Photocatalytic Degradation of para-Chlorobenzoic Acid and Perfluorooctanoic Acid

Using Titanium Dioxide and Hexagonal Boron Nitride Catalysts under Three Different

Treatment Scales

by

Jiefei Cao

A Thesis Presented in Partial Fulfillment
of the Requirements for the Degree
Master of Science

Approved July 2021 by the
Graduate Supervisory Committee:

Shahnawaz Sinha, Chair
Paul Westerhoff
Mahmut Ersan

ARIZONA STATE UNIVERSITY

August 2021

ABSTRACT

Nearly 2.1 billion people around the world to date do not have access to safe drinking water. This study proposes a compact (2-L) upflow photoreactor that uses widely available photocatalysts material, such as titanium dioxide (TiO_2) or hexagonal boron nitrate (hBN), to oxidize toxic micropollutants. Photocatalysts, such as TiO_2, can create powerful hydroxyl radicals (OH•) under UV irradiation to oxidize and disinfect water with various toxic pollutants present in untreated waters. The study assesses this along with few other photoreactors in terms of their performance with an indicator dye, such as methyl orange (MO), para-chlorobenzoic acid (pCBA), as an intermediate of pesticides, and perfluorooctanoic acid (PFOA), part of the per- and polyfluoroalkyl substances (PFAS), a highly persistent organic contaminant in water. This study also describes the various stages of evolution of this 2-L photoreactor, first using TiO_2 coated sand in maintaining a uniform (photocatalyst) bed in suspension along with few other modifications that resulted in a photoreactor with a 3 to 4-fold increase in contact time, is discussed. The final stage of this upflow photoreactor modification resulted in the direct use of photocatalysts as a slurry, which was critical, especially for hBN, which cannot be coated onto the sand particles. During this modification and assessment, a smaller bench-top photoreactor (i.e., collimated beam) was also built and tested. It was primarily used in screening various photocatalysts and operational conditions before assessment at this upflow photoreactor and also at a commercial photoreactor (Purifics Photo-Cat) of a larger scale. Thus, the overall goal of this study is to compare a few of these photoreactors of different designs and scales. This includes a collimated beam (at bench-scale), upflow photoreactor (at testbed scale), and a commercial photoreactor, Photo-Cat (at pilot-scale). This study also discusses the

i

performance of these photoreactors under different operating conditions, which includes evaluating two different photocatalyst types (TiO_2 and hBN), variable loading rates, applied UV doses, environment pH, and supplemental peroxide addition (as AOP) and with corresponding E_{EO} values.

DEDICATION

I dedicate this thesis to my loving parents Wang Min and Yong Cao. None of this would

have been possible without them.

ACKNOWLEDGMENTS

TABLE OF CONTENTS

LIST OF TABLES

LIST OF FIGURES

Figure   Page

x

CHAPTER 1

INTRODUCTION

1.1 Introduction

In recent years, photocatalysts, such as titanium dioxide (TiO_2), a semiconductor, is gaining much research and industrial interest with their applications in the paint, medical, food, cosmetics, coating, and many other industries. TiO_2 is also used in decontaminating micropollutants present in the air, water, municipal or industrial wastewaters. Under the UVC (254nm) light, TiO_2 can create powerful hydroxyl radicals (OH•) to oxidize micropollutants (e.g., trace organics, pesticides, metals) in the water. A process, where the photons (lights) are adsorbed onto the TiO_2 surface to excite its electrons from its ground orbital or valance band (VB) state to the higher conduction band (CB) state and create electron-hole pairs. These electron-hole pairs play a critical role in breaking down the water molecule adsorbed on the TiO_2 surface to form free radicals (e.g., OH•) for the effective oxidation of micropollutants.

To utilize some of the benefits of TiO_2 under UVC light (i.e., irradiation), Rice University (Houston, TX) built a small upflow photocatalytic reactor as a point of use (POU) system. The TiO_2 was coated onto sand particles (as substrate) to be uniformly suspended within the photoreactor using a UVC lamp, located vertically within the photoreactor core.

The upflow photoreactor proposed as part of this thesis which uses TiO_2 coated sands under UVC light is expected to provide both disinfection as well as oxidation of trace organic contaminants (such as pesticides, herbicides) in water. TiO_2 coated sands at its initial photoreactor design at Rice University were introduced tangentially from the bottom,

as side-entry, where TiO_2 coated sands flow spirally upward around the UVC lamp before exiting the reactor. Although this POU was effective in oxidizing micropollutants and/or disinfecting water in shorter-term tests, it failed to be operated under a longer-term test. Particularly, keeping the TiO_2 coated sand suspended within the photoreactor is a challenge to overcome. This was primarily due to the tangential flow entry design, causing poor suspension, inadequate mixing, and fluidization of particles. Moreover, the TiO_2 coated sand particle remains away from the UV lamp, which is located at the center of the reactor. The particle remains more toward the reactor wall, resulting in ineffective photocatalytic oxidation during its operation.

This study primarily focuses on improving the design of photoreactor to overcome some of these limitations and building a modified upflow photoreactor. First, the side entry design was replaced and was changed to a conical-shaped bottom-entry design for better particle introduction and improved particle suspension, mixing, and fluidization, which was proven first by a CFD (computational fluid dynamic) modeling and later implemented in the design. The system was built and operated in both batch and continuous modes with few modifications in removing some trace organic contaminants from water. These contaminants include an indicator dye, such as methyl orange (MO), para-chlorobenzoic acid (pCBA), as an intermediate of pesticides, and later, perfluorooctanoic acid (PFOA), part of the per- and polyfluoroalkyl substances (PFAS), a highly persistent organic contaminant in water. TiO_2 and two different hBN (hexagonal boron nitride) photocatalysts are used in this study for degrading these contaminants in water.

The modified upflow photoreactor was found to be effective in maintaining a uniform particle suspension with a steady fluidized bed. Later a recirculation pump was

added to this photoreactor to increase the contaminant contact time, particularly for the TiO$_2$ coated sand to improve overall contaminant degradation. Subsequently, this reactor was modified again to avoid the labor-intensive catalyst coating process (i.e., onto the sand) but to use the photocatalyst directly as a slurry without requiring coating. This modification was especially necessary for hBN as it could not be coated under repeated trials onto the sand particles (i.e., unstable and peels off). All these photoreactor modifications lead to a flexible photoreactor that provided a better mixing of both catalysts and longer particle contact time with the addition of recirculation pump and was able to maintain a uniform fluidized bed for coated sands.

During these periods of the above assessments and modifications, a smaller bench-top photoreactor, the collimated beam, was also built and tested. This bench-scale setup was used primarily for screening catalysts and assessing their optimal operational ranges or conditions before evaluating them at the upflow photoreactor (testbed-scale). Finally, a larger-scale (pilot) commercial photoreactor (Photo-Cat, Purifics) was also used and evaluated, particularly to evaluate hBN effectiveness in degrading PFOA.

Although EPA hasn't established any MCLs for PFAS, there is a health advisory limit (HAL) set for PFOA and PFOS in drinking water, which is 70 ng/L. In addition, six PFAS have been included in the Third Unregulated Contaminant Monitoring Rule (UCMR3) for monitoring. PFAS remains a significant challenge for many municipal water utilities, including the one in Arizona. It can be removed by conventional treatments, such as granular activated carbon (GAC) and ion exchange (IX) but is difficult to degrade or destruct completely in the water. Thus, photocatalysis is investigated here as part of this thesis effort in evaluating several photoreactors for their destruction.

1.2 Goals and Objectives

The overall goals of this study will be to assess the performance of few different types of the photoreactors that were built and utilized for degrading primarily two targeted contaminants (i.e., pCBA and PFOA) in water, that includes: a collimated beam (at bench-scale) and upflow photoreactor (at testbed-scale) and a commercial-scale photoreactor (Purifics, Photo-Cat) (at pilot-scale). Secondly, this study will evaluate two catalyst selections (TiO_2 *versus* two types of hBNs) and assess performance based on the degradation of the contaminant. Thirdly, to evaluate optimal operational conditions that will result in maximizing their removal.

The operational conditions range from contaminant's concentration levels (from ug/L to mg/L ranges), catalyst loading rates (mg/L), its contact time (0-3 hours), applied UV dose (mJ/cm^2), supplemental chemical addition (hydrogen peroxide (H_2O_2), as advanced oxidation process), feed water condition (such pH), etc., for removing contaminants such as MO (organic dye), along with pCBA, PFOA/PFAS from water.

Some of the specific objectives of this study include:

(1) Compare three different photoreactors setup (design) in terms of their removal efficiency

(2) Compare catalyst types, TiO_2 *versus* two hBNs (i.e., hBN#1 and hBN#2) for removing pCBA and PFOA from water

(3) Elucidate operational ease and/or challenges of these photoreactors

CHAPTER 2

BACKGROUND ON PHOTOCATALYSIS

In the photocatalysis process, when the irradiation of the light energy is equivalent or greater than the band gaps of the semiconductor (e.g., TiO_2), it promotes an electron to leave from its lowest energy or valance band (VB) state to its higher energy or conduction band (CB) state (Figure 2.1). During this process photogenerated pairs, electrons (e^-), and holes (h^+) are formed, which subsequently plays a critical role in forming successive reactive oxygen species (ROS) that ultimately participate in the oxidation-reduction process of contaminant degradation. Generally, electron (e^-) participates in the reduction process by creating superoxide species ($O_2^-\bullet$), while photogenerated holes (h^+) breaks/splits the water molecule and forms hydroxyl radicals (OH•) as shown in Figure 2.1, which participates in the oxidation process.

Conduction Band (CB)

$O_2 + e^- \rightarrow O_2^{\cdot-}$
$O_2^{\cdot-} + Pollutant \rightarrow H_2O + CO_2$

Reduction

Light (UV)

e^-

h^+

Valance Band (VB)

$h^+ + Pollutant \rightarrow H_2O + CO_2$
or
$h^+ + H_2O \rightarrow OH\cdot + H^+$
$OH\cdot + Pollutant \rightarrow H_2O + CO_2$

Oxidation
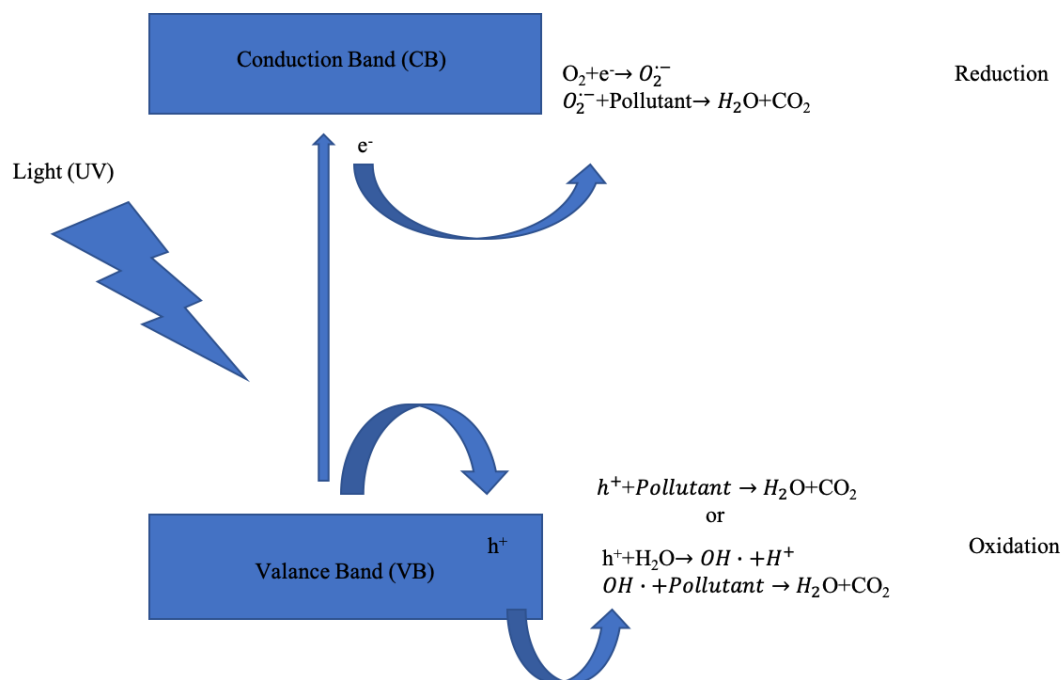
Figure 2.1 Mechanism of Semiconductor Photocatalysis

5

2.1 Photocatalytic Mechanism

The photocatalytic process is complex with multiple reaction processes and steps. Photocatalysts such as TiO_2 participates in the photocatalysis process by starting with photons (i.e., light) adsorption onto its surface to excite its electrons to leave its VB to CB. By exciting, it creates electron (e^-) and hole (h^+) pairs, as shown by equation (1) (below). The electron-hole pair then separates, only the electron (e^-) or the hole (h^+) migrates to the surface to drive either the reduction (equation 3) or the oxidation (equation 2) process, respectively (Guo et al. 2019). However, most electron (e^-) and hole (h^+) pair recombine and its energy is converted to thermal or vibrational energies and ceases to drive the reaction. The rapid charge recombination is one of the main limitations for many catalysts including the TiO_2 photocatalyst. To prevent such recombination is part of active and on-going catalyst research. It is done through photocatalyst modification, including doping, bringing defects, or structural induced changes, etc. (Guo et al. 2019).

$$TiO_2 + hv \rightarrow e^- + h^+ \tag{1}$$

$$\text{Oxidation: } H_2O\ +\ 2h^+ \rightarrow 2H^+ +\ +\frac{1}{2}O_2 \tag{2}$$

$$\text{Reduction: } 2H +\ + 2e^- \rightarrow H_2 \tag{3}$$

$$Overall: H_2O \rightarrow H_2\ +\frac{1}{2}O_2 \tag{4}$$
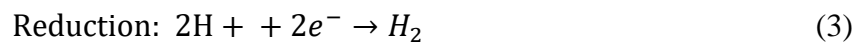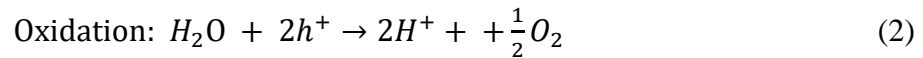
These photo-generated hole splits the water molecule (equation 2) on photocatalyst surface and leads to forming highly reactive oxygen species (ROS), such as hydroxyl radicals (OH•), which plays a critical role, especially in the photodegradation of contaminants by oxidation. The photo-generated electron (e^-) (equation 3) forms other reactive species for reducing contaminants. These reactive oxygen species (ROS) form on the surface of the catalysts and can directly oxidize or reduce pollutants in water. For the

6

redox reaction to occur with the pollutant, the pollutant first needed to be adsorbed onto the photocatalysts (TiO_2) surface (i.e., heterogeneous catalysis). The free radicals from this process react with the targeted contaminants onto the catalyst surface. These radicals degrade the organic micropollutants by breaking their C-C bonds or even stronger bonds (e.g., C-F bonds, if present). Photocatalysts in combination with other photocatalysts as bimetallic catalysts are explored that can effectively use photons in breaking these bonds are part of active photocatalytic material research.

Thus, the semiconductors material discovery has played a significant role and is being effectively used in converting light (solar) to energy (photovoltaic cell). It has many other important applications. The semiconductor industry uses these materials and develops them for various application. The selection of these catalysts is carefully done for targeted application with optimal band gaps that will maximize the energy utilization, which is an evolving field and are part of active material and application research.

Among all the photocatalysts, titanium dioxide (TiO_2) has remained one of the most widely used products by many industries. This is due to its favorable band gaps, high photothermal stability, and lower cost. However, due to its wider band gaps (3.0 to 3.2 eV), it only permits UV irradiation for its activity. It also tends to excite at a wavelength ranging from 266nm to 365 nm (Yang, 2019). It exists as anatase and rutile, but anatase (e.g., Degussa P25, a common commercial TiO_2 product) is widely used. This also due to its higher light adorability and hence photocatalytic activity. Commercial photocatalysts (such as P25) have been shown to oxidize air pollutants, toxic contaminants in water, and in disinfecting microbial contaminants in water. The rate of decomposition of the pollutants (e.g., inorganic, organic, and microbial) is dependent on its adsorbed concentration onto

the surface and hydroxyl radical (OH•) formation, which determines the rate of oxidation and degradation (i.e., kinetics). Similarly, photodecomposition of microorganisms occurs by breaking the cell wall (i.e., disinfection) due to the formation of ROS (Etacheri et al. 2015).

Although TiO_2 is effective in photo catalytically oxidize various types of contaminants in water, (e.g., colors, dyes, trace organics (pesticide, herbicides), inorganics (heavy metals), etc.), but it is less effective in removing strongly bonded, persistence organics or recalcitrant (such as C-F, strongest bond). The PFOA, as an example, has strong C-F bonds and is difficult to break. Other photocatalysts, such as hexagonal boron nitride (hBN), which is normally used as an electrical insulator due to its wide bandgap (~ 6.0 eV), is investigated and found to be effective in breaking such strong bonds (Duan, 2020). This wider bandgap leads to a narrower and lower absorbance spectrum (~208 nm) (Duan et al. 2020). However, bringing defects to hBN on edges as edge defects or with B or N vacancies can result in attaining higher absorbance in the UVC range, so that the electrons in its valence band (VB) transfer more effectively to its conduction band (CB) and become free photo-generated electrons. This is part of active research which is currently conducted at the Rice University. Based on this hypothesis, ball milling to introduce more defects within hBN is proposed and explored at Rice University. It is reported that there are two pathways of PFOA degradation using hBN as the catalyst. One is the direct reaction that the photogenerated holes in hBN interact with PFOA. This has been investigated by EDTA (as scavenger) experiment. The other reaction pathway is the hydro-defluorination pathway. This study uses silicon-carbide (SiC) photocatalysts in degrading PFOA degradation (Duan et al. 2020). In this case, some protons are reported to produce on the surface of SiC during

photocatalysis and react with the C−F bond directly in forming C−H and Si−F bonds *in situ* (Huang et al. 2018). Based on it, Duan et al. performed XPS on hBN and assumed PFOA can directly react with the B-H bond on the surface of hBN, as the equation shows below. The B−H bond is on the surface of hBN could be generated via photocatalyzed reaction with either proton or water and reported for hBN and fluorinated hBN in photocatalyzed water splitting (Duan et al. 2020).

$$C - F + B - \rightarrow C - H + B - F \tag{5}$$
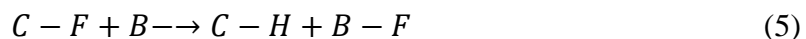
Apart from all these above advancements on photocatalytic degradation, is complex and remains at the research-level (e.g., hBN), and not yet practiced in a larger setup or implemented, especially the degradation of recalcitrant compounds, such as PFOA. Conventional treatments, like granular activated carbon (GAC) adsorption or ion-exchange (IX), or even reverse osmosis (RO) membrane are use and are effective in removing PFOA/PFAS from water. However, all of these treatments are non-destructive or physical separation technologies, meaning the contaminant remains, either adsorbed onto the media or concentrated as a waste product and not destructed. There are only a few limited technologies that can degrade PFOA by breaking the C-C and C-F bonds (Liu et al. 2017). However, some only transform their longer carbon chain (C-C) compounds (such as C8, PFOA) to shorter-chain compounds (C4, PFBS or C6, PFHxS), which is not preferred as the shorter chain of PFAS is more mobile, soluble, and stable than the longer-chain compound and is difficult to remove by conventional treatments. However, technologies such as thermolysis (decomposition by heating), or photocatalysis or electrocatalysis, can break the C-F bond which is more desirable and investigated to disintegrate the PFOA/PFAS to less toxic as non-fluorinated compounds (Gole et al. 2018).

Others have looked at other types of photocatalytic materials. Such as Zhao et al., found a significant level of PFOA degradation is possible with synthesized β-Ga_2O_3 and thought PFOA degradation was achieved by the reaction with the photogenerated electrons in the conduction band of β-Ga_2O_3 (Zhao et al. 2009). Li et al. have reported In_2O_3 as a promising photocatalytic in the decomposition of PFOA (Li et al. 2012). Sahu et al. synthesized and assessed a $Bi_3O(OH)(PO_4)_2$ photocatalyst, which has shown to be effective in PFOA degradation (Sahu et al. 2018). However, many of the photocatalyst and its assessment remains at the research or laboratory scale and may not be practical (e.g., costs or synthesis) for larger scale implementation. Photocatalysts such as hBN has proven to be effective in PFOA degradation but hasn't been evaluated or assessed at a larger scale. This study considers all the above advances and focuses on two primary photocatalysts, such as TiO_2 and hBN, evaluated under different treatment scales to remove pCBA and PFOA/PFAS as targeted contaminants in water.

2.2 Photoreactor Design

Photoreactor can be designed with several key approaches in utilizing the photocatalysts. However, two main approaches are either free dispersion of photocatalysts in water, like chemical addition as a slurry. However, the problem with this approach is the recovery of catalyst (as slurry) from the system for reuse. However, it can be overcome by having a separator, such as tight polymeric or ceramic membranes or other separator devices. There already exist some commercial photoreactor product (Photo-Cat system from Purifics) that is primarily used in industrial wastewater treatment using TiO_2 slurry with UVC light and ceramic membrane as separator, will be used in this study.

The other approach is immobilized photocatalyst coating, where photocatalyst such as TiO_2 is coated onto substrates (e.g., sands) in forming hierarchical structures at the macroscale, including nanoparticles coating onto optical fibers, packed bed media, and other materials (Westerhoff et al. 2016), a few are part of ongoing research.

CHAPTER 3

MATERIALS AND METHODS

3.1 Setup

3.1.1 Collimated beam

For the bench-scale study (collimated beam setup), a 4-inch diameter collimated

beam setup is built and used and is shown in Figure 3.1.

Figure 3.1 Collimated Beam (Bench-Scale Setup)

Around 120-ml of spiked water (e.g., pCBA or PFOA/PFAS) sample was poured

into the 4-inch diameter glass petri-dish with 1/2-inch deep. A gap of about 1-inch was

maintained between the bottom of the collimated beam (column) and the top of the petri

dish, as shown in Figure 3.1. Two tubular low-pressure (LP) UV lamps (17W and 60W;

total 77W) were used and placed horizontally inside an overhead collimated beam box.

Before the degradation study, the UV irradiance (uW/cm^2) onto the petri-dish was

measured using a handheld radiometer (AvaSpec-2048L) and found to be around 1000

uW/cm^2 (or 1 mJ/sec-cm^2). This irradiance value is used in calculating the expose time (min) needed to achieve a targeted UV dose (mJ/cm^2). During the UV irradiance or exposure study, the spiked water sample is gently mixed with a small magnetic stirrer in the presence (or absence) of catalysts.

A blank/dark spiked sample (without the catalyst or UV irradiation) is also prepared, which is mixed under similar contact time (minutes) required to achieve the targeted UV dose (mJ/cm^2). The blank/dark sample is collected and analyzed to determine if contaminant (spiked) is degraded due to photolysis or adsorption onto the catalyst.

Different UV doses are investigated for the contaminant at targeted concentration level to find an optimal UV dose for its removal. For example, a UV dose of 1000 mJ/cm^2, or 2000 mJ/cm^2 and 5000 mJ/cm^2 were evaluated for spiked pCBA sample (at 1 mg/L) for degradation. For example, to achieve an UV dose of 1000 mJ/cm^2, 2000 mJ/cm^2 and 5000 mJ/cm^2, approximately will require 17 minutes, 33 minutes and 83 minutes of UV exposure time (contact time), respectively. After UV-irradiation, samples were collected in 50-mL centrifuge tubes for analysis.

3.1.2 Upflow photoreactor

TiO$_2$ Coated Sands

For the testbed study, TiO$_2$ coated sand is used as the photocatalyst for below upflow photoreactor, located within MobileNEWT testbed.
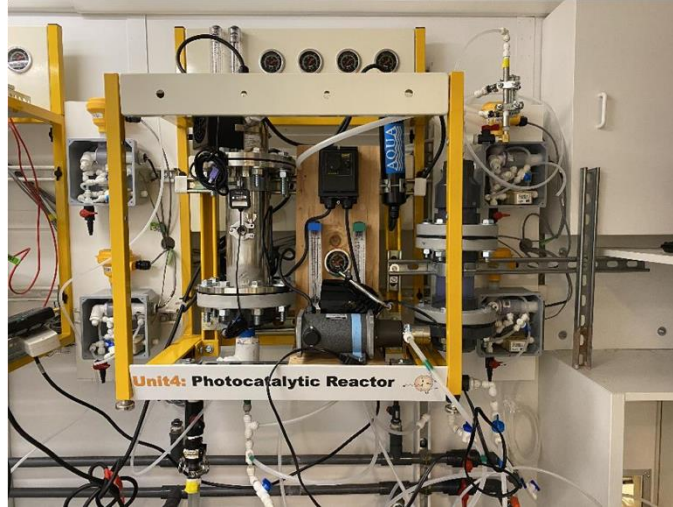
Figure 3.2 Upflow Photoreactor (Testbed Setup)

The 2L upflow photoreactor was custom designed and built at ASU (after CFD modeling and analysis) and is used with a single 60W (254 nm) LP (low pressure) UV lamp at the core of this stainless steel (SS) photoreactor, as shown in Figure 3.2. TiO_2 coated sand is used, prepared by Rice University (Houston, TX) and loaded (250 g/L, 1% wt. of TiO_2, which is equivalent of 2500 mg/L as TiO_2) into the photoreactor before the study. A fine 60-mesh screen is used at bottom of the photoreactor plate (flanges) to retain the catalyst within the reactor. Feed water is introduced from the bottom of this upflow photoreactor using conical-shaped bottom or distributor. Feed water spiked with targeted contaminant enters the reactor bottom and flows uniformly through the reactor and then exits from the top (i.e., upflow-mode). The incoming flow lifts the TiO_2 coated sands uniformly (as particle-bed) and fluidize it to targeted fluidization level (50% of photoreactor height). Contaminant is spiked continuously in the feed line and using a dosing pump (PULSAtron, FL) for continuous operation (otherwise spiked to feedwater once for batch operation). A needle valve is used in carefully controlling the influent flowrate (L/min) to the photoreactor (for particle fluidization).

The UV dose applied at upflow photoreactor is based in residence time (seconds) within the reactor and hence based on the flowrate (L/min). For example, of the flow rate of 3 L/min, will provide a contact time of around 0.7 minute (i.e., volume 2L, flowrate 3L/min), representing a UV dose of 500 mJ/cm^2. Similarly, a contact time of 2-minute, or 4-minutes, represents a UV dose of 1000 mJ/cm^2, or 2000 mJ/cm^2, respectively, under continuous mode of operation. The UV dose (mJ/cm^2) calculation is based on a previously conducted chemical actinometry study (with photosensitive dye) for this photoreactor. It provides UV irradiance (measured by the handheld radiometer (AvaSpec-2048L) and related the flowrates (for contact time) to determine UV dose (mJ/cm^2). The photoreactor was operated continuously at least two column volumes for each targeted UV dose (mJ/cm^2) and sampled at midway through the run to get representative (dye) samples.

A recirculation pump (Tuthill PM8014) is added to the setup with a recirculation chamber. The addition of this recirculation pump allows the upflow photoreactor to increase the contact time of the contaminant with the TiO$_2$ coated (sand) fluidized bed. During this initial stage of photoreactor assessment, methyl orange (MO) is used as the contaminant and relate its degradation under different contact times (with recirculation) using TiO$_2$ coated sand (as catalyst). The required feed flow rate, which includes both incoming feed flow rate and the recirculation rate, was targeted to maintain at 4 L/min (combined) to achieve the targeted fluidization (i.e., 50%) and to avoid any particle washout of the reactor. The flowrate is based on sand particle size (180-220 um) and density (2.2 g/cc) (prior modeling effort using Ergun equation also indicated particle size/density for targeted fluidization).

During MO study, a chemical dosing pump (PULSAtron, FL) was used for providing continuous spike of MO at targeted concentration level to the feed water. The system was operated at continuous flow mode with different recirculation rate using a variable frequency drive (VFD) (MotorTec 2002) controller. Both of influent and effluent samples were collected in 50-mL centrifuge tubes for subsequent analysis.

Upflow (Slurry) Photoreactor

The above upflow photoreactor (Figure 3.2) was modified to a 'slurry' based photoreactor (Figure 3.3) to use catalyst directly without requiring coating (e.g., TiO_2 and hBN loaded as slurry) for removing pCBA and PFOA, respectively. This slurry-based photoreactor could be operated in continuous or batch-mode (with recirculation). The fine mesh at bottom the reactor is removed to allow the slurry to enter and leave the reactor freely. The slurry is retained and recycled within the photoreactor using the ceramic filter (Dalton Rio 2000) in a 10-inch filter housing (Figure 3.3). The gear pump (Tuthill PM8014) used in the upflow photoreactor (Figure 3.2) is replaced with a larger multi-stage centrifugal pump (Grundfos 96081032 Vertical Multi-stage pump), which can circulate slurry without damaging the pump impeller or crushing the catalyst (slurry), which could occur in the gear-pump, thus was replaced.

Figure 3.3 Slurry Photoreactor (Testbed Setup)

3.1.3 Photo-Cat

The Photo-Cat (Serial 0700) system is used for pilot-scale assessment. This system is a 16-L system and is integrated four (4) UV lamps (each 75-Watt, LP mercury lamp) and uses a ceramic (silicon carbide) membrane separator. This system is controlled by a PLC (programmable logic controller) (Figure 3.4). These LP lamps emit UV light at a wavelength of 254 nm. The PLC allows light operation and catalyst circulation, separated by an ultrafiltration (UF) ceramic (silicon-carbide) membrane. In addition, under the recirculation mode the Photo-Cat system allows for variable power output to control one or multiple lamps simultaneously (Stancl et al. 2015). For this study, the system is usually operated (or recirculated with catalysts) at a constant flow rate of 25 L/min (under batch operation).

Figure 3.4 Photo-Cat from Purifics (Pilot-Scale Setup)

3.2 Material

3.2.1 Methyl orange (MO)

Preparation

Methyl orange (MO) was used in degradation study, particularly in assessing the upflow photoreactor (Figure 3.2) with TiO_2 coated sand study. Around 18-L of concentrated MO solution is prepared at concentration of 80 mg/L. A dosing pump (PULSAtron, FL) is used for adding targeted MO dose to feed water. To prepare this concentrated MO solution, about 1.44 g of MO is dissolved into a 1-L volumetric flask and later add with nanopure water to mark and then poured into the 18-L container and then fill with nanopure water to mark. Initially, around 1-L of this solution is run through the system and is used in preparing (or washing) the system for the study, remaining 17-L is used for the degradation study.

All MO samples (before and after) of the study are collected in 50-mL centrifuge tubes. Samples are analyzed by spectrophotometer (HACH DR5000). Samples are measured under single wavelength of 460-nm with a 50-mm rectangular quartz cell. Standards are measured along with samples as quality control, calibration curve is used in correlating absorbance to concentration (mg/L).

3.2.2 para-Chlorobenzoic acid (pCBA)

Preparation

The pCBA solution was prepared in an alkaline solution (i.e., NaOH) in a partially filled volumetric flask with sonication approach. After sonication, the pH is adjusted to pH 6-7 with a diluted acid (i.e., HCl). After acid addition, the volumetric flask is added with nanopure water to the mark.

Sample Analysis

All samples collected are filtered with 0.45-um syringe filters (Cole-Parmer with nylon membrane), a 5-mL syringe is used to draw sample and is then filtered into 2-mL glass vials. Samples are analyzed by HPLC (Waters 2695) with a Photodiode Array detector at 239 nm. The RP18 column (100 mm × 4.6 mm) is used with a mobile phase mixture of water-acetonitrile aqueous solution at 60:40 (v:v) at a flow rate of 0.6 mL/min. Samples are measured with standards and blanks each time (as quality control) and correlated with the peak area.

3.2.3 Perflurooctanonic acid (PFOA)

Preparation

The PFOA sample was prepared by dissolving measured amount of PFOA sample in a partially filled volumetric flask with nanopure water and sonicated then then add with nanopure water to mark.

Sample Analysis

All samples of the study are filtered with 0.45-um PES syringe filters (Thermo Scientific), a 5-mL syringe is used to draw sample and is filtered into 2-mL glass vials. Samples are analyzed by HPLC (Waters 2695) with a Photodiode Array detector at 210 nm. The C18 column (250 mm × 4.6 mm) is used and the mobile phase was a mixture of 0.005 M NaH_2PO_4-acetonitrile aqueous solution at 50:50 (v:v) at a flow rate of 0.8 mL/min. Samples are measured with standards and blanks (as quality control) each time and correlated with the peak area.

3.2.4 Photocatalysts

Two types of photocatalyst are used in this study, that includes TiO_2 and two types of hBNs. For TiO_2, Degussa P25 (ACROS), a commercial product, widely available is used for this study. This product is used in assessing TiO_2 (P25) effectiveness (either as coated onto the sand particle or added directly as slurry) in degradation of targeted contaminant in water.

For hBN, two types are used in this study. One received, initially from Panadyne (donated; Montgomeryville, PA), widely used hBN used by various industries and is designated as hBN#1. The other is from Saint-Gobain (Malvern, PA), received from Rice University (Houston, Texas) and is defined as hBN#2.

The hBN#1 is highly hydrophobic, widely used, and has good affinity for oils and polymer resin and serves as a good mold release agent for the molten metals and salts, was

investigated in this study. While hBN#2, is surface treated by the manufacturer or functionalized and is less hydrophobic or partially of hydrophilic in character and meant for different application and or use (Figure S1.). Both hBNs were used and tested to understand their similarities and difference in character and effectiveness in removing targeted contaminant from water under different treatment conditions.

CHAPTER 4

DEGRADATION OF PARA-CHLOROBENZOIC ACID AND PER-

FLUOROOCTANOIC ACID WITH BENCH-SCALE SETUP (COLLIMATED BEAM)

This chapter focuses mainly on removing contaminants such as para-chlorobenzoic acid (pCBA) and per-flurooctanoic acid (PFOA) from water using the bench-scale, the collimated beam setup. Two different catalysts, mainly titanium dioxide (TiO$_2$) and two hexagonal boron nitrides (hBN#1 and hBN#2) as slurry is used in this setup (Figure 3.1). Around 120-ml of nanopure water spiked with either pCBA or PFOA at targeted concentration level of 1.0 ppm (6 uM) and 25 ppm (60 uM) respectively, were evaluated. Sample is poured carefully into a shallow glass petri-dish (4-inch diameter with 1/2-inch deep). The two-tubular low-pressure (LP) UV lamps are used for the collimated beam setup to provide 1000 uW/cm^2 (or 1 mJ/sec-cm^2) of UVC exposure on top of the petri-dish. This irradiance value is used with the exposure time (min) to attain the targeted UV dose (mJ/cm^2).

During the UV exposure study, water sample is gently mixed with a small magnetic stirrer in the presence or absence of UV light or the catalysts. A dark study (with spiked sample), but without UV irradiation or catalysts, is conducted under similar contact time (minutes for targeted UV dose) as it would be with be for photocatalytic process (i.e., UV with catalyst). This is to determine contaminant degradation or removal by the photolysis or adsorption (only), respectively and to compare them against UV irradiance in the presence of catalysts. The following discusses some of these results from bench-scale study.

4.1 pCBA Degradation

For pCBA degradation study, a comprehensive experiment matrix is developed, as shown in Table 4.1. This table shows pCBA degradation under different catalyst types (TiO_2 and hBNs) and loading rates (0-10,000 mg/L). It also shows the effect of applied UV dose (ranging from 0-6000 mJ/cm^2) and under different pH conditions (pH 3.0-11.0) and in presence or absence of hydrogen peroxide (H_2O_2) addition as advanced oxidation process (AOP), are investigated.

Two types of hBNs were used in this study, as described in Chapter 3. Both are commercially available hBN products. One is received from Panadyne (designated as hBN#1). The other hBN received from Saint Gabion (designated as hBN#2). It is a surface treated or functionalized hBN powder, which is less hydrophobic or partially of hydrophilic character to hBN#1. Both hBNs were used and tested in the collimated beam study to understand the difference or similarities and compare their effectiveness in removing pCBA under different treatment scenarios. The concentration of pCBA in the water sample was spiked at 1.0 ppm level (which is around 6 uM) and measured by HPLC as discussed in Chapter 3.

Table 4.1

Experiment Matrix for pCBA

pCBA Degradation	Exp #	Catalyst Type	Catalyst Dose (mg/L)	UV Dose (mJ/cm^2)	pH	H$_2$O$_2$ (mg/L)
Effect of Photolysis	1	None	0	4000	6.2	None
Effect of Adsorption	2	TiO$_2$	2500	0	6.2	None
	3	hBN#1	2500	0	6.2	None
Effect of Loading Rate	4-8	TiO$_2$	500-1000-2500-5000-10000	2000	6.2	None
	9-13	hBN#1	500-1000-2500-5000-10000	2000	6.2	None
	14-18	hBN#2	500-1000-2500-5000-10000	2000	6.2	None
Effect of UV Dose	19-21	TiO$_2$	2500	2000-4000-6000	6.2	None
	22-24	hBN#1	2500	2000-4000-6000	6.2	None
Effect of pH	25-27	TiO$_2$	2500	2000	3.0-6.2-11	None
	28-30	hBN#1	2500	4000	3.0-6.2-11	None
Effect of Peroxide Addition	31-33	TiO$_2$	2500	2000	6.2	1-5-10
	34-36	hBN#1	2500	4000	6.2	1-5-10

All samples for the collimated-beam study were prepared with nanopure water. Few of the initial experiments, such as experiment #1 (Table 4.1) was conducted to evaluate the effectiveness of photolysis (without catalyst present) in pCBA degradation. Experiments

#2 and #3 were conducted in the dark (absence of UV irradiance) for both TiO_2 and hBN#1, respectively, to see the effect of adsorption.
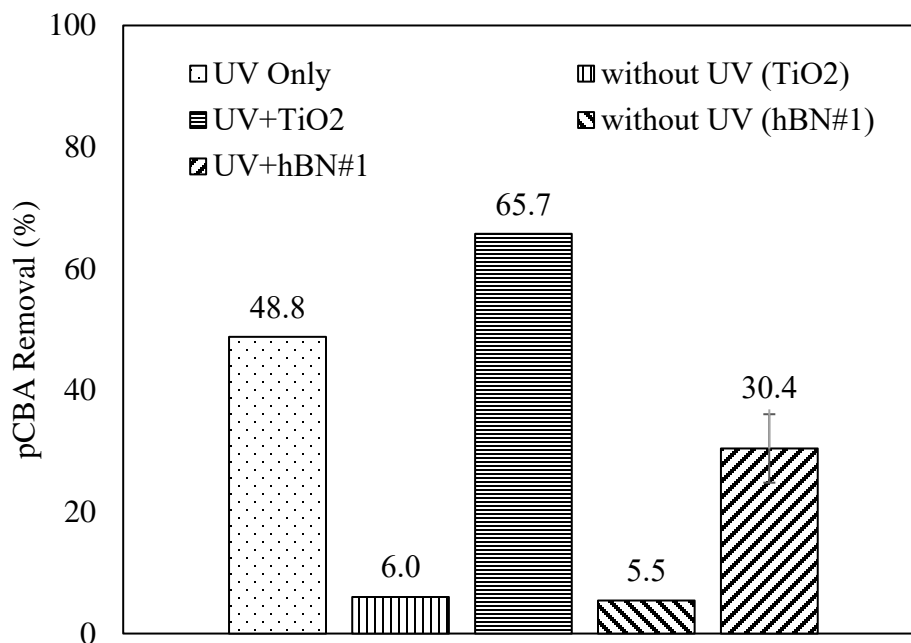
Figure 4.1 Effect of Photolysis and Adsorption [Time of irradiance: 67 min (UV dose: 4000 mJ/cm^2); Loading rate: 2500 mg/L; pH 6.2]

The above figure shows pCBA can easily be degraded with photolysis only. About 49% of pCBA was degraded by a UV dose (only) at 4000 mJ/cm^2 (which is a substantial UV dose but used in assessing photolysis). This figure also shows, in absence of UV dose (dark), TiO_2 can only remove around 6% of pCBA (by adsorption) at a loading rate of 2500 mg/L. However, TiO_2 in presence of UV irradiation resulted in a synergistic effect, much higher amount of pCBA degradation (66%) is noted. This nearly 17% increase (beyond photolysis) is due to the formation of the hydroxyl radicals, which helps on the removal/degradation process.

Above figure also shows, a direct comparison between TiO_2 and hBN#1, it shows for a similar loading rate (2500 mg/L) the uptake is like TiO_2, ~6% by adsorption (dark)

for hBN#1. However, in the presence of UV light, it degrades around 30% of pCBA, which is much lesser than TiO_2 and hence further reduction to photolysis (is discussed below).

Above results suggest that TiO_2 is more effective than to hBN#1 (with an equal loading rate) for pCBA removal at the collimated beam study. Figure 4.2 shows TiO_2 could be well-dispersed in the petri-dish without causing any types of agglomeration, aggregation, or clumping. Unlike TiO_2, hBN#1 is more hydrophobic than TiO_2 and causes such aggregation and clumping (Figure 4.3). Agglomeration can also limit the catalysts surface area and its exposure (and blocks) UV light, which may lead to a lesser amount of pCBA degradation by hBN#1. It was also found, clumped hNB#1 also floats on the surface (due to hydrophobicity), which can also block the UV light for catalyst and irradiation, as shown in Figure 4.3. All these results suggest, due to the inherent difference between TiO_2 and hBN#1 (e.g., hydrophilicity versus hydrophobicity), a better dispersed or well-mixed hBN (as slurry) would be necessary to improve overall pCBA removal.

Figure 4.2 TiO_2 Well Dispersed in pCBA Solution
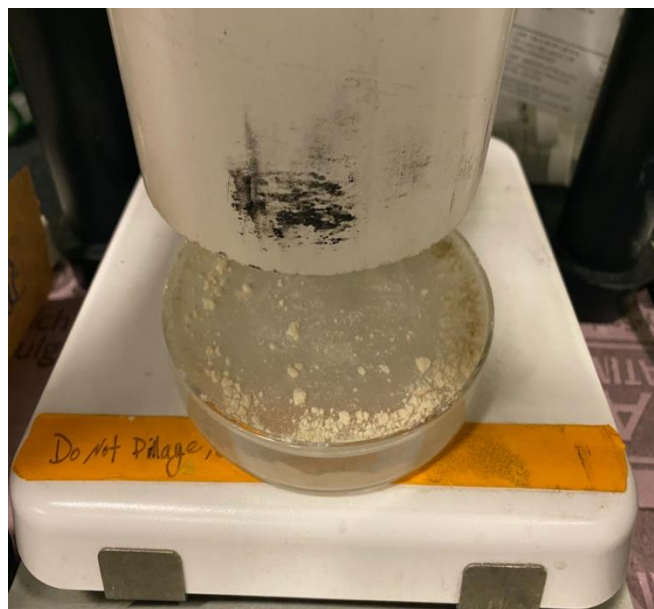
Figure 4.3 hBN#1 Floating on the Surface

4.1.1 Optimizing TiO$_2$ for pCBA degradation

Next, a series of tests were conducted for TiO$_2$ in the collimated beam by changing

its loading rate, pH, peroxide addition to further improve and optimize pCBA degradation

using TiO$_2$, are discussed below.

Effect of Loading Rate
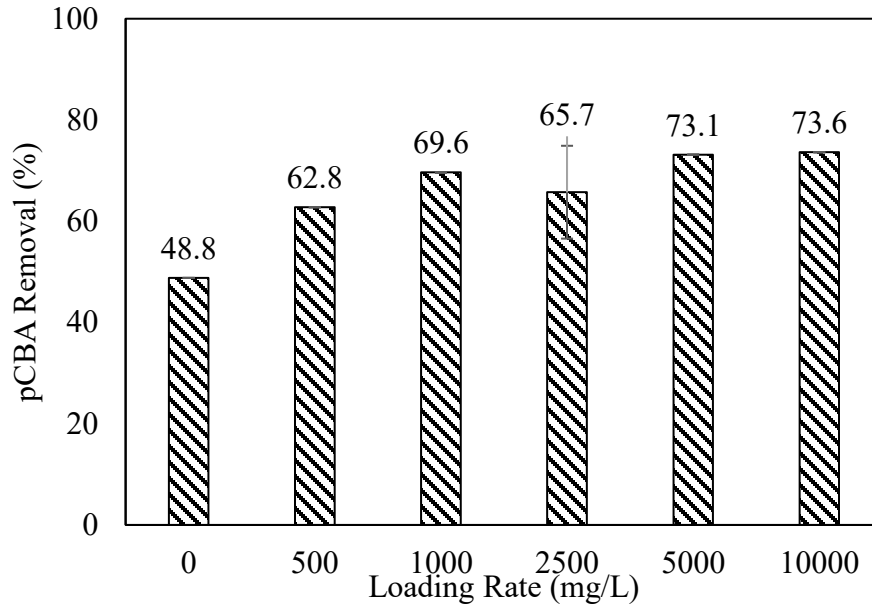
Figure 4.4 Effect of Loading Rate (TiO$_2$) [UV Dose: 2000 mJ/cm^2; pH 6.2]

The TiO$_2$ loading rate can play an important role in pCBA degradation. Figure 4.4, it shows as TiO$_2$ loading rate increases from 0 mg/L (none; i.e., photolysis) to 10,000 mg/L for a fixed UV dose of 2000 mJ/cm^2 and under ambient pH condition (pH 6.2), the pCBA degradation also increases significantly from 48% (photolysis; no catalysts) to 74% under higher TiO$_2$ loading rates. However, the optimal loading rate tends to be around 1000 to 2500 mg/L, as higher loading only slightly improves overall removal. The higher pCBA removal with the increased loading rate is due to an increase in TiO$_2$ particle concentration and hence higher surface area and exposure resulting in a higher hydroxyl radical formation, which lead to a higher pCBA removal.
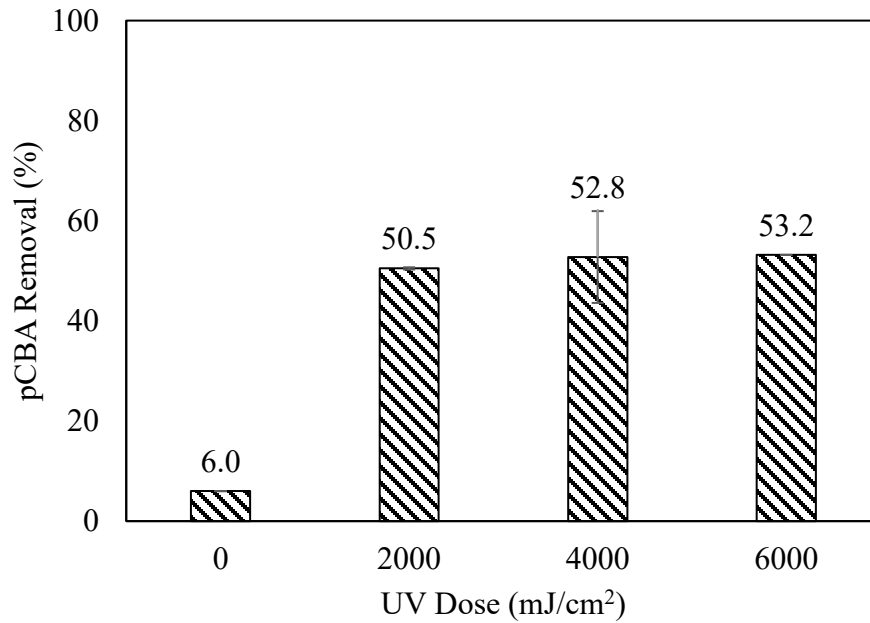
Figure 4.5 Effect of UV Dose (TiO$_2$) [Loading Rate: 2500 mg/L; pH 6.2]

Likewise, the loading rates, variation of UV dose (mJ/cm^2), could also play an important role in pCBA degradation and is investigated for a fixed TiO$_2$ loading rate (2500 mg/L) and at ambient pH condition (pH 6.2). The above figure (Figure 4.5) shows there is no significant effect of UV dose on pCBA removal for TiO$_2$. Thus, a dose from 2000 mJ/cm^2 to 4000 mJ/cm^2 tends to be adequate for pCBA removal.

Effect of pH
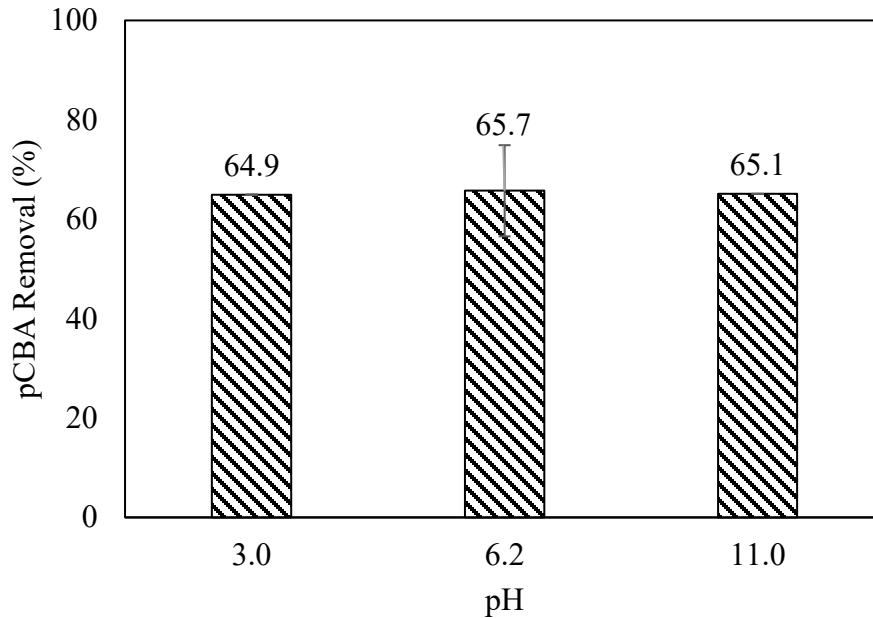
Figure 4.6 Effect of pH (TiO$_2$) [UV Dose: 2000 mJ/cm^2; Loading Rate: 2500 mg/L]

The effect of pH on pCBA removal could equally be important and thus was investigated for TiO$_2$. Three different pH levels were investigated, ranging from pH 3 to pH 11. The study was conducted at collimated beam for a fixed (optimal) loading rate (2500 mg/L) and fixed UV dose (2000 mJ/cm^2), while varying the pH. The effect of pH is shown in Figure 4.6, which indicates no significant effect of pH on pCBA removal for TiO$_2$.

Above results (Figure 4.1 and Figures 4.4 to 4.6) suggest that TiO$_2$ effectiveness in pCBA removal is dependent on loading rate (mg/L). If the UV dose is within the optimal ranges, it shows it has lesser effect with UV dose variation. Above results also suggests pH tends to have less impact on TiO$_2$ on pCBA removal in collimated beam study.

Effect of Peroxide Addition
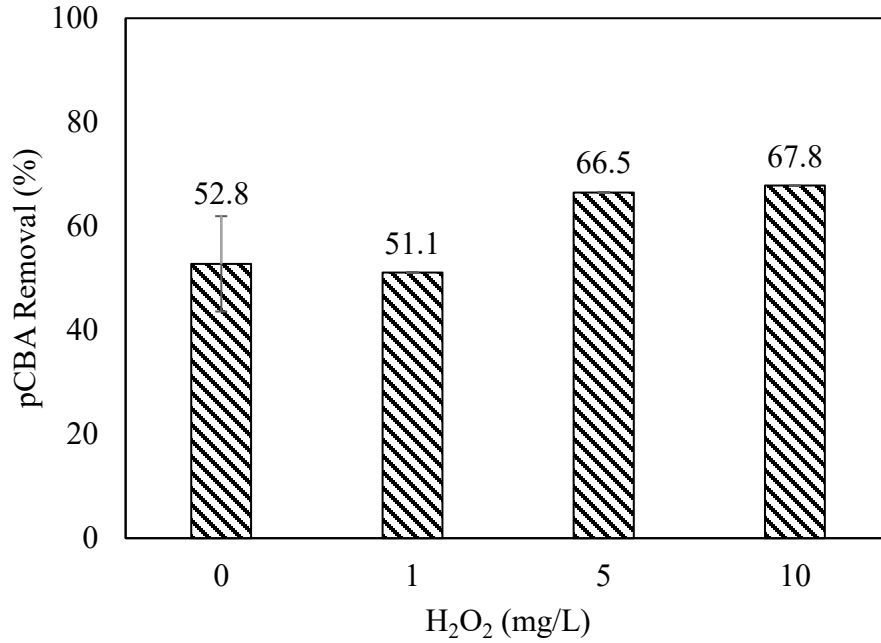
Figure 4.7 Effect of Peroxide Addition (TiO$_2$) [UV Dose: 2000 mJ/cm^2; Loading Rate: 2500 mg/L; pH 6.2]

The advanced oxidation process (AOP), using H$_2$O$_2$ in presence of UV light has shown to be effective in removing various types of micropollutant in water, thus is it is investigated in absence and presence of TiO$_2$ (photocatalyst) under UV. Both AOP (UV+H$_2$O$_2$) and photocatalysis (UV with TiO$_2$), creates hydroxyl radicals (OH•) and is investigated for pCBA removal. Figure 4.7 shows, the peroxide addition tends to have a slight positive impact on pCBA degradation, and it improves it removal by an additional 15%.

Overall, these results suggest photolysis (i.e., without catalysts) by itself, is highly effective in pCBA removal (49-50%). However, the addition of TiO$_2$ as a catalyst, improves the pCBA degradation due to the formation of hydroxyl radicals (OH•). However,

effect of UV dose or pH tends to have less of an impact in collimated beam, whereas peroxide addition (as AOP) shows a slight improvement.

4.1.2 Optimizing hBN for pCBA Removal
Effect of Loading Rate
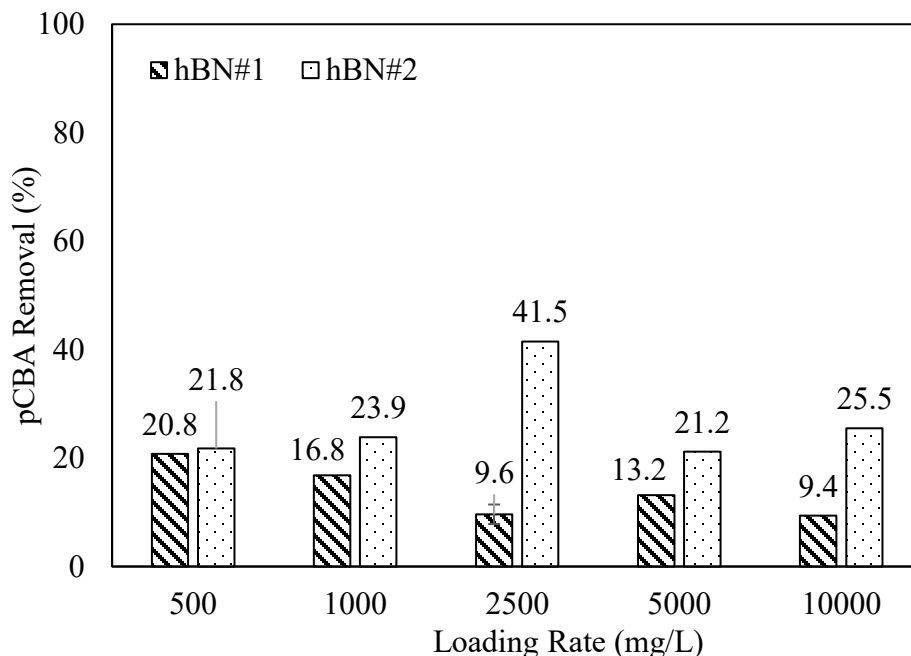
Figure 4.8 Effect of Loading Rate [UV Dose: 2000 mJ/cm^2; pH 6.2]

Likewise, TiO$_2$, a series of experiments were conducted, using both hBNs (i.e., hBN#1 and hBN#2) to see if further optimization in terms of loading rate, or UV dose, pH or AOP can improve pCBA removal. The Figure 4.8 shows pCBA removal with hBN#1 and hBN#2 catalysts. Unlike TiO$_2$, an increase in hBN#1 loading rate does not increase pCBA removal. Poorer removal for hBN#1 for pCBA removal could be due to the issue that was previously discussed in Figure 4.3 (i.e., agglomeration and clumping). Thus, with the higher hBN#1 loading, causes hBN to aggregate and accumulate, which minimizes both surface area and hence UV exposure, resulting in a poor pCBA removal with increased loading rates. However, hBN#2, which is less hydrophobic, and surface treated

(functionalized by manufacturer) can be well-mixed in the petri-dish but it settles down in the shallow petri-dish (Figure 4.13; will be further discussed below) with increase loading, even with constant magnetic-stirrer mixing. Yet, hBN#2 still found to have better performance on pCBA removal than to hBN#1 as shown in the Figure 4.8. hBN#1 performance becomes poorer with increased loading rate, whereas hBN#2 tends to improve overall removal with loading rates, but then decreases as the loading rates increases.

Effect of UV Dose
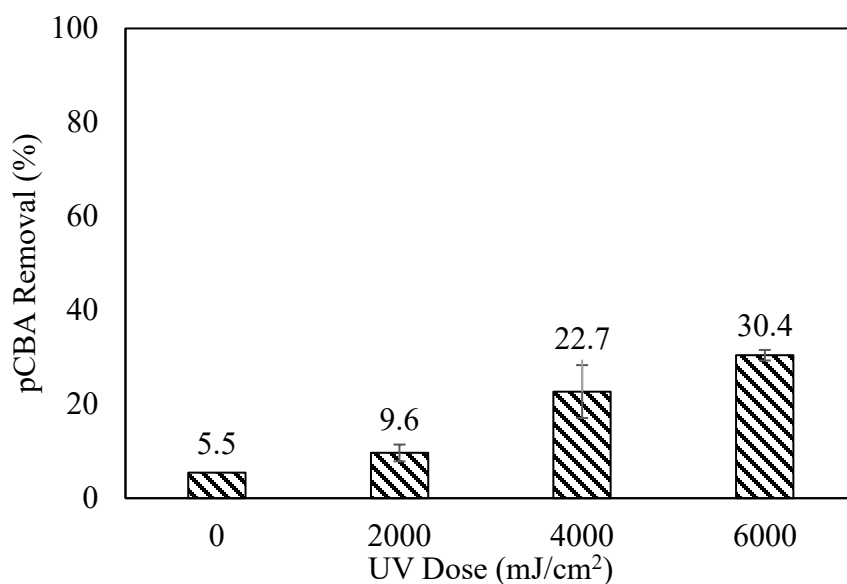
Figure 4.9 Effect of UV Dose (hBN#1) [Loading Rate: 2500 mg/L; pH 6.2]

Although all previous experiments with hBN#1 indicated its addition in the collimated beam (petri-dish) is not ideal for the pCBA removal due to its agglomeration, clumping and floating (Figure 4.3). Yet, the effect of UV dose for hBN#1 was still investigated as part of the study, is to verify if higher UV and other factors (discuss below) could improve overall the pCBA degradation. During this study, the effect of UV dose with hBN#2 was not investigated but assumed it would have better performance than hBN#1.

Figure 4.9 shows the effect of UV dose on hBN#1 for pCBA removal under a fixed loading rate of 2500 mg/L at ambient pH. This figure suggests that a higher UV dose can improve pCBA removal from 10% (at 2000 mJ/cm^2) to 30% (at 6000 mJ/cm^2).

Effect of pH
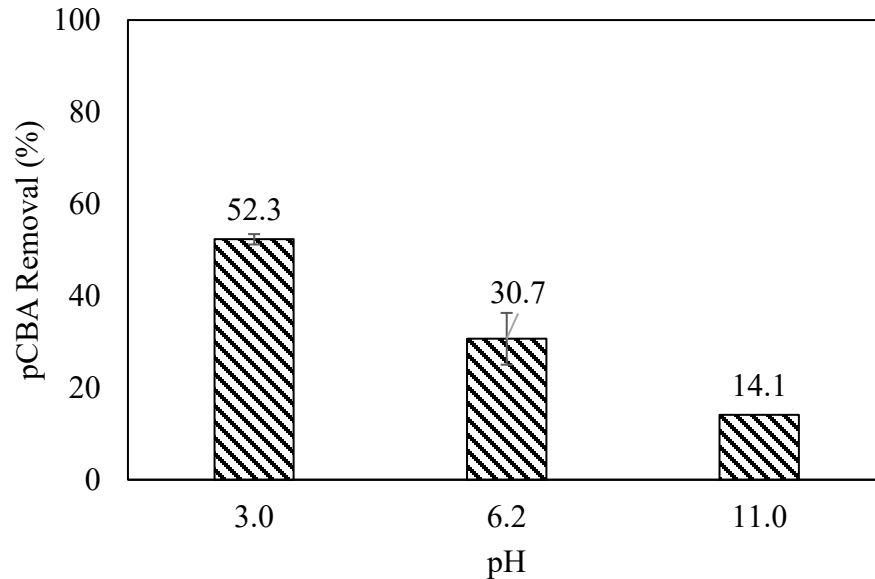
Figure 4.10 Effect of pH (hBN#1) [UV Dose: 4000 mJ/cm^2; Loading Rate: 2500 mg/L]

Next a series of tests were conducted for hBN#1 to study the effect of pH on pCBA removal. The Figure 4.10 shows pH seems to have a significant impact on hBN#1 performance on pCBA removal. Lowering pH from ambient pH condition to pH 3.0 significantly improves the hBN#1 performance from 30% at pH 6.2 to 52% at pH 3.0. Thus, lowering pH tends to provide an optimal environment for the hBNs (i.e., hBN#1). It may be because lowering the pH (i.e., pKa of hBN is around 2.8) allows hBN to become more positively charged to adsorb negatively charged pCBA. However, a higher pH of 11, hBN becomes less photo-catalytically active and becomes more negatively charged and tends to have an opposite effect on pCBA removal as shown in Figure 4.10.

Effect of Peroxide Addition
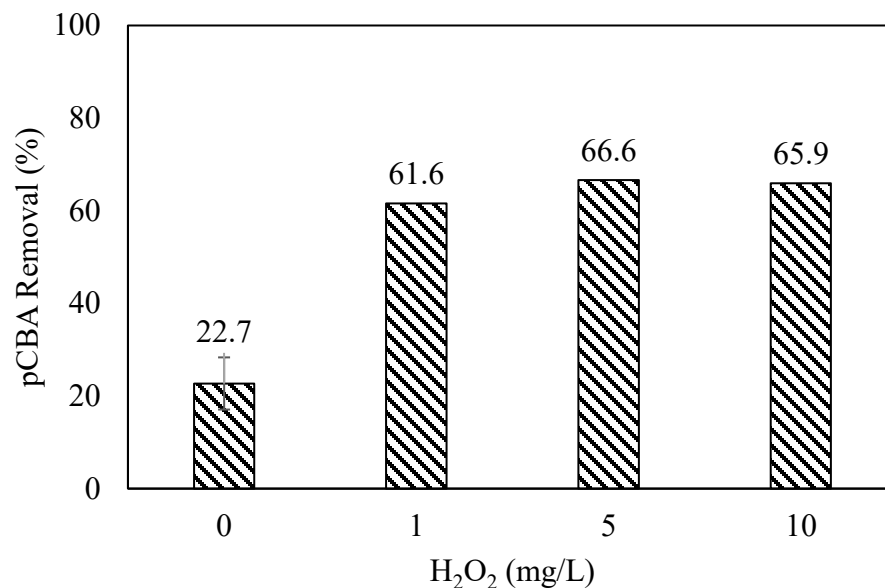
Figure 4.11 Effect of Peroxide Addition (hBN#1) [UV Dose: 4000 mJ/cm^2; Loading Rate: 2500 mg/L; pH 6.2]

The effect of peroxide addition was also investigated for hBN#1. Figure 4.11 shows H$_2$O$_2$ addition contributes positively to pCBA removal. However, adding a higher level of peroxide beyond 5 mg/L shows no additional benefit for pCBA removal. It may be because the hydroxyl radicals produced from peroxide addition formed in the bulk solution (homogeneous catalysis) may interfere with hBN photocatalytic reactivity (heterogeneous catalysis) or may interfere or occupy the active sites, which may result in a less adsorption of pCBA. These are only hypothesized but are beyond the scope of this study, still critical to provide much needed insights.

Overall, all these results suggest photolysis (i.e., without catalysts) is effective in pCBA removal. However, presence of hBN#1 slurry in collimated beam study, does not significantly improve pCBA degradation due to agglomeration and clumping. However,

lowering the pH to 3.0, increasing the UV dose, or adding peroxide (as AOP) improves

hBN#1 performance significantly from 30% to 60%. hBN#2 tends to be more favorable

since it does not aggregate or clumps as seen for hBN#1 but found to be difficult to keep it

suspended in the shallow depth petri-dish of the collimated beam setup.

4.2 PFOA Degradation

Next, a series of experiments were conducted in the collimated-beam setup, but this

time for removing PFOA using both TiO_2 and hBNs (i.e., hBN#1 and hBN#2) as catalysts,

as shown in Table 4.2. This table shows PFOA degradation under different catalyst types

(TiO_2 and hBNs), loading rates (500-10,000 mg/L), applied UV dose (ranging from 2000

to 11,000 mJ/cm^2), pH (3.0-11.0) and addition of hydrogen peroxide (H_2O_2) (as AOP) for

PFOA removal.

Both hBNs (i.e., hBN#1 and hBN#2) were used in this study. The concentration of

PFOA in the water sample was at 25 ppm level (which is around 60 uM) and measured by

HPLC as discussed in Chapter 3.

Table 4.2

Experiment Matrix for PFOA

PFOA Degradation	Exp #	Catalyst	Catalyst Dose (mg/L)	UV Dose (mJ/cm^2)	pH	H$_2$O$_2$ (mg/L)
Effect of Photolysis	1	None	0	4000	6.2	None
Effect of Adsorption	2	hBN#2	2500	0	6.2	None
Effect of Loading Rate	3-7	TiO$_2$	500-1000-2500-5000-10000	4000	6.2	None
	8-12	hBN#2	500-1000-2500-5000-10000	4000	6.2	None
Effect of UV Dose	13-16	hBN#1	2500	2000-4000-6000-8000	6.2	None
	17-21	hBN#2	2500	2000-4000-6000-11000	6.2	None
Effect of pH	22-24	hBN#2	2500	6000	3.0-6.2-11	None
Effect of Peroxide Addition	25-27	hBN#2	2500	4000	6.2	1-5-10
Optimal Condition	28-29	hBN#2	2500	11000	3.0	0-10

All samples were prepared in nanopure water. Experiment #1 (Table 4.2) is conducted first to see the effect of photolysis (without catalyst) and then experiment #2 is followed (dark), to see the effect of adsorption with hBN#2. Most of the study for PFOA removal was investigated with hBN#2 over hBN#1, as it was found to be more difficult to suspend. Yet, assessed to see if the pCBA degradation could be further improved for few

selected experiments using with both hBNs (hBN#1 and hBN#2) and compared for PFOA degradation.
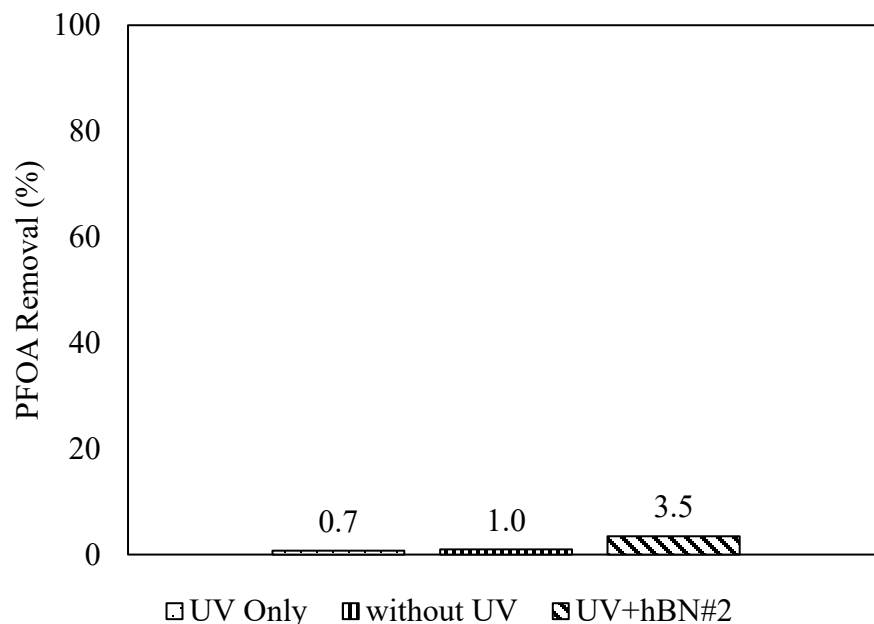
Figure 4.12 Effect of Photolysis and Adsorption [UV Dose: 4000 mJ/cm^2 (67 min); Loading Rate: 2500 mg/L; pH 6.2]

Figure 4.12 shows, no significant PFOA degradation ($< 3\%$) using hBN#2 at fixed UV dose of 4000 mJ/cm2 at loading rate of 2500 mg/L at pH 6.2. This result also suggests, unlike pCBA (which showed $> 50\%$ or higher removal at ambient pH condition), hBN#2 is found to be ineffective for PFOA degradation. This figure also shows, unlike pCBA, UV cannot photolyze PFOA (at UV dose of 4000 mJ/cm^2). Additionally, this figure also suggests, hBN#2 addition does not improve PFOA removal. Previously, hBN#2 was noted to settles in the petri-dish, even under constant mixing and resulted in moderate to poor removal. Overall, it could be concluded, the collimated beam setup is nonideal for hBN photocatalyst for the degradation study. Although, hBN#1 performance for pCBA removal

was shown to improve by lowering the pH (pH 3.0) or improved slightly with peroxide addition. A similar, approach is taken here for the PFOA degradation, but using hBN#2, to assess any variation in loading rate (mg/L) or altering the pH condition, higher UV dose, or peroxide addition (mg/L) may improve PFOA degradation. However, it is important to note here, hBN#2 although causes less agglomerate, clumping as hBN#1, but it is challenging to suspend it in the collimated beam's (shallow) petri dish even with constant stirring, as shown in Figure 4.13.
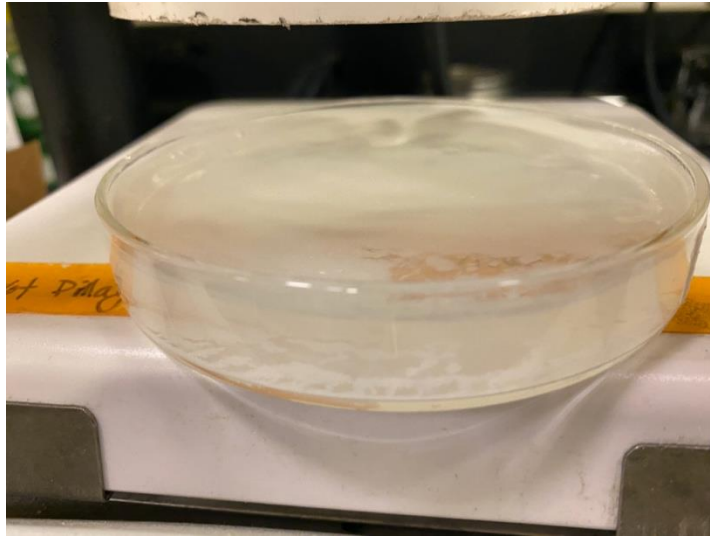
Figure 4.13 hBN#2 Settle Down at the Bottom of the Petri-dish

Effect of Loading Rate
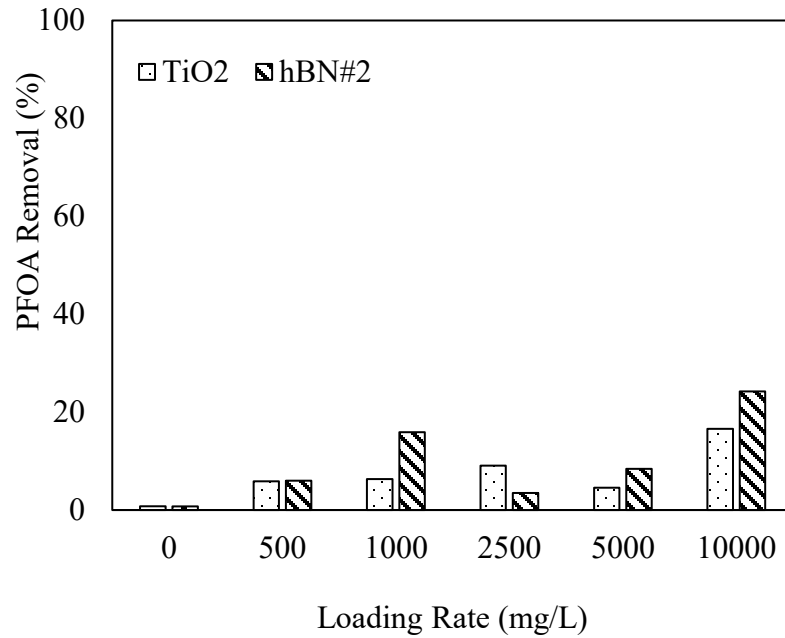
Figure 4.14 Effect of Loading Rate [UV Dose: 4000 mJ/cm^2; pH 6.2]

Figure 4.14 shows PFOA degradation using both of TiO$_2$ and hBN#2. Both were found to be less to moderately effective for PFOA degradation under collimated beam study (i.e., shows photolysis in ineffective). Between TiO$_2$ and hBN#2, this figure shows hBN#2 is found to be more effective to TiO$_2$ in PFOA degradation, although the removal ranges are low and varied from 1-16%, as shown in Figure 4.14. Based on these results, it could be suggested hBN tends to be more effective to TiO$_2$ for PFOA removal. All experiment listed on the Table 4.2, i.e., lowering pH or increasing the UV dose (mJ/cm^2) or addition of peroxide are still investigated as part of the study to improve hBN performance in PFOA degradation.

Effect of UV Dose
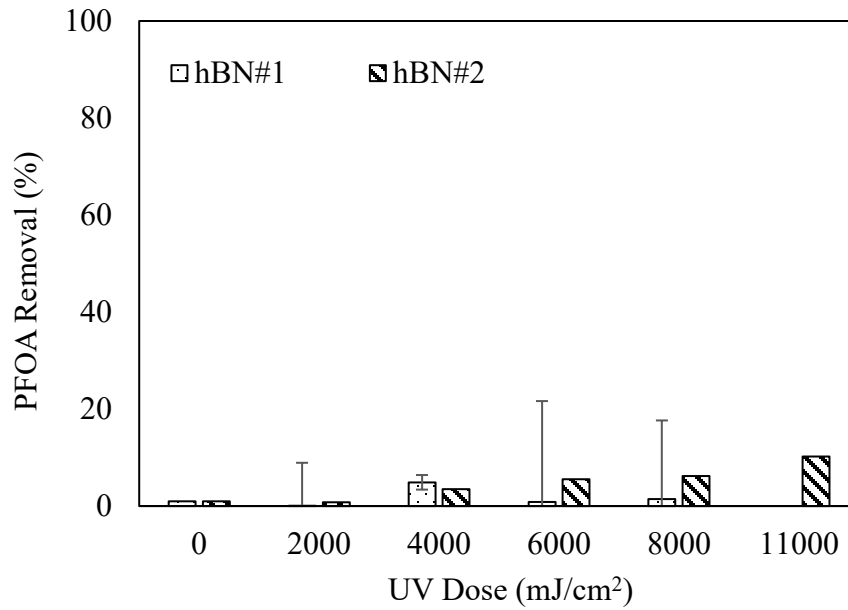
Figure 4.15 Effect of UV Dose [Loading Rate: 2500 mg/L; pH 6.2]

Increasing or decreasing the UV dose did not improve PFOA removal for both of hBN#1 and hBN#2 under ambient pH condition, as shown in Figure 4.15, the removal remains low even at significantly higher UV dose of 11,000 (mJ/cm^2). Between the two hBNs, hBN#2 is again found to be slightly more effective in PFOA removal. However, the removal is still poor (1-10%) using hBN#2. The aggregation of hBN#1 and floating/clumping on the surface prohibited the light in the petri-dish, may resulted in poor performance. While hBN#2, settles down and cannot be fully suspended in shallow petri-dish, may also have resulted in poor PFOA removal, overall, in spite of high UV dose under ambient pH condition, this treatment condition was found not to be favorable for PFOA degradation.
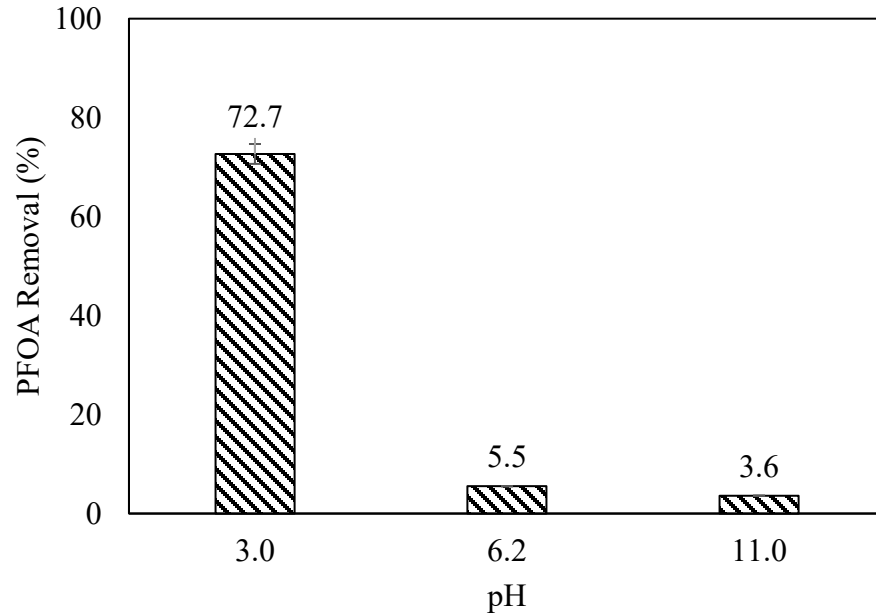
Figure 4.16 Effect of pH (hBN#2) [UV Dose: 6000 mJ/cm^2; Loading Rate: 2500 mg/L]

Yet, a series of tests were conducted for hBN#2 to investigate the effect of pH on PFOA removal. The pH was found to have a profound impact on PFOA removal, increasing the removal from low 5% at ambient pH to as high as 73% at pH 3 condition and under a higher UV irradiance (6000 mJ/cm^2). It was also demonstrated previously that lowering the pH tends to help hBN with pCBA degradation. Similarly, lowering pH here, also tends to improve hBN#2 performance in PFOA degradation. Thus, it could be concluded under acidic conditions, hBN tends to be more effective and can remove a higher amount of PFOA through photocatalytic degradation.

Effect of Peroxide Addition
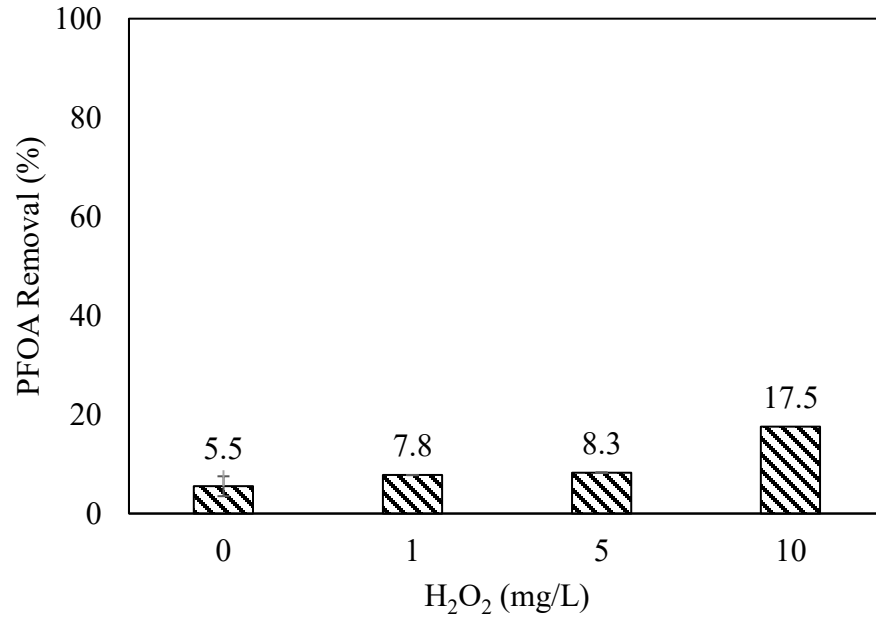
Figure 4.17 Effect of Peroxide Addition (hBN#2) [UV Dose: 6000 mJ/cm^2; Loading Rate: 2500 mg/L; pH 6.2]

The effect of peroxide addition in presence of UV for PFOA removal by hBN (under ambient pH), is investigated. It shows a slightly positive impact of H_2O_2 addition under ambient pH, with a slight improvement (12-15%) on PFOA degradation. The removal efficiency increases slightly with the increase of H_2O_2 addition. The optimal H_2O_2 dose is around 10 mg/L. However, this removal was not as drastic as the lower pH condition, as seen above (Figure 4.16), which improved PFOA degradation significantly.

Optimal Condition
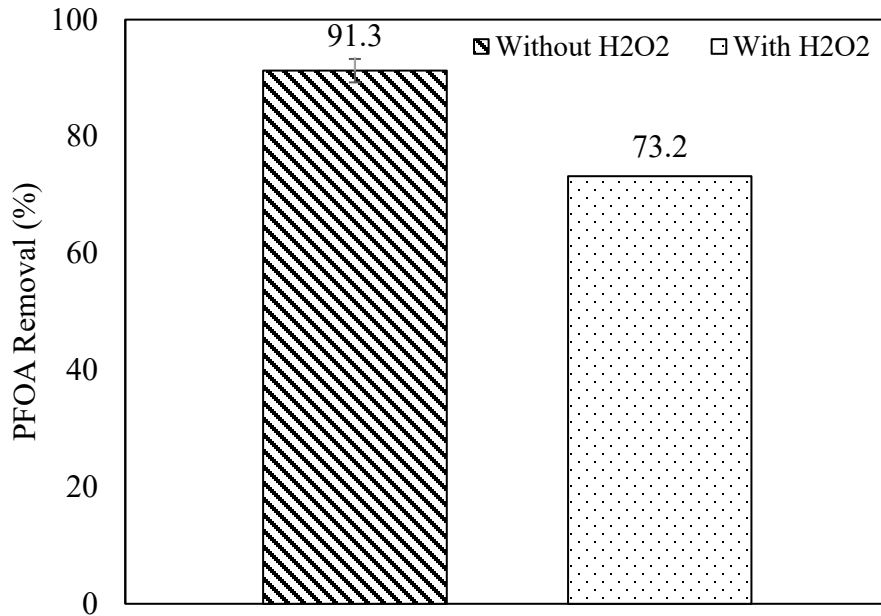
Figure 4.18 PFOA Degradation under Optimal Condition (hBN#2) [Loading Rate: 2500 mg/L; UV Dose: 11000 mJ/cm^2; pH 3.0; H_2O_2 Dose: 10 mg/L]

Next, an additional experiment was conducted, but under optimal condition to increase overall PFOA degradation. The condition is selected based on above PFOA degradation results, i.e., lowering the pH (to pH 3.0), further increasing the UV dose of 11,000 mJ/cm^2, (although this UV dose is considered to be too high but applied to assess performance), along with adding peroxide dose (10 mg/L) in improving PFOA degradation. Under such optimal condition, it was found PFOA degradation could be significantly improved to 91% for hBN#2 but occurs in absence of peroxide. In presence of peroxide, the removal is still high (73%), but lesser than to without peroxide. A slightly lower removal due to H_2O_2 addition and under higher UV irradiation is unclear. AOP tends to be considered as homogeneous catalysis, where OH• radical formation occurs within the bulk

solution, whereas the photocatalytic process, the OH• radical formation occurs on catalyst surface, i.e., surface mediated process (heterogeneous). Probably formation OH• in bulk, could be less conducive to PFOA degradation, needed to be further investigated. Nevertheless, a 73% to 91% PFOA reduction at lower pH (pH 3.0) with and without peroxide addition, respectively at significantly elevated UV dose, is promising result for PFOA/PFAS, may be difficult to practice at field setting or maybe cost prohibitive (pH lowering at pretreatment and increasing at post treatment, along with higher UV dose), but is noteworthy to mention, especially for PFOA destruction (with limited available treatment options).

4.3 Comparison of Catalysts

The photocatalytic degradation of pCBA and PFOA in the collimated beam provided some added insights to the photocatalyst. The E_{EO} value are not reported for the collimated beam but will be reported for the larger reactors (Chapters 5 and 6). All two catalysts type (i.e., TiO_2, hBN#1 and hBN#2), under the same condition were compared here for comparison in pCBA degradation, as shown below.
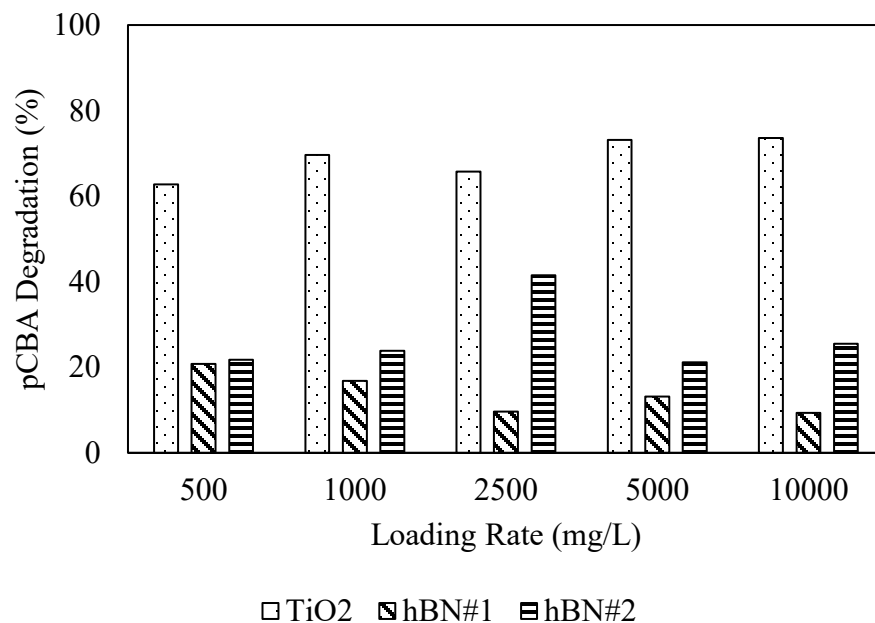
Figure 4.19 Comparison of pCBA Degradation at Collimated Beam [pCBA Concentration: 1 ppm; UV Dose: 2000 mJ/cm^2; pH 6.2]

The Figure 4.19 shows all three catalysts, a side-by-side comparison under variable loading rates. It shows pCBA degradation with TiO_2 increases from 63% to 74% with increase in loading rate (50% removal to occur by photolysis alone). This figure also shows the effect of loading rate for both hBN#1 and hBN#2 for pCBA removal. Unlike TiO_2, there are no trend on hBN loading rate for pCBA removal. Overall, TiO_2 was found to be more effective than hBN under neutral pH condition at the collimated beam.
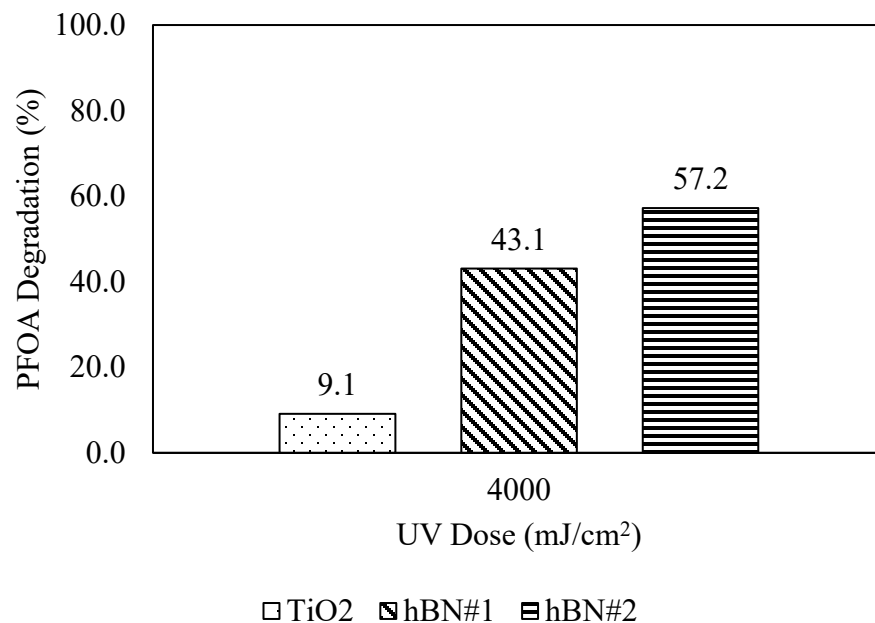
Figure 4.20 Comparison of PFOA Degradation at Collimated Beam [PFOA Concentration: 25 ppm; Loading Rate: 2500 mg/L; pH 3.0]

The Figure 4.20 shows PFOA degradation by all three catalysts under same UV dose of 4000 mJ/cm^2 and pH of 3.0. PFOA degradation is highest for hBN#2 under reduced pH condition and shows it has a profound impact on PFOA degradation. This figure also shows hBN#1 performance to hBN#2 under the lower pH condition, showing hBN#2 performed better than hBN#1. Both of hBN#1 and hBN#2 are equally difficult either to mix and keep them suspended in the collimated beam setup, but lowering the pH tends to improve its overall performance.

4.4 Conclusions

The overall conclusion drawn from this chapter on the collimated beam (bench-scale) study is multifold. First, it shows a small-scale setup, such as collimated beam is a good tool in screening catalysts and assessing treatment conditions. It conveniently uses only a small volume of sample (120-mL) and can effectively show the differences in

catalysts performances before the larger-scale (testbed or pilot) studies are to be conducted. This study also shows mixing issues and/or differences remains, between TiO_2 to hBNs in the collimated setup, which may (may not) be faced in the larger system (yet to be investigated) if not adequately mixed or addressed. It also shows the differences between the TiO_2 and hBNs performance in pCBA and PFOA removal which can differ significantly. The study shows changing the catalysts loading rates or altering the pH or increasing the UV dose or adding hydrogen peroxide – all can have positive or negative or no effect at all, based on the contaminants assessed as part of the screening. This study also provided some of these valuable insights of these photocatalysts and their expected outcomes before testing at other treatment scales (e.g., testbed and pilot) for both pCBA and PFOA degradation.

Between the pCBA and PFOA, above results also show the catalyst uptake (adsorption) of contaminants (pCBA and PFOA) is low (<5%) in absence of UV light (dark). However, it was shown that pCBA tends to easily photolyzed (50%) under UV light without requiring any catalysts (TiO_2 or hBN) addition, whole PFOA cannot be photolyzed. However, adding the catalyst (particularly TiO_2) to UV irradiation, photocatalytically improves the pCBA degradation. Between pCBA and PFOA, the later (i.e., PFOA), as mentioned above, was found to be more difficult to photolyze ($< 5\%$) (in absence of catalysts) or removed in presence of catalyst. Unlike TiO_2, hBN was found to be very difficult to disperse or mixed in solution of the shallower petri-dish, especially it was more difficult to mix, particularly for hBN#1 to hBN#2, but again hBN#2 is more difficult to suspend. These observations suggest unfavorable condition in testing hBNs in the collimated beam setup. Yet, with all these difficulties, hBN was still investigated at

48

collimated beam study, to investigate the effect of increasing the UV dose, lowering pH (from ambient to pH 3.0) and adding hydrogen peroxide in assessing degradation. The pH was shown to have much profound impact on both hBNs (i.e., hBN#1 and hBN#2) to TiO_2 for both pCBA and PFOA degradation. Also, it shows increasing the UV dose significantly (11,000 mJ/cm^2, which may be difficult to apply) and lowering pH can improve PFOA degradation but its implication with cost-benefit analysis needed to be carefully assessed. All these insights are helpful for both pCBA and PFOA (and PFAS) photocatalytic degradation and will be relevant to larger scale studies. All of this information will provide benefit in assessing these catalysts at the testbed (upflow photoreactor in Chapter 5) and commercial pilot-scale photoreactor (Photo-Cat system in Chapter 6), yet to be assessed and will of further discussion in the next chapters.

CHAPTER 5

DEGRADATION OF PARA-CHLOROBENZOIC ACID AND PER-FLUOROOTANIC

ACID WITH TESTBED SETUP (UPFLOW PHOTOREACTOR)

This chapter mainly focuses and discusses the effectiveness of the upflow photoreactor (Figure 3.2) and slurry-based upflow photoreactor (Figure 3.3) (at testbed-scale) in removing methyl orange (MO) by using TiO_2 coated sands and later pCBA and PFOA removals at the upflow slurry-based photoreactor, respectively using both TiO_2 and hBN as slurry.

The upflow photoreactor (Figure 3.2) was first modified by adding a recirculation pump to increase contaminant's contact time within the photoreactor and tested using methyl orange (MO) only for its initial assessment. Later, this upflow photoreactor was further modified to a slurry-based photoreactor (Figure 3.3) to use catalyst directly as a slurry (e.g., TiO_2 and hBN) without requiring coating onto the sand particles for removing pCBA and PFOA, respectively.

Effect of recirculation for the Upflow Photoreactor

The addition of the recirculation pump (Tuthill PM8014) to the upflow photoreactor increased the contaminant contact time within the reactor and was studied for MO removal using TiO_2 coated sand (as catalyst) at loading rate of 250 g/L (1% wt. as TiO_2, i.e., 2500 mg/L as TiO_2). The required feed flow rate, which includes both incoming feed flow plus the recirculation flow was targeted to be maintained around 4 L/min, which is targeted in order to achieve 50% fluidized bed in the photoreactor. This 50% catalyst fluidization to the total photoreactor height provided some added benefits, provided oxidation of targeted

contaminants within the catalyst bed, while the clear water column sitting above the bed (with no catalysts) provided disinfection (due to UV lamp irradiation).

The targeted flowrate (4 L/min) to maintain 50% fluidization, is based on the sand particle size (180-220 um) and density (2.2 g/cc) assessed by previous modeling effort (Ergun equation). A lower flow rate < 4 L/min, will decrease the bed height (collapses) while a higher flow rate will expand the bed height that can also result in both lowering the bed density (thinning) and can also result in catalyst loss, respectively, thus was avoided. The targeted flow rate (4 L/min) was maintained in the upflow photoreactor, either solely by incoming feed flowrate (with no recirculation) or by combining the incoming flowrate with recycling/recirculation flowrate. Lowering the incoming feed flowrate while increasing the recirculation rates to maintain the targeted flowrate (4 L/min), increases the contaminant contact time within the reactor, allowing a typical 15-second contact time (with no recirculation) to an increased 50 seconds contact time (nearly a minute), which is a nearly 4-fold increase in contact time, as shown in Figure 5.1
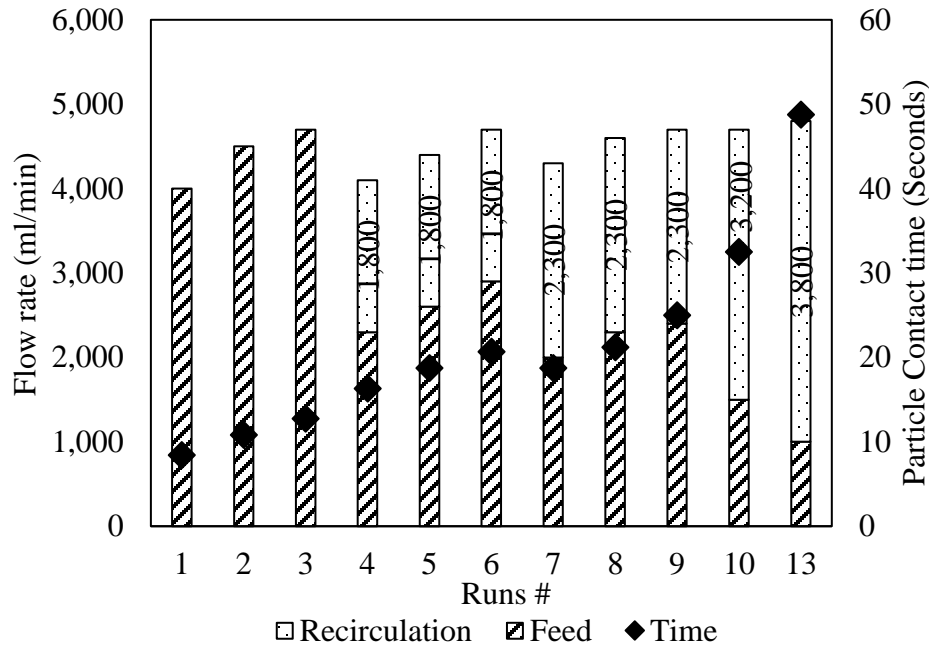
Figure 5.1 Effect of Recirculation

Methyl Orange (MO) degradation by Upflow Photoreactor
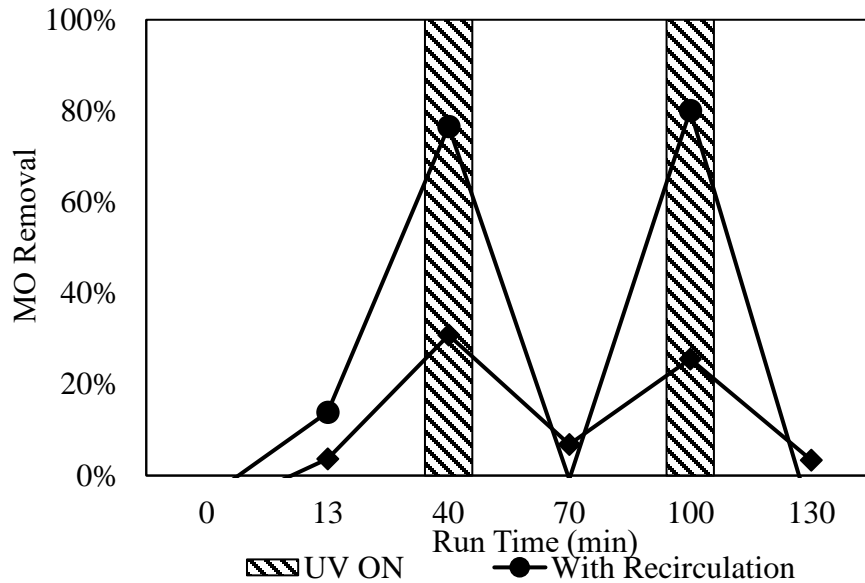
Figure 5.2 Effect of Recirculation on MO Removal [MO Concentration: 0.09 ppm;

Loading Rate: 2500 mg/L; pH 7; Water Type: tap water]

The methyl orange (MO) with and without recirculation, i.e., under increased

contact time (11 seconds *versus* 22 seconds; similar to run#8, as shown in Figure 5.1) was

investigated in the upflow photoreactor using TiO_2 coated sand for MO removal at loading rate of 250 g/L (1% wt. as TiO_2, i.e., 2500 mg/L as TiO_2) and under ambient pH condition. Above figure (Figure 5.2) shows, significantly higher amount of MO reduction from 25% to around 80% by recirculation. Thus, increasing the MO contact time to even higher contact (i.e., increasing the recirculation rate higher contact time, such as run# 10 or #13 as shown in Figure 5.1) will result in even greater MO degradation.

During this period of TiO_2 coated sand particle (as catalyst) assessment at the upflow photoreactor was realized, i.e., unlike TiO_2, which can easily be coated onto the sand particles, the hBN photocatalysts could not be coated onto the sand particles. Several different coating protocols were tried (calcination) to coat hBN onto the sand particles (and other substrates) at Rice University by following the same protocol as of TiO_2, but hBN failed to be coated onto the sand particles. The hBN peeled off easily from sand particle and would not fuse or stick to the sand particles during calcination or it use. As hBN could no longer be successfully coated onto the sand particles, an alternative option to introduce the catalysts to photoreactor was investigated. Alternative option was chosen, to introduce catalyst directly to the upflow photoreactor as slurry, such that both catalysts (i.e., TiO_2 and hBN) could be introduced similarly and can be compared equally. Which meant the current upflow photoreactor (Figure 3.2) could no longer be used, especially for hBN utilization and thus the photoreactor was modified one more time and was converted to a slurry-based upflow photoreactor (Figure 3.3) by primarily altering the feed pump (from gear pump to multi-stage centrifugal pump) for its operation.

Upflow (slurry-based) photoreactor

After modification of the upflow photoreactor to upflow slurry-based photoreactor, it was assessed for both pCBA and PFOA degradation. Around 7-L of spiked water (deionized water, DI) sample is used, spiked either with 5.0 ppm (30 uM) and 35 ppm (85 uM) ppm of pCBA or PFOA, respectively, were evaluated. The upflow slurry-based photoreactor was operated in batch-mode (but if needed could also be operated under continuous mode), where the slurry is separated and recycled back into the photoreactor by using a ceramic membrane in 10-inch filter housing (Figure 3.3). As mentioned in Chapter 3 (section 3.1.2), the gear pump for the upflow photoreactor was replaced with a larger multi-stage centrifugal pump, which can circulate slurry without damaging the pump or the catalyst as particles/powder during its operation.

Sample is fed into the upflow photoreactor (priming) using small feed pump (Tuthill PM8014) before the run to fill the photoreactor fully and its ancillary piping and the ceramic filter housing (Figure 3.3) for batch-scale operation. A tubular low-pressure (LP) UV lamp (same as the upflow reactor) is used, located at the core of the reactor to provide 1000 uW/cm^2 (or 1 mJ/sec-cm^2) of UV-C exposure. This irradiance value is used with the exposure time (min) to attain targeted UV dose (mJ/cm^2).

To assess the effect of UV dose (mJ/cm^2), the spiked water sample is constantly circulated and mixed using the multi-stage centrifugal pump in the presence or absence (dark) of the UV light with the catalyst as slurry. A blank and dark sample is collected, in presence of UV light (without catalysts) only, and in absence of UV light, but with catalyst only (dark). Both were run for similar run length (minutes) to attain the targeted UV dose (mJ/cm^2). This is to determine the contaminant degradation by the photolysis or adsorption

(only), respectively and compared against the UV irradiance in presence of catalyst (i.e., photocatalysis). The following discusses these results.

5.1 pCBA degradation

Deionized (DI) water was used for slurry reactor experiments using both TiO_2 and hBN as catalyst. Initially, experiment #1 (Table 5.1) was contacted before conducting other experiments as listed on this table to assess the effect of photolysis (without catalyst) in the upflow slurry reactor for pCBA degradation.

Table 5.1

Experiment Matrix for pCBA

pCBA Degradation	Concentration (ppm)	#	Catalyst	Catalyst Dose (mg/L)	pH	H_2O_2 (mg/L)
Effect of Photolysis	5	1	None	0	7	None
Effect of Loading Rate		2-3	TiO_2	500-1000	7	None
Effect of pH		4-6	TiO_2	1000	3-7-11	None
		7-8	hBN#1	1000	3-7	None

Experiment #1 was conducted first (Table 5.2) as mentioned above, to assess the effect of photolysis (without the catalyst), then a series of other experiments were conducted as shown on this table.
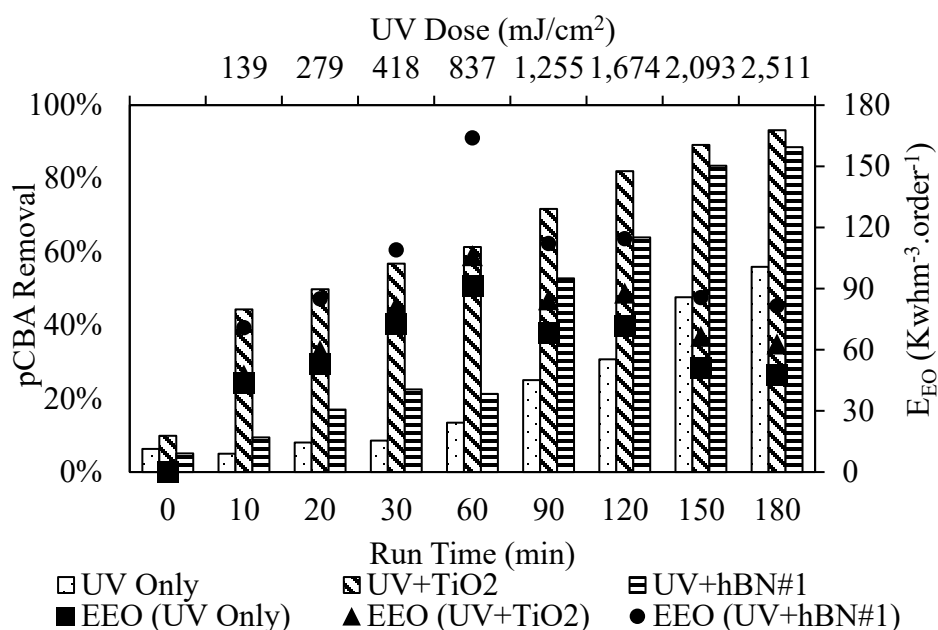
Figure 5.3 Effect of Photolysis [pCBA Concentration: 5 ppm; Loading rate: 1000 mg/L; pH 7]

Figure 5.3 shows, the slurry-based upflow photoreactor performance for pCBA degradation under UV (photolysis) irradiance and with TiO$_2$ and hBN#1 (as slurry) in the presence of UV light. The UV alone (photolysis) was found to be effective (50%) in pCBA removal, which is similar to what was observed previously in the collimated beam study. Although hBN#1 was found to aggregates and clump in shallow petri-dish in the collimated beam study resulting in poor to moderate removal, but it was not the case in the upflow slurry-based photoreactor. This could be due to the design of the photoreactor and of larger sample volume (7-L) with effective mixing due to the recirculation pump, thus avoiding the clumping and aggregation issue as of the collimated beam's shallow petri-dish This result also suggests, some of the issues that were found for the hBN#1 (in the petri-dish of the collimated beam study for pCBA removal) became less of an issue at the slurry-based

photoreactor. It shows significant amount pCBA removal (>85%) is achievable using hBN#1, as shown in the figure.

The figure also shows the system was operated for more than 2-hour to reach UV dose to about 2,500 mJ/cm^2, also shows the corresponding E_{EO} value with pCBA removal. Samples were collected over time which correspondence to corresponding UV dose (mJ/cm^2) as shown on the secondary (top) x-axis. This figure (Figure 5.3) shows, the effectiveness of TiO$_2$ and hBN#1 slurry result at ambient pH condition at catalysts loading rate of 1000 mg/L (as slurry). The TiO$_2$ slurry is found to be more effective (10-20%) than to hBN#1 for pCBA removal. This figure also shows, TiO$_2$ tends to be more effective to hBN#1 at UV dose less than 850 mJ/cm^2 as shown in Figure 5.3. However, as the UV dose increases (> 1000 mJ/cm^2) the differences between the two catalysts narrow. Although, a smaller amount of hBN (less than 5%) settled down in the ceramic filter housing bottom (and are trapped), as shown in Figure 5.4, which was mostly due to exit-port design/elevation in the bottom of filter housing.

This figure (Figure 5.3) also shows, pCBA could be effectively removed by photolysis (UV only) that can range from 5-50% with increase UV doses. Moreover, adding catalysts, such as TiO$_2$ and hBN#1, both increases the removal from 50% (photolysis) to 90% for TiO$_2$ addition, while hBN removal was similar, around 85% with increased UV dose, which is significantly higher than that of the collimated beam study, posing no significant mixing/settling issues of hBNs. This figure also shows the E_{EO} value significantly lower when the catalysts are used, from more than 90 kW/m^{-3}order^{-1} to less than 20 kW/m^{-3}order^{-1} with catalyst (at UV dose of 2500 mJ/cm^2). These E_{EO} values are reasonable and acceptable for photocatalytic degradation. Overall, these results show

although UV (photolysis) is effective for partial removal (maximum 50%) of pCBA, but adding catalysts has synergistic effect, improving the overall removal (85% -95%) due to formation of the OH• radical, that can further enhance pCBA removal. This is similar (synergistic) to what was found in the collimated beam study using TiO_2. Overall it shows pCBA removal by TiO_2 is higher over hBNs (at lower UV doses, however, narrows at higher doses), moreover this figure shows adding the catalysts reduces the E_{EO} value substantially.

Figure 5.4 hBN#1 Settle Down in the Housing.

Effect of Loading Rate
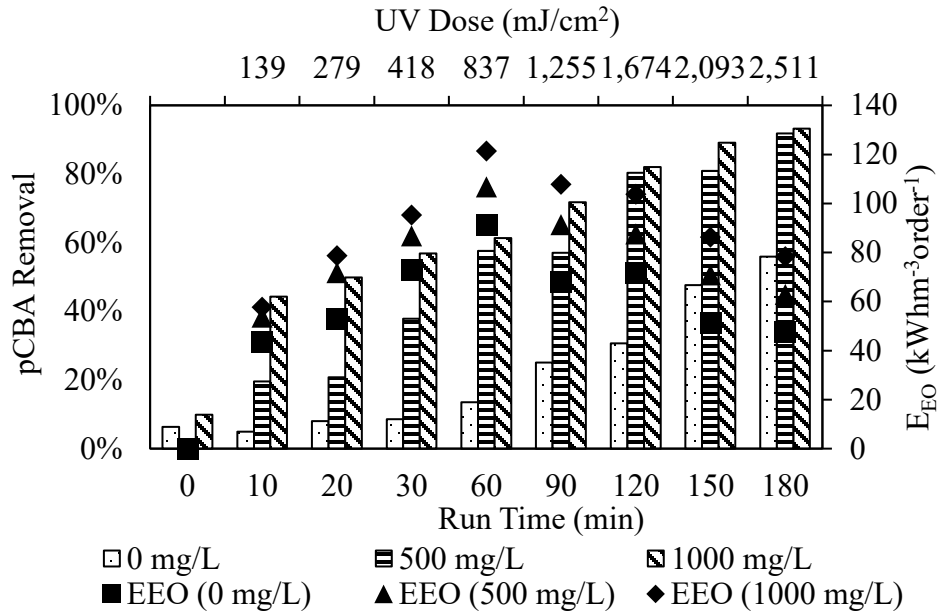
Figure 5.5 Effect of Loading Rate (TiO$_2$) [pCBA Concentration: 5 ppm; pH 7]

Next a series of tests were conducted at various TiO$_2$ loading rates (ranging from 0, 500 to 1000 mg/L) for pCBA degradation in the slurry-based photoreactor. This figure shows the loading rate has a positive effect on pCBA degradation. At lower UV doses (< 400 mJ/cm^2; shown on second x-axis), loading rates (500 *versus* 1000 mg/L) tends to have differences in pCBA removal, but at higher UV dose (> 1250 mJ/cm^2) the difference in loading rates narrows on pCBA removal. Photocatalysis, i.e., the addition of catalyst with UV, can further reduce E$_{EO}$ value from 90 to less than 20 kW/m^{-3}order^{-1}.

Effect of pH
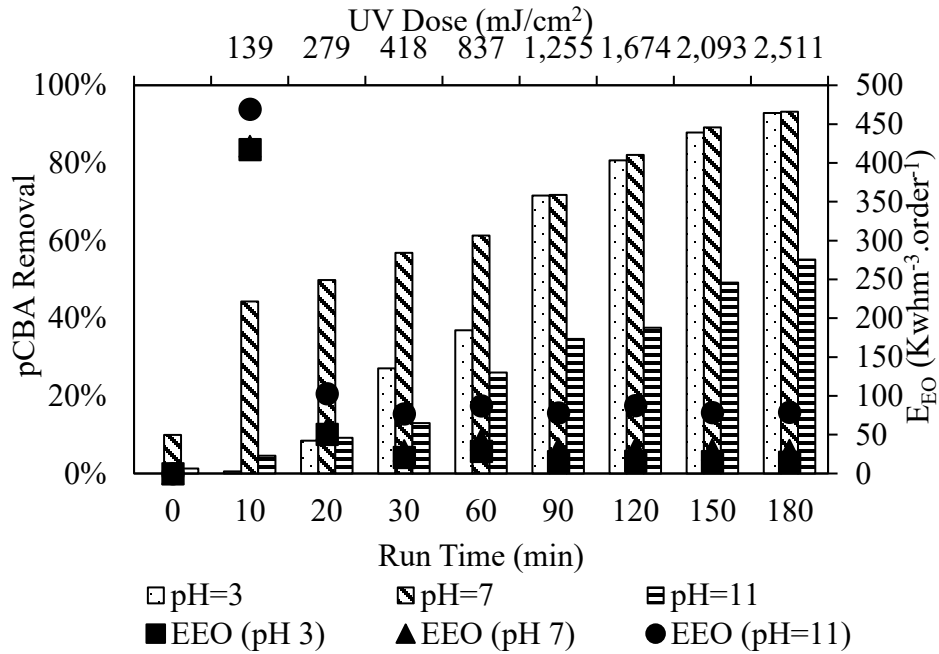
Figure 5.6 Effect of pH (TiO$_2$) [Loading Rate: 1000 mg/L]

Next, series of tests were contacted under various pH condition for TiO$_2$ slurry, ranging from pH 3 to pH 11, as shown in Figure 5.6. The results show TiO$_2$ is less affected by pH in pCBA removal at UV dose greater than 1000 mJ/cm2, where both pH 3.0 and pH 7.0 are equally effective, which is similar to what was found previously in the collimated beam study. However, pH 11 as shown in the figure, is found to be less effective in pCBA removal. The optimal pH for TiO$_2$ for CBA removal is at around neutral pH condition. This figure also shows, the E$_{EO}$ values tends to decrease at lower pH value. All of these are important findings in improving pCBA degradation and in reducing the energy requirements.
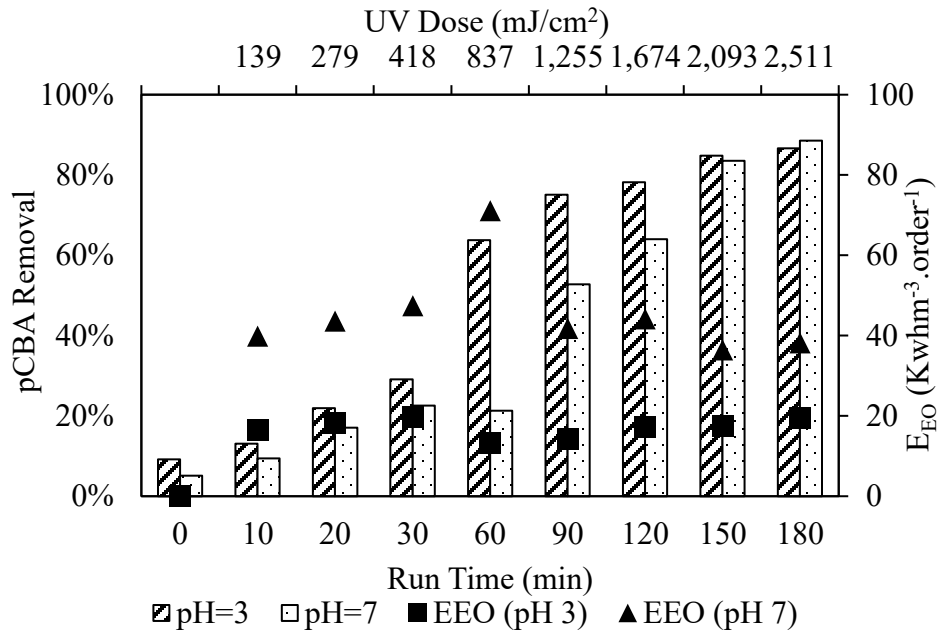
Figure 5.7 Effect of pH (hBN#1) [Loading Rate: 1000 mg/L]

Likewise, TiO_2 (Figure 5.6), the pH effect on pCBA removal, the hBN#1 was investigated as shown in Figure 5.7. This figure shows, unlike TiO_2 which is not sensitive to pH variation (acidic or neutral), hBN tends to be highly sensitive to pH. Its performance tends to be impacted, especially at UV dose below 1700 mJ/cm^2, but then the pH effect narrows at higher UV doses. The pH effect is like what was found in the collimated beam study, where lower pH played favorable role for hBN#1. Thus, lowering the pH to pH 3.0 along with higher UV dose >1700 mJ/cm^2 (for hBN#1), results in increasing pCBA degradation and lowering the E_{EO} values as shown on this figure.

5.2 PFOA degradation

Next a series of run were made on the upflow slurry-based photoreactor using TiO_2 and with hBNs (i.e., hBN#1 and hBN#2) for removing PFOA from 35 ppm (85 uM) spiked DI water.

Table 5.2

Experiment Matrix for PFOA

PFOA Degradation	Concentration (ppm)	#	Catalyst	Catalyst Dose (mg/L)	pH	H_2O_2 (mg/L)
Effect of Photolysis	35	1	None	0	7	None
Effect of Loading Rate		2-4	hBN#2	500-1000-2500	3	None
Effect of pH		5	hBN#1	1000	3	None
		6-8	hBN#2	1000	3-7-11	None
Effect of Peroxide Addition		9-11	hBN#2	1000	3	10
Optimal Condition		12-13	hBN#2	1000	3	0-10

We first conducted experiment #1 (Table 5.2) first to see the effect of photolysis (without the catalyst) then run other scenarios as listed in Table 5.2.
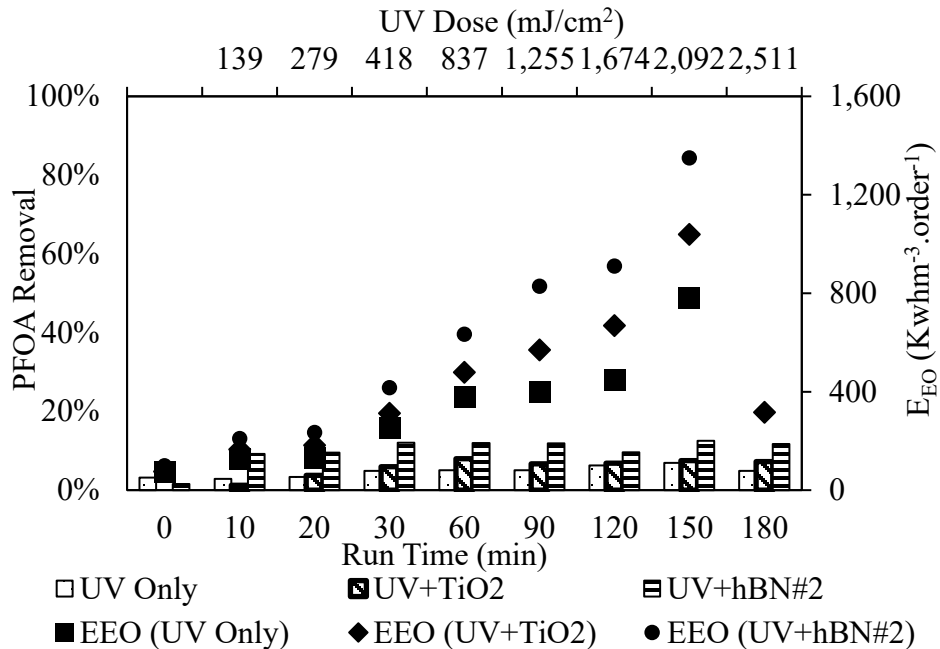
Figure 5.8 Effect of Photolysis [PFOA Concentration: 35 ppm; Loading Rate: 1000 mg/L; pH 7]

Unlike pCBA, PFOA degradation with photolysis with UV only (Figure 5.8) is found to be lower (<10%). This is due to PFOA's strong C-F bond, which makes it highly stable, recalcitrant and is difficult to degrade by photolysis. It is expected a higher UV irradiance is necessary with the photocatalysts to degrade PFOA.

In dark (without UV) both TiO_2 and hBN#2 can remove PFOA, but the removal remains lower (<10%), which is similar to what was found in the collimated beam study (Figure 4.1 and 4.12), mainly the removal is due to adsorption onto the photocatalyst. Between TiO_2 and hBN#2, the hBN#2 was found to be better in PFOA degradation (although the removal seems low < 10%, as shown in Figure 5.8), this is due to ambient pH condition run, may not be favorable for hBN for PFOA degradation based on the collimated beam study.

Effect of Loading Rate
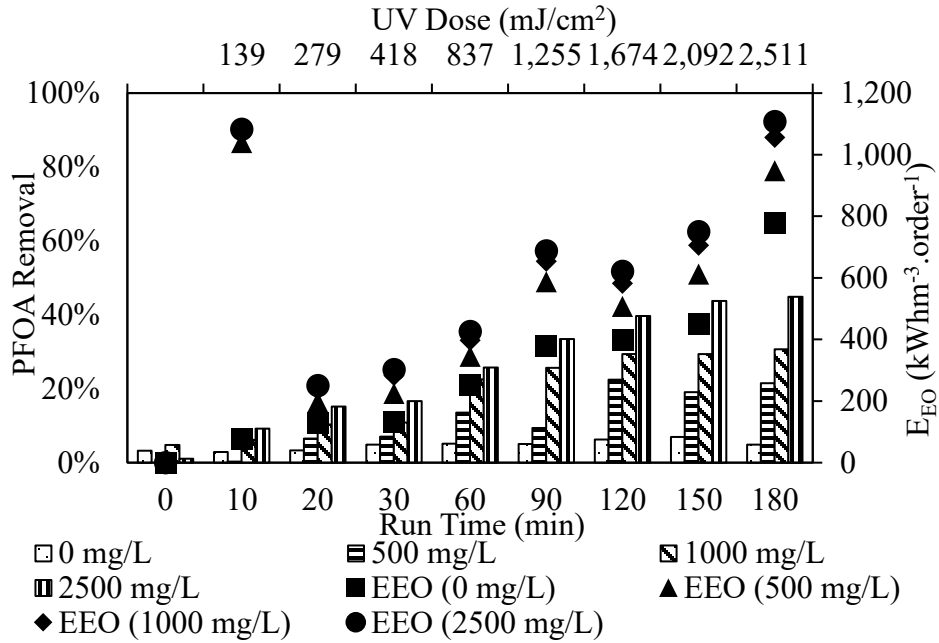
Figure 5.9 Effect of Loading Rate (hBN#2) [PFOA Concentration: 35 ppm; pH 3]

Next a series of run were made using hBN#2 but under different loading rates at pH 3. The increase in catalyst (hBN#2) loading rate (Figure 5.9) resulted in a higher amount of PFOA degradation due to the increase in the surface area of the hBN#2, which then can result in higher PFOA degradation. It shows higher loading can improve removal by an additional 10-15%. This figure also shows PFOA is difficult to remove by photolysis only, less than 5% of PFOA removal occurs by it (i.e., without hBN#2 loading). But adding hBN (with increasing loading rate), can improve its removal from 5% to 40%, while the optimal hBN#2 loading rate for PFOA degradation is around 1000 mg/L to 2500 mg/L ranges. This figure also shows E_{EO} for the different loading rates, suggesting the E_{EO} values lowers from 800 kW/m^{-3}order^{-1} for UV only to <100 kW/m^{-3}order^{-1} for the use of hBN#2, which is significantly higher than the pCBA degradation, meaning PFOA requires higher UV energy for its degradation.

Effect of pH
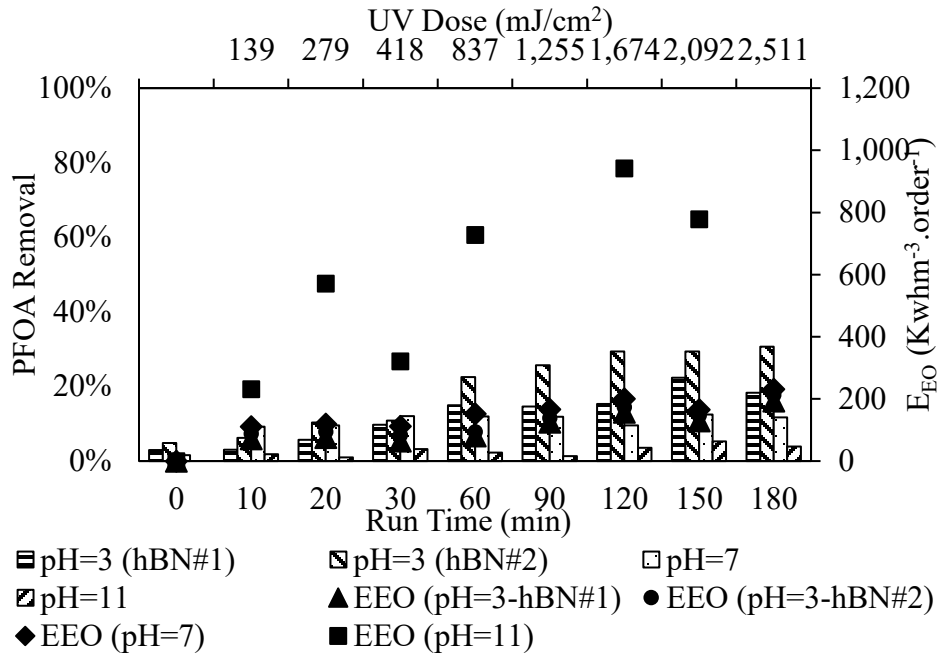
Figure 5.10 Effect of pH [PFOA Concentration: 35 ppm; Loading Rate: 1000 mg/L]

Next, the impact of pH on PFOA removal was investigated using hBN#2 in the upflow slurry-based photoreactor. The pH was varied from pH 3, pH 7 and pH 11. Both hBN#1 and hBN#2 were investigated. First, this figure shows PFOA tends to be more degraded at a lower pH (acidic) than at the alkaline pH condition (pH 11), similar to what was seen at the collimated beam study. Between the hBN#1 and hBN#2, hBN#2 is again found to be more effective than hBN#1 in PFOA degradation. Moreover, due better mixing capabilities within the photoreactor (compared to the collimated beam), resulted in a better PFOA degradation. Although, overall removal by hBN for PFOA remained low (30%) even with higher UV dose of 2500 mJ/cm^2 level, this removal is primarily due to photocatalysis (as oppose to photolysis).

Effect of Peroxide Addition
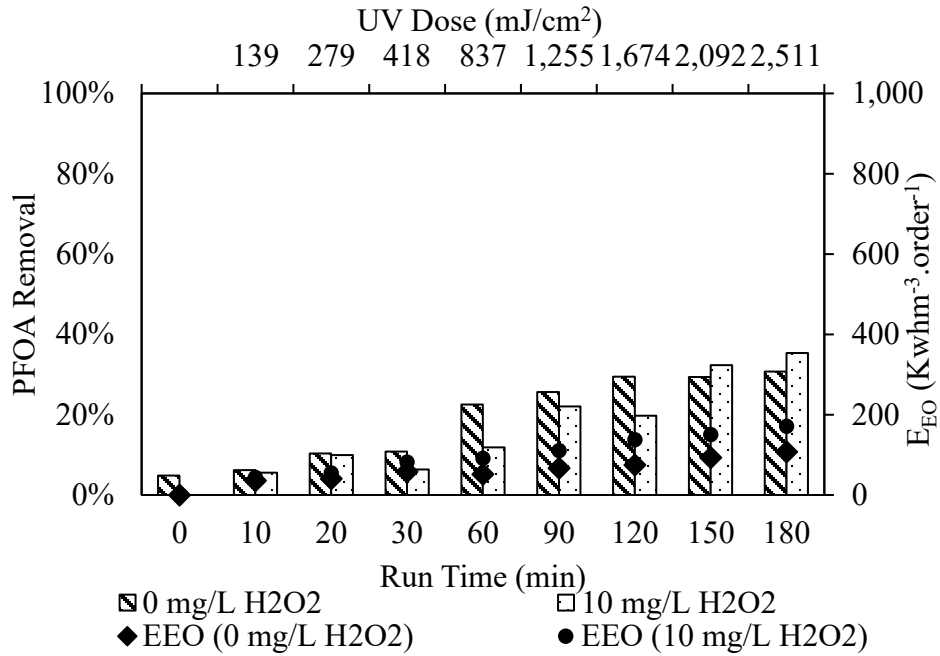
Figure 5.11 Effect of Peroxide Addition (hBN#2) [Loading rate: 1000 mg/L; pH 3]

The effect of peroxide addition on PFOA degradation by hBN#2 was also investigated. It shows a slight impact of H_2O_2 addition at pH 3 on PFOA degradation, with only ~5% improvement was observed, although a higher degradation was expected in presence of peroxide. However, PFOA degradation with peroxide still remains moderate at ranges 30-40%.

Optimal Condition
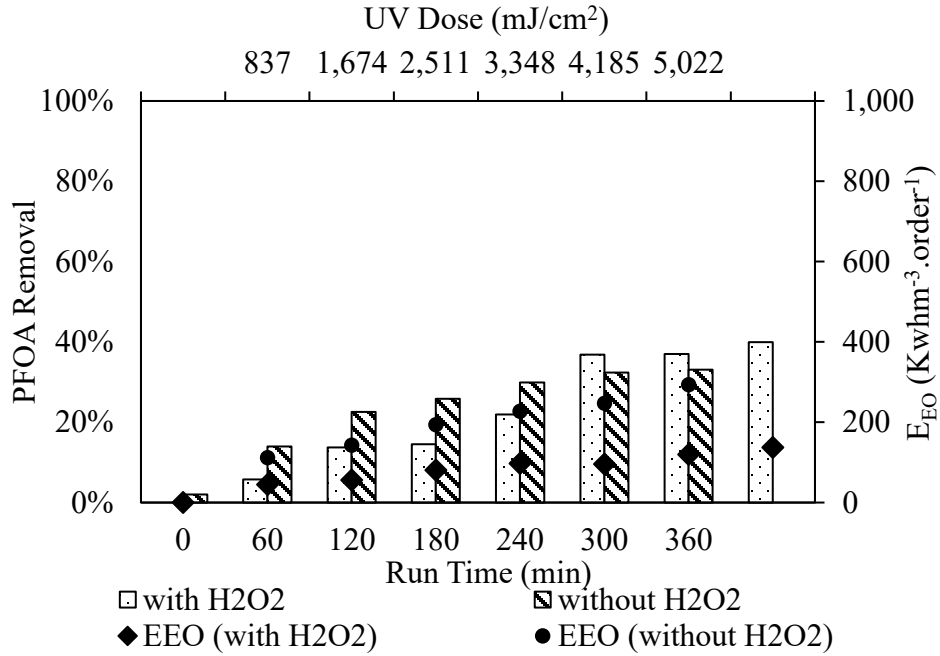
Figure 5.12 Optimal Condition (hBN#2) [Loading Rate: 1000 mg/L; pH 3]

Next, another series of run were made, but under increased UV dose (by increasing the overall run length from 3 hours to 6 hours). However, increasing the UV dose from 2511 mJ/cm^2 to a higher level did not increase PFOA degradation. It is important to note a significantly higher PFOA degradation (70-90%) was achievable at the collimated beam, but the UV dose (11,000 mJ/cm^2) was twice as much, but was not investigated at the upflow (slurry) photoreactor since it will require a much longer operational run. Suggesting a higher PFOA degradation could still be achievable at lower pH condition but with a significantly higher UV dose.

5.3 Comparison of Catalysts

The photocatalytic degradation of pCBA and PFOA were compared on side by side basis for the upflow (slurry) photoreactor. Below compare the degradation results and E_{EO} values among two catalysts (TiO$_2$, hBN#1 and hBN#2), all under similar treatment condition.
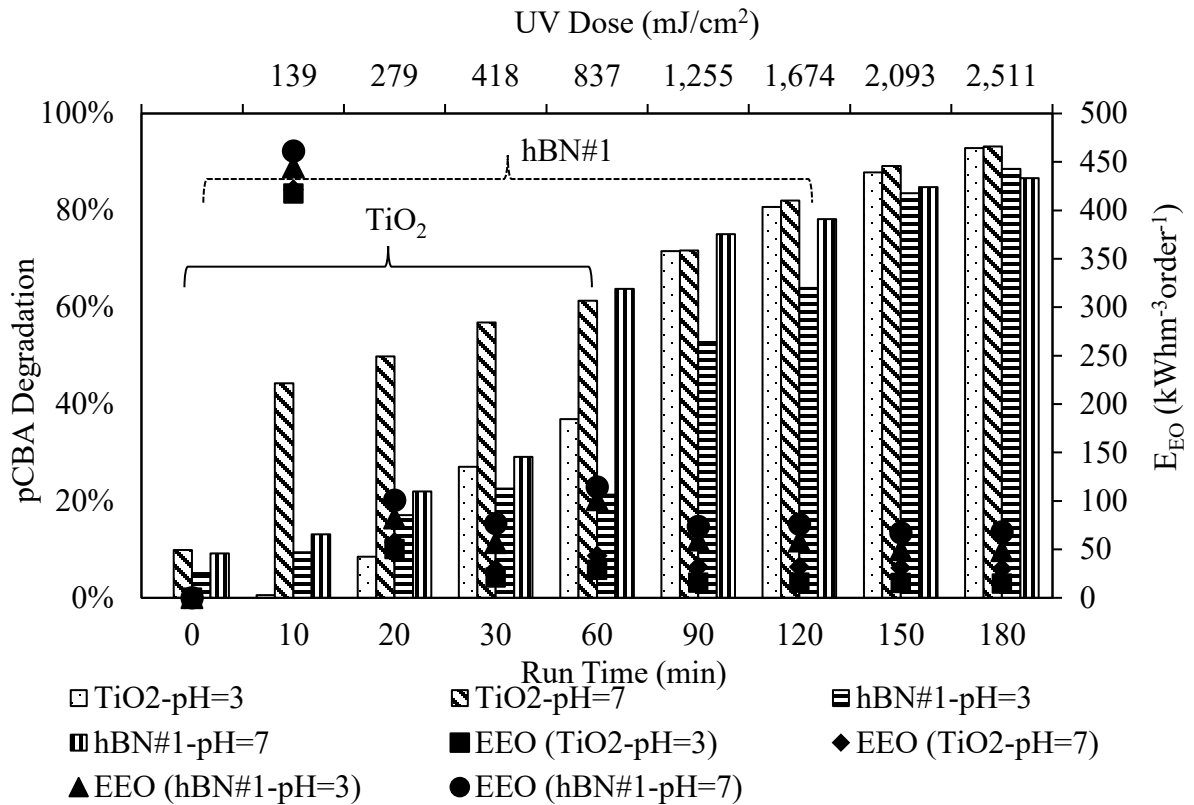
Figure 5.13 Comparison of pCBA Degradation at Slurry Photoreactor [pCBA Concentration: 5 ppm; Loading Rate: 1000 mg/L]

Above figure shows pCBA degradation with TiO$_2$ and hBN#1 at the upflow photoreactor under two different pH conditions (pH 3 versus pH 7). The figure shows pH tends to have an impact on pCBA degradation with TiO$_2$ up until 1000 mJ/cm^2 UV dose, but this difference narrows when the UV dose increases beyond ~1250 mJ/cm^2. At a UV dose of 2500 mJ/cm^2, there is no difference in pH, both are equally effective in degrading

68

more than 90% of pCBA. For hBN#1, the pH difference exists until a UV dose of ~1700

mJ/cm^2 and beyond that, the difference narrows. This figure suggests, unlike TiO$_2$, hBN#1

tends to have significant pH effect (lower pH better) at UV dose, although the difference

narrows at higher UV dose, which needed to be further investigated (to further study the

impact of pH to UV doses). Overall, TiO$_2$ and hBN both performed equally on pCBA

degradation (>90%) at final stage of the run. Both E_{EO} for TiO$_2$ or hBN#1 were reasonable

and less than 100 kWhm^{-3}order^{-1}, the values is lower for pCBA than to hBN. The E_{EO} value

will be discussed further in Chapter 7.
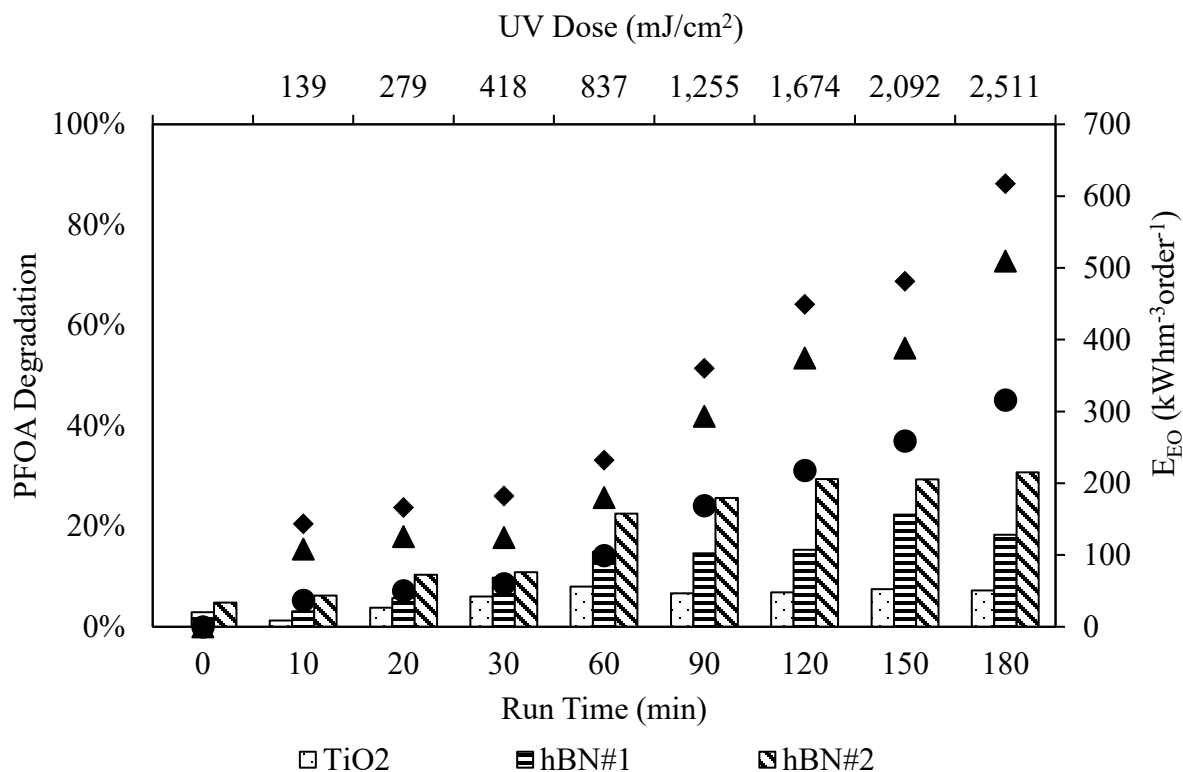
Figure 5.14 Comparison of PFOA Degradation at Slurry Photoreactor [PFOA

Concentration: 35 ppm; Loading Rate: 1000 mg/L; pH 3]

The performance of all three catalysts at pH 3 are compared in Figure 5.14. TiO$_2$

was proven to be ineffective in PFOA degradation regardless of pH variation as illustrated

on this figure and shown previously in the collimated beam study. This figure also shows hBN#2 seems more effective in PFOA degradation than hBN#1 and TiO_2 at pH 3. Also, E_{EO} with hBN#2 is the lowest among three catalysts, around $100\,kWhm^{-3}order^{-1}$. However, it is much higher compared to pCBA degradation, indicating PFOA will require higher energy input for its degradation. E_{EO} value will be further discussed in Chapter 8.

5.4 Conclusions

The overall conclusion that can be drawn from this chapter could be, the upflow (slurry) photoreactor at the testbed, using both TiO_2 and hBN catalysts (as slurry) for pCBA and PFOA degradation is effective. It also provided some valuable insights on pCBA to PFOA degradation to the previous collimated beam study (at Chapter 4). Some of the shortcoming of the collimated beam, especially hBN#1 and hBN#2 were hBN mixing or settling issues but both were overcome with better mixing capabilities at the upflow photoreactor. The effect in terms of catalyst loading rate, UV dose, pH and peroxide addition (as AOP) and their assessment provided much needed insights to upflow photoreactor and provided much needed guidance of further testing or improving these catalysts at pilot-scale (Purifics Photo-Cat) (Chapter 6).

The result also shows, pCBA tends to easily photolyzed (50-56%) under UV light without requiring any photocatalysts (TiO_2 or hBN) addition in the upflow (slurry) photoreactor. In comparison, PFOA was found to be more difficult to photolyze (~5%) (in absence of catalysts). Both of TiO_2 and hBNs can significantly improve pCBA (~90%) degradation but with moderate PFOA (40-45%) removal only by further optimization for the upflow (slurry-based) photoreactor.

70

However, TiO_2 was found to be less effective to hBN in PFOA degradation. Unlike TiO_2, hBN was found to perform much better by increasing its loading rate and by lowering the pH to pH 3.0 at moderately high UV dose 2500 mJ/cm^2. The pH impact was more profound for the hBN than to TiO_2 for both pCBA and PFOA degradation up until certain UV doses, however at higher UV dose the pH impact was seen to narrow. Addition of hydrogen peroxide (H_2O_2) was found not to be an important factor in overall PFOA degradation. All these insights are considered to be important for both pCBA and PFOA (and PFAS) degradation. This information will be helpful in assessing the Photo-Cat (at pilot-scale) system and will be discussed in the next chapter (Chapter 6).

It is important to note here, particularly for the PFOA degradation for this study, where PFOA is spiked at significantly higher (35 mg/L) concentration level than what is found at concentration (mostly at ng/L level) in nature. Thus, the UV dose (mJ/cm^2) applied and other optimal conditions selected to improve PFOA degradation for this high concentration (mg/L) level, will still be applicable in natural setting. The higher level PFOA spiking was selected, due to the current analytical capability at our lab with detention limit of PFOA is higher to ng/L (minimum detection limit at 1.0 mg/L). A lower PFOA spiking, with lower detection limit (ng/L) will require sending PFOA samples to outside labs, at significantly higher cost, thus avoided. Nevertheless, the overall goal of this study shows, the upflow (slurry) reactor can remove 40-50% of PFOA (at such high concentration level) is a good indicator that the upflow photocatalytic will be effective for PFOA/PFAS degradation in real water. However, the background water organics and presence of co-occurring ions/salts (iron, silica, etc.) and metals or matrix effect in natural

water may interfere in catalysts performance, which still needed to careful investigated.

Chapter 5 (Photo-Cat) investigates on PFAS degradation, also for a natural groundwater.

CHAPTER 6

DEGRADATION OF PARA-CHLOROBENZOIC ACID AND PER-

FLUOROOTANOIC ACID WITH PILOT-SCALE SETUP (PHOTO-CAT)

A commercial, pilot-scale photoreactor (Photo-Cat) from Purifics (London, Canada) was used during this study. The pilot unit was donated to ASU nearly 13-15 years ago and was used, primarily with TiO_2 (P25) as slurry in few past photocatalytic related research studies over the years. The unit was used for this study for removing pCBA and PFOA degradation using both TiO_2 and hBNs (hBN#1 and hBN#2 as photocatalysts). This is a larger system (19L) requires larger volume of spiked water sample and catalyst volume in batch operation. During initial assessment only TiO_2 and hBN#1 were used. Thus, hBN#1 was used in preliminary assessment and later in subsequent study. The system was operated in batch-mode as described in detail in Chapter 3.

6.1 pCBA Degradation

Since Photo-Cat pilot unit was unused for a long time, the system was initially checked for its operation before the catalysts assessment. The pCBA was used as the system-check using both catalysts (i.e., TiO_2 and hBN#1). The experimental matrix is shown in below table.

Table 6.1

Experiment Matrix for System Check

pCBA Degradation	Concentration (ppm)	Exp #	Catalyst	Catalyst Dose (mg/L)	pH	Power/Volume Ratio (Watt/L)
Effect of Photolysis	39	1	None	0	7	7.5
		2	TiO$_2$	1000		
		3	hBN#1	1000		
Effect of Loading Rate		4-6	hBN#1	100-500-1000		

Nanopure water was used for the Photo-Cat system under batch operation. The results of pCBA degradation results are discussed below.
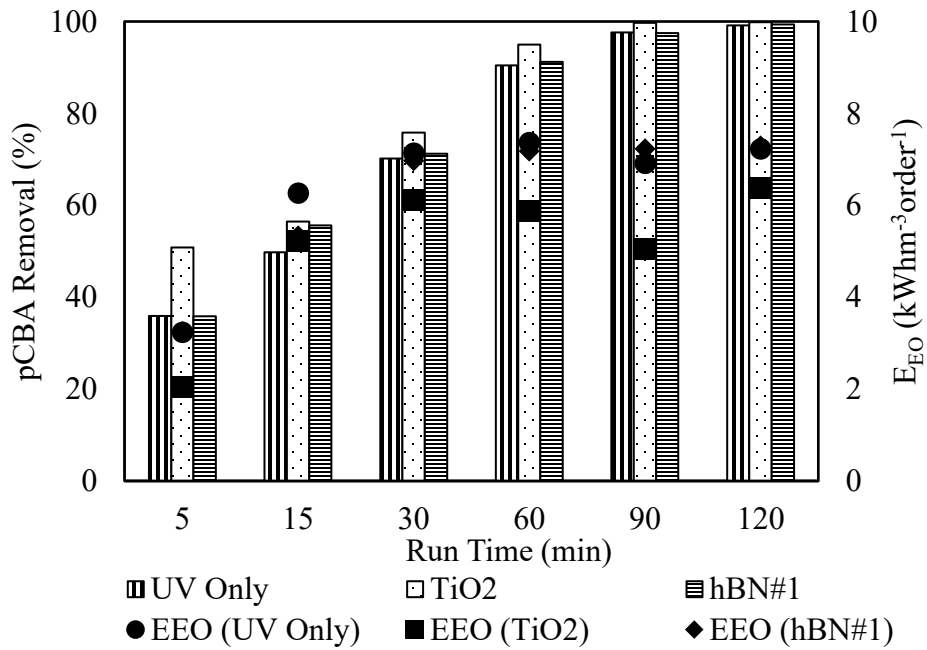
Figure 6.1 Effect of Photolysis [Loading Rate: 1000 mg/L; pH 7]

74

Above figure shows, the UV only (photolysis) was highly effective in completely removing pCBA from water (~100%). This was even with using only one of the UV lamp (75W), while the other three (3) were turned off. This result is unlike both, the collimated beam and the slurry reactor, where photolysis was effective in removing only 50% of pCBA from spiked water under photolysis. The catalyst loading rate (1000 mg/L), pCBA concentration (5 mg/L) and pH (pH 7.0) for the Photo-Cat study are alike to that of the collimated-beam or the upflow (slurry) photoreactor study, but yet, the Photo-Cat shows a significantly higher amount of pCBA degradation. Which are indicatives of a higher UV irradiation (mJ/cm^2), where the exact UV dose (mJ/cm^2) applied to Photo-Cat is unknown due to the lack of the actinometry data. But it is understood it to be higher, as this unit is much larger in size to upflow photoreactor with higher power to volume ratio, and also equipped with multiple UV lamps and its design photoreactor diameter to lamp diameter is much smaller to the upflow photoreactor, may have played a positive role.

Effect of Loading Rate
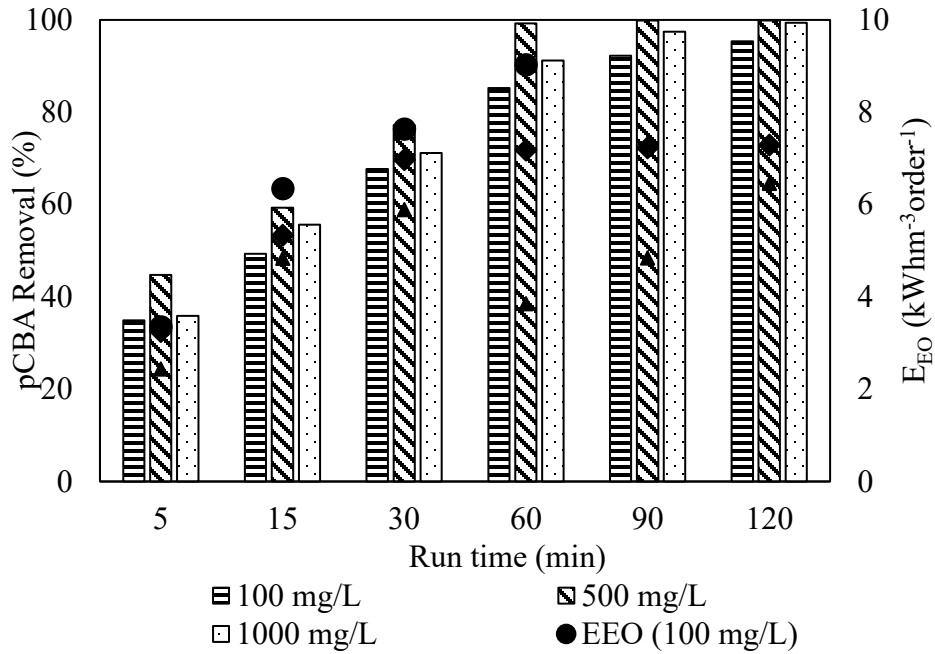
Figure 6.2 Effect of Loading Rate (hBN#1) [pH 7]

Next, a series of runs were made on Photo-Cat by varying hBN#1 loading rate, as shown in Figure 6.2. This plot does not show photolysis (UV only), which will be similar as to Figure 6.1. Suggesting, most of the pCBA removal was occurring due to UV only (photolysis). The impact of catalyst loading rate (mg/L) is not significant. However, this figure shows as the hBN#1 loading rates increases to 1000 mg/L, it shows lesser amount of pCBA removal. Suggesting higher light scattering from a higher photocatalyst concentration in the water may also negatively impact the removal due to lamp design (i.e., lamp diameter to housing diameter is much narrower to the upflow photoreactor, with lesser opening to bring the catalysts closer to the lamp). The competing mechanisms may lead to an optimal photocatalyst concentration, which may require further investigation. Specifically, the optimal hBN dose for pCBA degradation was found to be around 500 mg/L at Photo-Cat based reactor, as shown on Figure 6.2.

76

6.2 PFOA Degradation

Next, an experiment matrix for PFOA degradation at Photo-Cat is shown below.

Table 6.2

Experiment Matrix for PFOA

PFOA Degradation	Concentration (ppm)	Exp #	Catalyst	Catalyst Dose (mg/L)	pH	Power/Volume Ratio (Watt/L)
Effect of Catalyst	50	1	TiO_2	1000	7	30
		2	hBN#2	1000		
Effect of pH		3	hBN#2	1000	3	

Nanopure water was used for Photo-Cat runs, spiked with targeted PFOA concentration in assessing both TiO_2 and hBN#2 for PFOA removal, are discussed below.
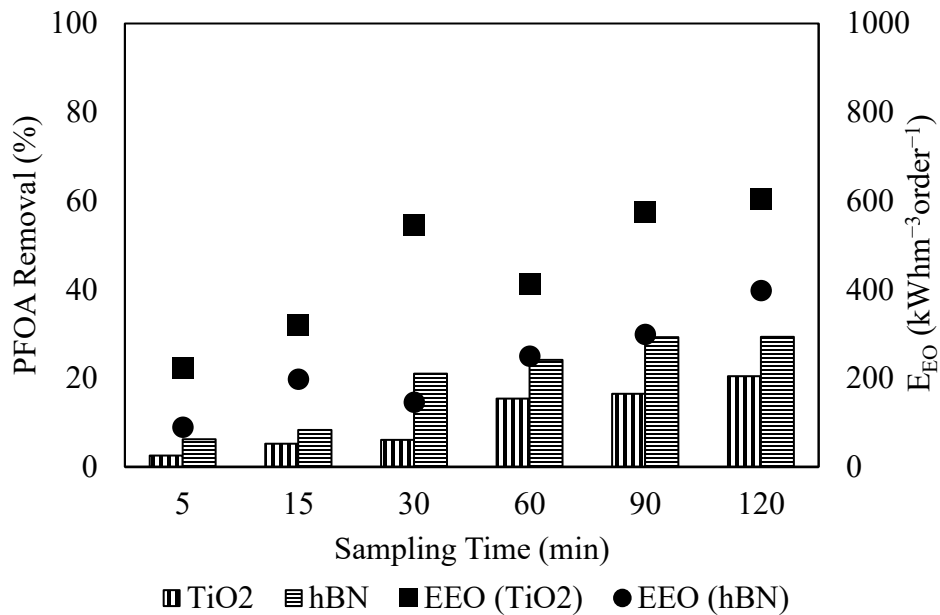
Figure 6.3 Effect of Catalyst [Loading Rate: 1000 mg/L; pH 7]

Figure 6.3 shows PFOA degradation with TiO_2 and hBN#2 at ambient pH condition under an equivalent loading rate of 1000 mg/L. This result is similar to what was seen before in the upflow photoreactor (Figure 5.8), where hBN#2 was found to be slightly more effective than TiO_2 (~5% better) in PFOA degradation, although the PFOA degradation remains low, about 20-25% at Photo-Cat under an ambient pH condition. Although the effect of UV only (photolysis) is not shown in the figure, but is expected to be lower for hBN, as seen previously in upflow photoreactor (Figure 5.8). Slightly higher PFOA degradation with hBN#2 than with TiO_2 which also agrees with previous collimated beam and the upflow (slurry) photoreactor, could be the difference between the degradation mechanisms, where TiO_2 achieves degradation by OH• radical (due to electron hole and water dissociation), whereas hBN follows similar but slightly different mechanism with water hydrolysis (direct interaction with holes), which is still under investigation at Rice University. These differences play a critical role in PFOA degradation.

78

Unlike Chapter 4 and 5, where the photocatalyst was compared to each other under different experimental conditions (e.g., loading rate, peroxide addition, etc.). These were not done for the Photo-Cat system, except the pH experiment, thus cannot be compared.

Effect of pH
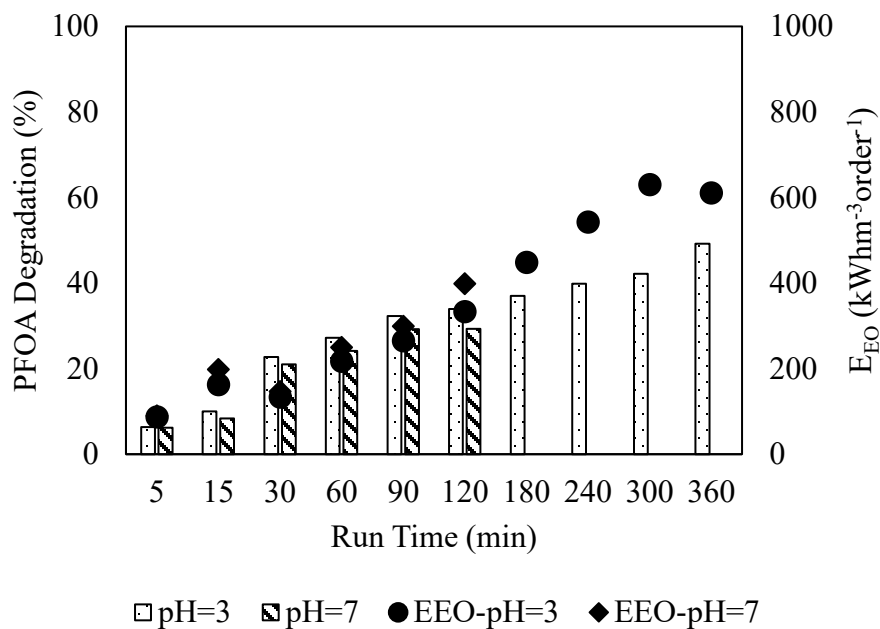
Figure 6.4 Effect of pH (hBN#2) [Loading Rate: 1000 mg/L]

Figure 6.4 shows PFOA degradation with hBN#2 under two different pH conditions (i.e., pH 3 and pH 7) and under two different run lengths (i.e., longer run length results in higher UV dose) for an equivalent loading rate of 1000 mg/L. This result is similar to what was seen before at the upflow (slurry) photoreactor (Figure 5.10), where PFOA was found to be more degraded at a lower pH condition (acidic), which was also seen at the collimated beam study (Figures 4.16 and 4.18). Also, with a higher UV dose (i.e., with a longer run), PFOA degradation also increases from < 25% at ambient pH (Figure 6.3) to around 50% at pH 3.

6.3 Conclusions

Overall, the Photo-Cat system shows pCBA could be completely degraded (100%) by photolysis only, unlike collimated-beam and upflow photoreactor, where only 50% degradation occurred by photolysis. Higher removal by Photo-Cat could be due to higher UV irradiance and/or better reactor design, or other unknow reasons, yet to be investigated, which resulted in higher pCBA degradation and removal. A chemical actinometry, if doable, will provide UV dose (mJ/cm^2) data with the reactor run length. Unlike, collimated and upflow (slurry) photoreactors where the catalyst addition (i.e., TiO$_2$) in presence of UV improved pCBA degradation (synergy), this could not be assessed at the Photo-Cat, as photolysis completely (100%) degraded pCBA.

However, for the PFOA degradation, the Photo-Cat was able to degrade PFOA partially (<30%). The results also show the difference between the photocatalysts, where hBN was found to be moderately more effective (<30%) to TiO$_2$ for PFOA degradation, but at ambient pH condition. This is similar with what was found at slurry based photoreactor, but at higher UV dose and/or lower pH level, the removal could be further improved to 50%. Further study on optimization may be necessary to assess and provide greater insights into improving Photo-Cat performance to overall PFOA degradation. All these findings from this and previous chapters are important to provide greater insights in photocatalytic degradation of pCBA and PFOA among the three photoreactors of scale.

CHAPTER 7

COMPARISON OF PARA-CHLOROBENZOIC ACID AND PER-FLUOROOTANIC

ACID DEGRADATION AMONG DIFFERENT SCALE SETUPS

This chapter primarily focuses on all three photoreactors performance in side-by-side comparison study and in terms of their overall effectiveness in degrading these two targeted contaminants in water. It also compares E_{EO} values between the upflow (slurry) photoreactor and Photo-Cat and investigates the reaction kinetic of contaminant degradation.

7.1 pCBA Degradation

All three photoreactors that are tested in this study for photocatalytically degrade pCBA is compared below. Although the initial concentration of pCBA varied among three scales. pCBA degradation for all three scales but E_{EO} values for the upflow (slurry) photoreactor and Photo-Cat are compared.

7.1.1 pCBA degradation with TiO₂
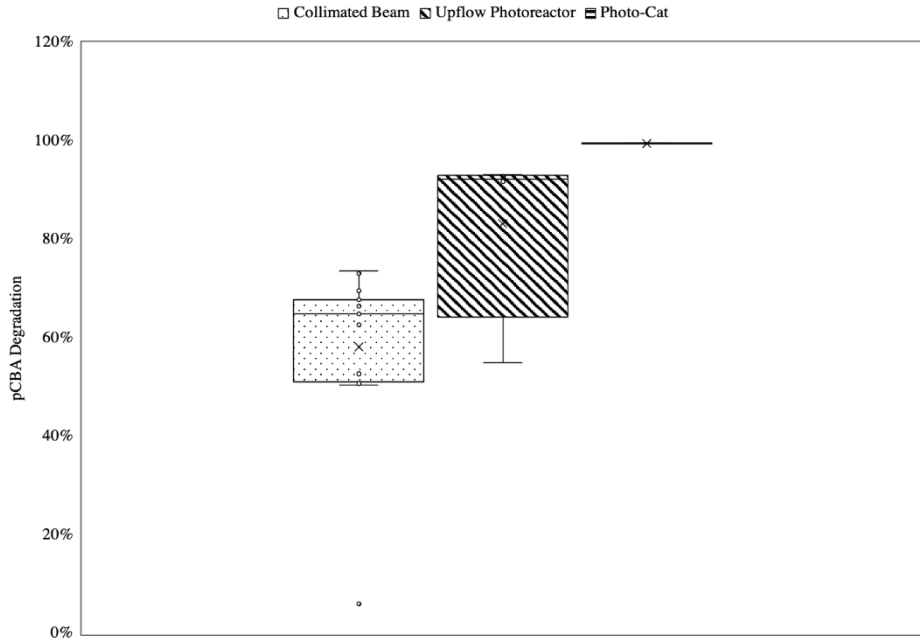
Figure 7.1 Comparison of pCBA Degradation (TiO₂)

Figure 7.1 shows box and whisker plot for pCBA degradation for all three photoreactors using TiO_2, these include: collimated beam, upflow (slurry) photoreactor and Photo-Cat system. The spread of the boxes (collimated and slurry photoreactor) indicate variation in pCBA removal and outcomes, which are based on several experimental runs that were discussed in detail in previous chapters. However, a narrower box indicates tightness of data (e.g., Photo-Cat) or the data based on only one single run, thus not showing much difference in removal or spread of the box as outcome. These figure shows, pCBA degradation at the collimated beam varied (45-70%) with a median value of removal around ~ 65%. Whereas the upflow photoreactor pCBA removal varied from 60-80%, with a median value around 82% degradation. It is important to note, photolysis by itself was able to degrade 50% of pCBA at both photoreactors, however addition of the catalyst

improved removal. For the Photo-Cat, the box is narrower, due to only one single run, with 100% removal of pCBA by photolysis alone.
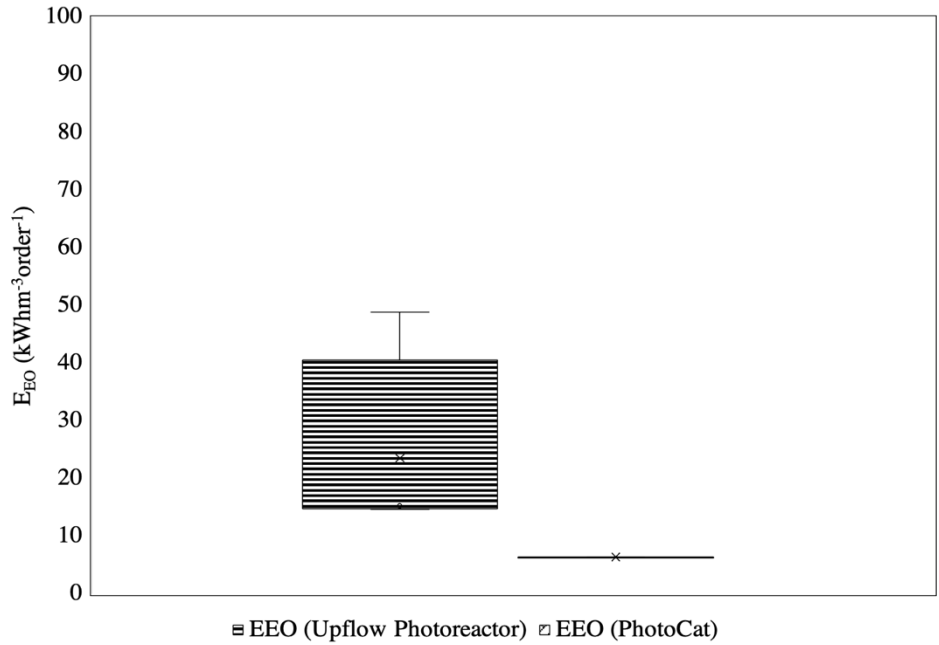
Figure 7.2 Comparison of E_{EO} for pCBA degradation (TiO_2)

Figure 7.2 shows E_{EO} values at the upflow photoreactor and Photo-Cat. E_{EO} values are comparable, but slightly higher for the upflow (slurry) photoreactor than for the Photo-Cat due to variability of experimental runs. It decreases from 40 kWhm^{-3}order^{-1} for the upflow (slurry) photoreactor to nearly 10 kWhm^{-3}order^{-1} for the Photo-Cat, respectively. However, these values are still higher for practical water treatment application (desired < 10 kWhm^{-3}order^{-1}), which could be due to a higher pCBA concentration (mg/L) (spiking) during experimental runs.

Below figure shows pCBA degradation (decay) curve over time for the TiO_2 for the upflow (slurry) photoreactor (Figure 7.3).
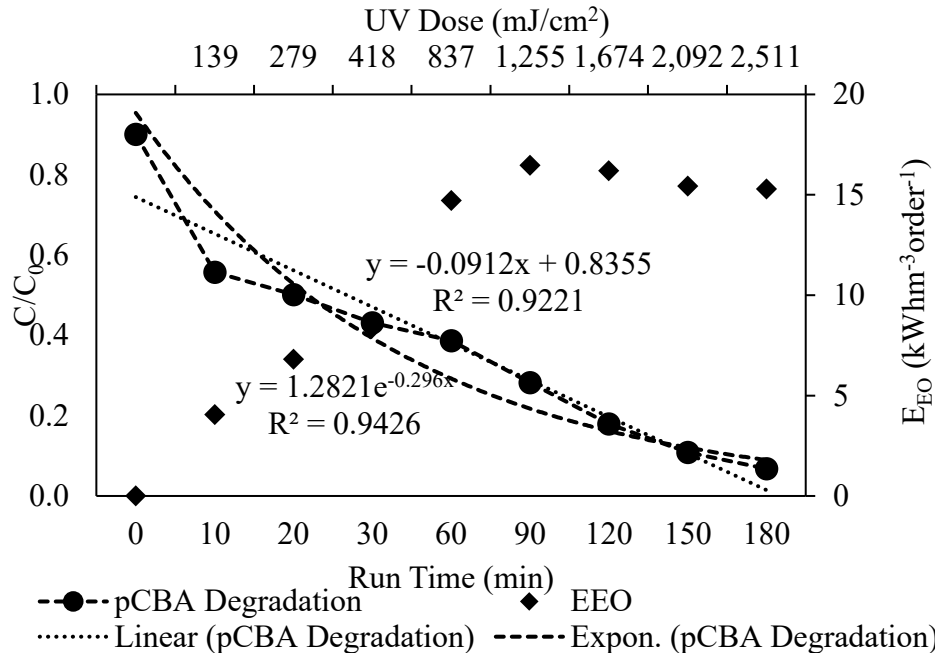
Figure 7.3 Decay Curve of pCBA Degradation with TiO_2 at Upflow Photoreactor [Loading Rate: 1000 mg/L; pH 7]

This figure shows, pCBA degrades rapidly within the first 30 minutes (at UV dose of <400 mJ/cm^2) and thereafter decreases gradually as UV irradiation (mJ/cm^2) increases over time. A liner, to designate a zero-order kinetics, while an exponential fit, to indicate first order decay plots are shown on this figure. The results suggest, pCBA degradation data for the first 30-minutes fits a first order decay and after 30-minutes it fits zero order degradation. The first order rate constant is around 0.296 min^{-1} (<400 mJ/cm^2) while from 60 to 180 minutes (>1000 mJ/cm^2), under zero-order, the rate constant of 0.401 mg/L/min.

7.1.2 pCBA Degradation with hBN
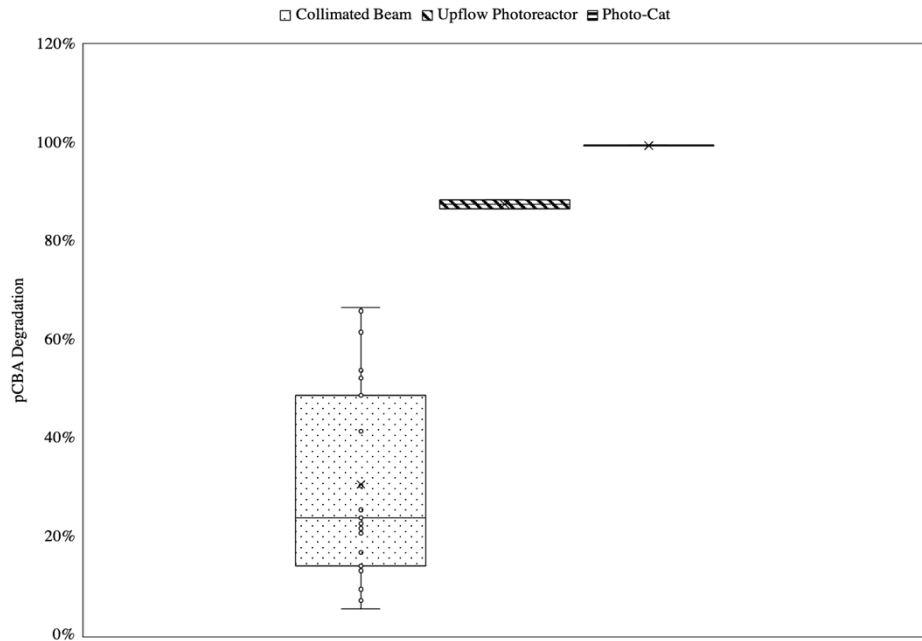
Figure 7.4 Comparison of pCBA Degradation (hBN)

Figure 7.4 shows the pCBA degradation for the hBN. For collimated beam, the pCBA degradation varies from 15-50% with median is around 22%, which seems low. The lower removal was due to the hBN aggregation, clumping or settling in the collimated beam setup (i.e., petri-dish). This result indicates the collimated beam is not an appropriate setup for pCBA degradation, especially for using hBN, as hBN could not be well mixed. However, this lower amount of degradation increases significantly to 80-85% and 100%, at the larger upflow (slurry) or Photo-Cat photoreactor due to better reactor design and mixing.
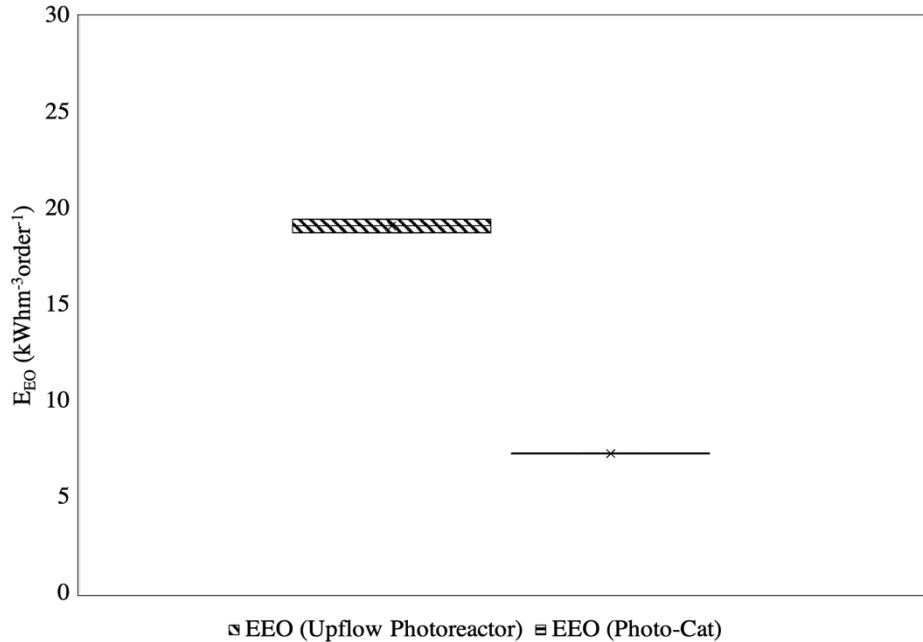
Figure 7.5 Comparison of E_{EO} for pCBA degradation (hBN)

Above Figure 7.5 shows E_{EO} value for both the upflow (slurry) photoreactor and Photo-Cat; are both comparable to each other, but slightly higher for the upflow photoreactor to the Photo-Cat. The E_{EO} value decreases from 20 $kWhm^{-3}order^{-1}$ for the upflow photoreactor to nearly 7 $kWhm^{-3}order^{-1}$ for the Photo-Cat for pCBA degradation.

Next a series of decay curves were developed for hBN in degrading pCBA for the upflow photoreactor.
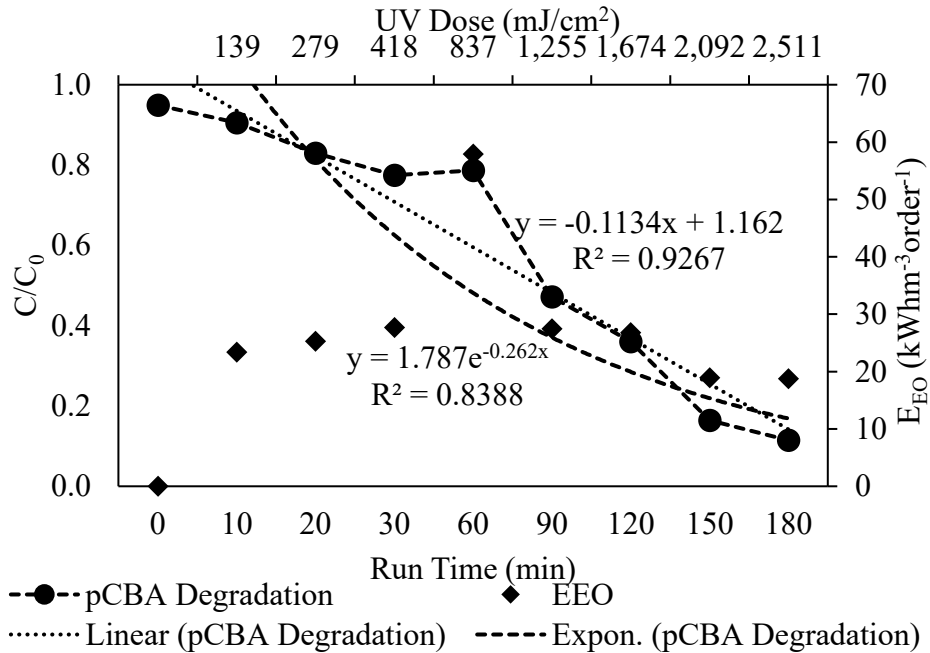
Figure 7.6 Decay Curve of pCBA Degradation with hBN at Upflow Photoreactor [Loading

Rate: 1000 mg/L; pH=3]

Above Figure 7.6 shows pCBA degradation over time and suggests pCBA degrades

gradually for the first 60 minutes of the run (UV dose < 850 mJ/cm^2) and then decays faster

after 60 minutes. A liner line, to designate a zero-order kinetics, while the exponential fit,

to indicate the first order decay are shown on the figure. These results suggest, the pCBA

degradation for hBN does not follow first order but is combination of two zero orders. The

reaction rate for the first 60 minutes (850 mJ/cm^2) around 0.009 and after 60 minutes 0.016

(mg/L)/min (> 850 mJ/cm^2), respectively.

7.2 PFOA Degradation

All three photoreactor photo-catalytically degradation of PFOA are compared here.

Although the initial concentration of PFOA varied (collimated bean at 25 mg/L and for

upflow (slurry) and Photo-Cat at 35 mg/L) among the scales. The PFOA degradation at all

three scales and E_{EO} at the upflow (slurry) photoreactor and Photo-Cat are compared here.

E_{EO} at the collimated beam is excluded from this study, only larger photoreactor are compared.

7.2.1 PFOA degradation with TiO_2
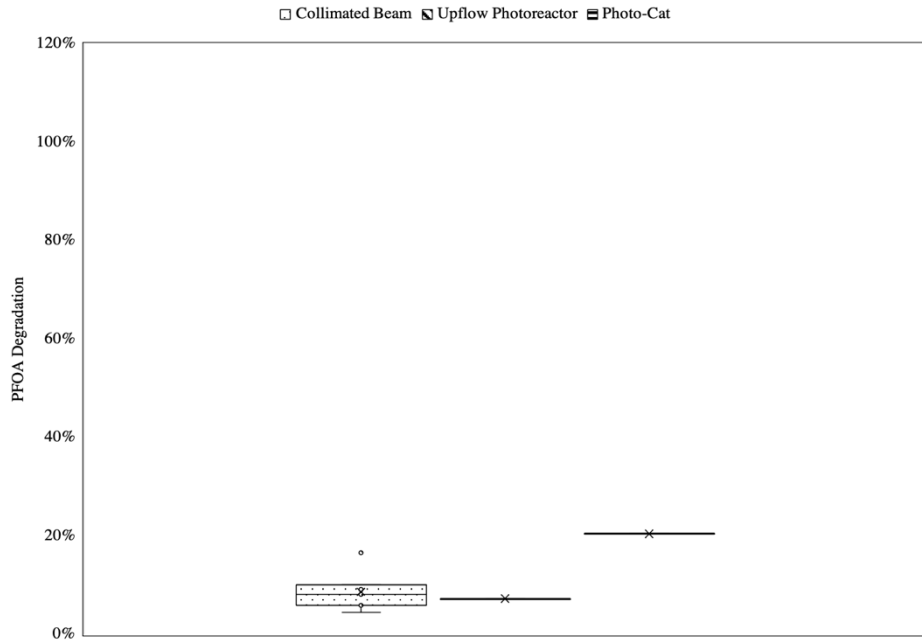
Figure 7.7 Comparison of PFOA Degradation (TiO_2)

Above figure, the Figure 7.7 shows box and whisker plot for all three photoreactors for PFOA degradation using TiO_2, these include: collimated beam, upflow (slurry) photoreactor and Photo-Cat. This figure shows, PFOA degradation for all photoreactors using TiO_2, remains lower, around 10% for the collimated beam and the upflow (slurry) reactor, while 20% removal for the Photo-Cat. It is important to note, photolysis is unable to degrade PFOA by photolysis (< 5-10%; Figure 5.8).
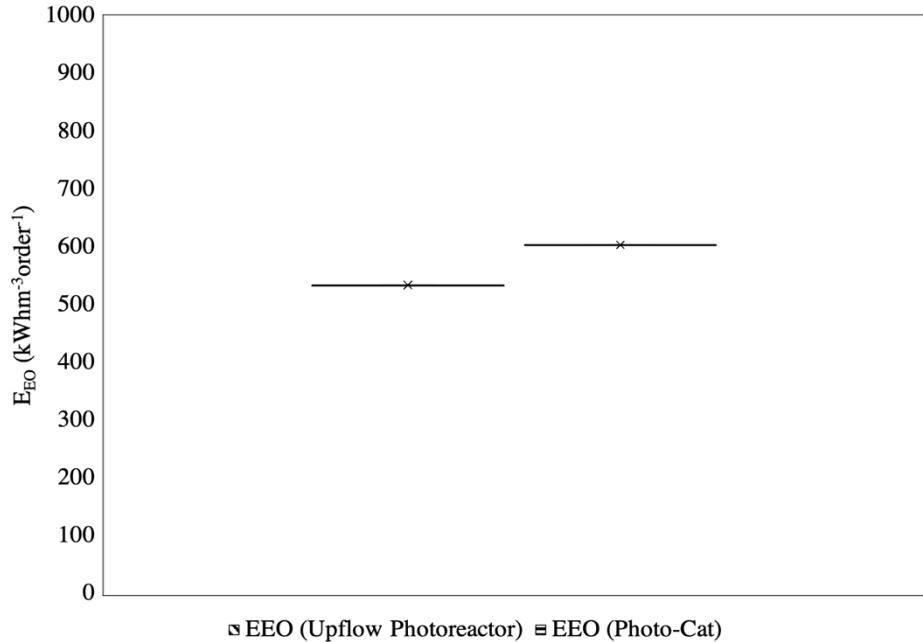
Figure 7.8. Comparison of E_{EO} PFOA Degradation (TiO_2)

Above figure, Figure 7.8 shows E_{EO} value for the upflow (slurry) photoreactor and Photo-Cat. The E_{EO} value for these two photoreactors are similar, but slightly lower for the upflow (slurry) photoreactor than to the Photo-Cat. The E_{EO} value for the upflow (slurry) photoreactor is around 500 $kWhm^{-3}order^{-1}$ and it increases to 600 $kWhm^{-3}order^{-1}$ for the Photo-Cat, this could be due to a higher initial spiked feed concentration for Photo-Cat (35 ppm *versus* 50 ppm, respectively).

Next a series of decay curve were developed for PFOA degradation using TiO_2 at the upflow (slurry) photoreactor is discussed below.
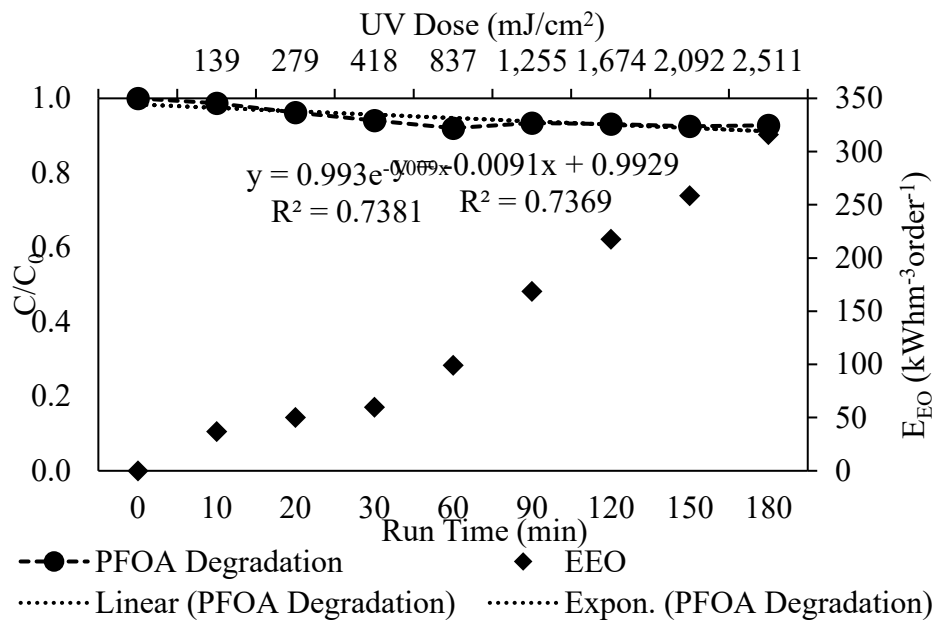
Figure 7.9 Decay Curve of PFOA Degradation with TiO_2 at Upflow Photoreactor [Loading

Rate: 1000 mg/L; pH 3]

Above figure, Figure 7.9 shows, PFOA degradation over time. This figure suggests,

PFOA does not degrade well by TiO_2, but if degrades, it degrades gradually (i.e., slowly)

for the entire run (where the UV dose ranges from 0-2500 mJ/cm^2). A liner line, to

designate a zero-order kinetics curve (fitted), to indicate the zero-order decay using TiO_2.

The reaction rate determined from this curve results in 0.209 mg/L/min.

7.2.2 PFOA degradation with hBN
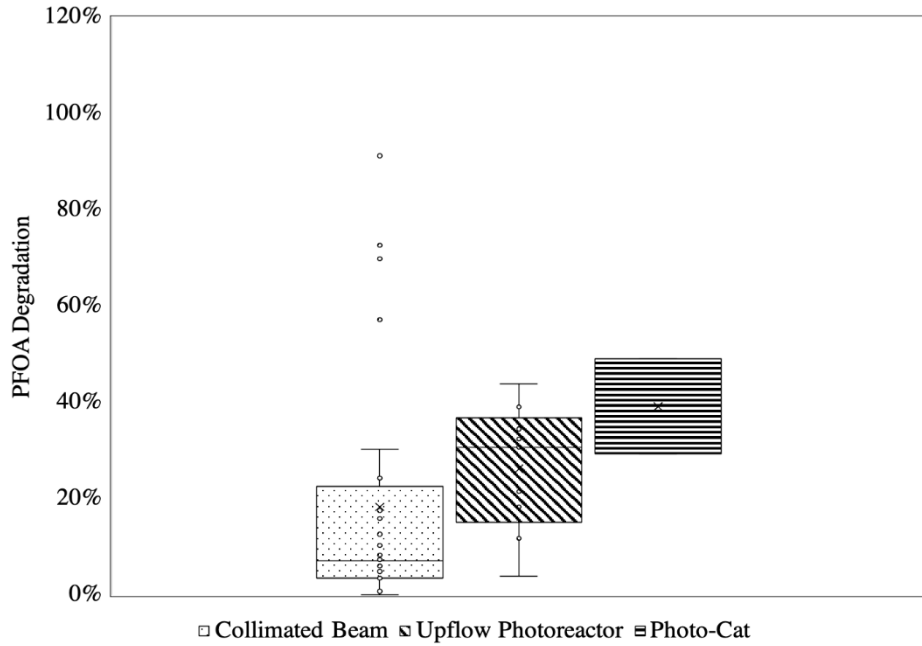
Figure 7.10 Comparison of PFOA Degradation (hBN)

Figure 7.10 shows PFOA degradation among three scales. The PFOA degradation at the collimated beam is lower (median 10%) than that of the upflow (slurry) and Photo-Cat (i.e., 20-50%) photoreactor using hBN. This figure also shows, between the upflow photoreactor and Photo-Cat, the Photo-Cat shows slightly better in PFOA removal than to the upflow slurry reactor, which was possible by further optimization steps undertaken for both photoreactors (e.g., a higher applied UV dose and/or lowering the pH for the hBN), resulted in higher PFOA degradation (30-50%).
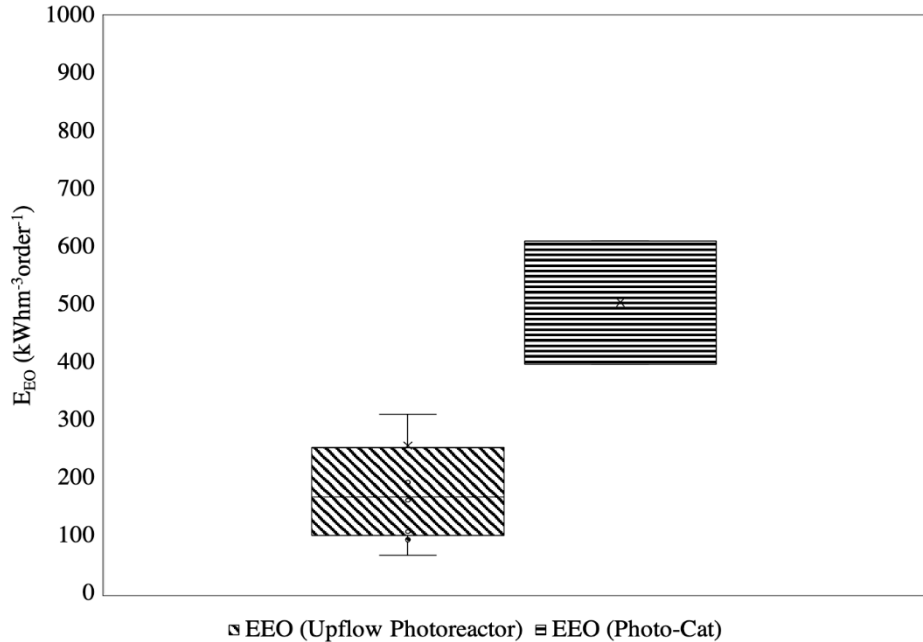
Figure 7.11. Comparison of E_{EO} PFOA Degradation (hBN)

Figure 7.11 shows E_{EO} value for the upflow photoreactor and Photo-Cat. E_{EO} values are significantly higher for both upflow (slurry) photoreactor and Photo-Cat for PFOA degradation in comparison to the pCBA removal (Figure 7.5, which is < 20 kWhm^{-3}order^{-1}). The E_{EO} values for the upflow photoreactor is about 200 kWhm^{-3}order^{-1} and 500 kWhm^{-3}order^{-1} for the Photo-Cat, which due to a higher feed (spiked) concentration (35 ppm *versus* 50 ppm, respectively) or use of higher power/volume ratio.

Later to further improvement on PFOA degradation was achievable for both upflow (slurry) and Photo-Cat photoreactors under optimizing the treatment condition by lowing pH and increasing the UV dose, also resulted in lower E_{EO}. However, the maximum amount of PFOA degradation remains around 40-50% and could not be further improved. The PFOA decay curve for the upflow (slurry) photoreactor under an optimal condition is shown below.
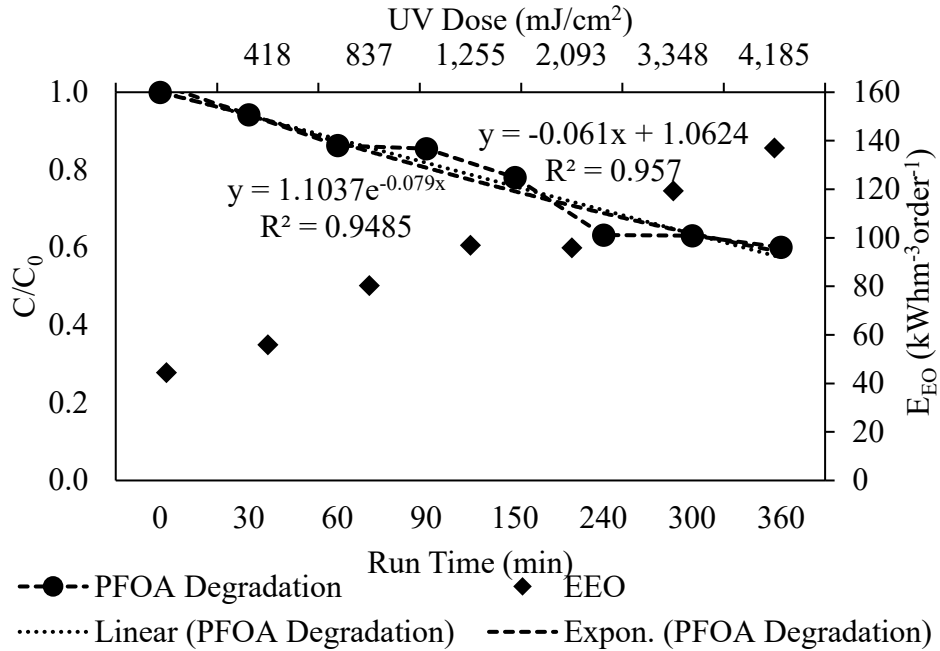
Figure 7.12 Decay Curve of PFOA Degradation with hBN at Upflow Photoreactor

[Loading Rate: 1000 mg/L; pH 3; Peroxide Addition: 10 mg/L]

Figure 7.12 shows PFOA degradation curve for the upflow (slurry) photoreactor using hBN. This figure shows, PFOA degradation over time and the figure suggests, PFOA degrades over time slowly. A liner line, to designate a zero-order kinetics (fitted), to indicate that it fits zero-order decay (to first order decay, not shown). The reaction rate is 1.34 mg/L/min.
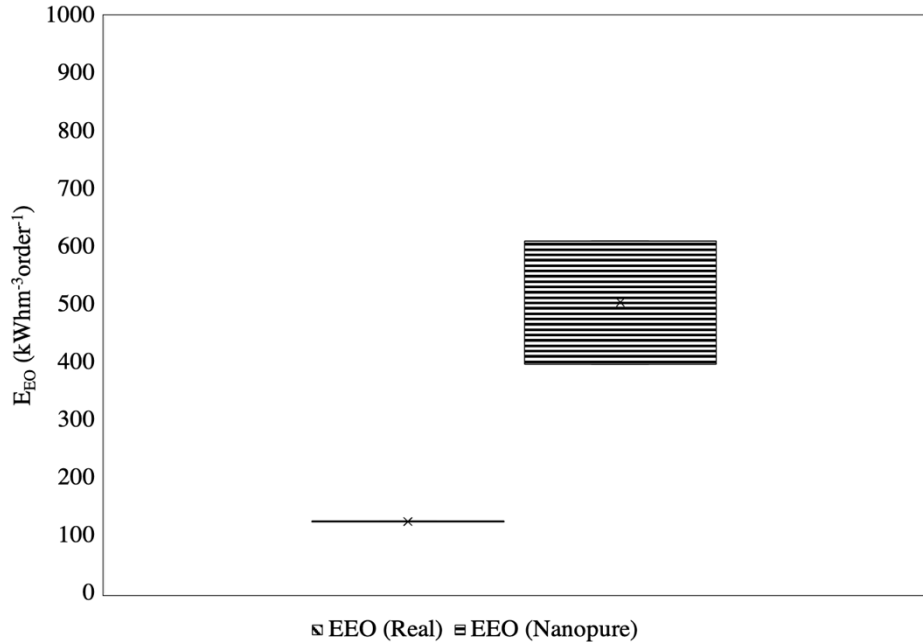
Figure 7.13. Comparison of E_{EO} between Real Water and Nanopure spiked Water

Figure 7.13 shows E_{EO} value for real water collected from a PFAS contaminated groundwater-well in California (see Appendix A.2; Report title: *UV, UV/H$_2$O$_2$, and O$_3$/H$_2$O$_2$ PFAS Treatability Screening Using Real Groundwater*) and nanopure (PFOA spiked) water for the Photo-Cat. The E_{EO} value for the real water is about 100 kWhm^{-3}order^{-1} for PFOA degradation in comparison to the nanopure water, which is five times higher, at about 500 kWhm^{-3}order^{-1}, since the PFOA concentration for the nanopure water sample is much higher (mg/L) than to the real water (ng/L) as shown on Table S2.

7.3 Conclusions

Overall, this chapter was able to show performance of various photoreactor in a side-by-side comparison. It also assesses their overall performance in removing the two targeted contaminants (i.e., pCBA and PFOA) from water. These results show between pCBA and PFOA, the PFOA is more difficult to remove at all treatment scales and will also requires higher E_{EO} or energy requirement to degrade it. Although the E_{EO} value for

the collimated beam are not reported but reported and compared against the two larger photoreactors, which are designed as a modular unit for implementation. The upflow (slurry) and the Photo-Cat photoreactors performed similarly in contaminant removal and their E_{EO} values were also of similar in ranges. However, due to the difference in initial contaminant concentration (spiked) in synthetic (nanopure; with higher PFOA concentration in mg/L) to natural waters (with lower PFOA concentration in ng/L) the performance differed. The PFOA removal performance varied between the scales (particularly, collimated beam). It is noteworthy to mention here, the PFOA degradation for both upflow (slurry), and the Photo-Cat was able to improve from its lower removal (<20-25%) to moderate (40-50%) removal by further optimization (i.e., lowering the pH with higher UV doses).

CHAPTER 8

SUMMARY AND CONCLUSIONS

The photocatalytic degradation study was primarily conducted for two different contaminants, these are pCBA and PFOA and using three different photoreactors of scales and with two different photocatalysts (i.e., TiO_2 and hBN). Photoreactor included the collimated beam (at bench-scale), upflow (slurry) photoreactor (testbed-scale), and Photo-Cat system (pilot-scale). Below is a summary table to qualitatively describe the advantages and disadvantages of these three reactors based on the results of this study.

Table 8.1

Qualitative Table

Parameters	Collimated Beam	Upflow (slurry) Photoreactor	Photo-Cat
Reactor Type	Small, bench-top unit	Compact, modular, testbed mounted	Commercial (PLC equipped), larger unit
Advantage	Small sample volume needs & easy to operate	Easy to operate under both batch or continuous operation, modular, regular power supply (110-120V)	Proven, commercial product, automated (PLC controlled)
Disadvantage	Poor mixing (e.g., catalyst settling)	Catalyst settling at filter housing (although low < 5%)	Hard to disassemble, troubleshoot, heavy (bulky); requires higher voltage (230V)

pCBA Degradation	TiO$_2$	Moderate	Good	Good
	hBN	Poor (due to poor mixing)	Good	Good
PFOA Degradation	TiO$_2$	Poor	Poor	Poor
	hBN	Poor (improves with lower pH)	Moderate	Moderate
Application		To Screen catalysts & quickly assess operational condition	Field assessment (using real water)	Field assessment (using real water)
E$_{EO}$		High (not reliable)	Moderate for pCBA, but higher for PFOA	Low for pCBA but higher for PFOA

The overall observations for both pCBA and PFOA degradation show lowering the pH tends to have a profound impact on hBNs performance for all three photoreactor at scale. The removal is also dependent on applied UV doses (or run length). While the acidic (pH ~ 3) or alkaline (pH ~11) condition has a lesser effect on TiO$_2$, while neutral pH seems optimal. Also, increasing the UV (mJ/cm^2) and peroxide dose (mg/L) differed by the contaminant type (pCBA or PFOA) and their overall degradation. However, some issues at the bench scale (collimated beam) remains, were mostly related to the two hBNs photocatalysts to mixing or settling. Since hBN#1 is more hydrophobic than hBN#2, it

tends to aggregate and clump-up more at the collimated beam (petri-dish) setup. In contrast, hBN#2, which is surface treated (by manufacturer), is slightly hydrophilic, does not agglomerate as much, but was prone to settling in the shallower petri-dish in collimated beam setup, even under continuous mixing. However, hBN's clumping or setting was overcome in the upflow (testbed) and Photo-Cat (pilot) photoreactor system with better mixing and recirculation (pump) with larger volume sample for these setups.

Although TiO_2 and hBN were found to be effective in pCBA degradation, yet TiO_2 was found to ineffective in PFOA degradation. Furthermore, both hBNs were found to perform better than TiO_2 for PFOA degradation, while hBN#2 overall performed better. Although the degradation remains low to moderate (<20-25%) at the bench-scale, but lowering the pH to pH 3.0 improves the hBNs performance significantly and moreover under higher UV dose (i.e., 11000 mJ/cm^2), PFOA degradation at collimated beam was shown to improve significantly (>90%). Most of these findings are consistent through all three scales and throughout this study. The addition of hydrogen peroxide (H_2O_2), improved performance in pCBA degradation for TiO_2, but less so for PFOA degradation, and remains unclear. It could be due to some inherent differences between these two photocatalysts and their interactions with water layer and contaminants and/or types. Differences in catalysts may include differences in band gaps (i.e., 6.2 eV for hBN *versus* 3.2 eV for TiO_2), or surface hydrophobicity (i.e., hBN is being more hydrophobic to TiO_2) and/or surface charge (i.e., hBN is of lower PZC of ~ 2.8 to TiO_2 of ~6). Additionally, it could also be due to the difference in photocatalyst surface characteristics and its surrounding water layers (or coverage) and their interaction with catalysts (TiO_2 *versus* hBN) or surrounding co-ions, or surface-active sites – which is

98

beyond the scope of this research. These differences as alike or unlike are essential to understand to provide much-needed insights into the performance of these catalysts at fundamental level, some of which are being currently addressed at Rice University.

Between the upflow (slurry) photoreactor and Photo-Cat system, both systems performed equally. Besides assessing the photoreactor's performance, there are some physical and operational differences between these two units. From the field-testing or intended application perspectives, the selection of a photoreactor will be based on its proposed use, size and application, selected by considering some of these inherent differences as listed in Table 8.1. All of these are to be carefully considered before the selection of such a unit for further assessment. In terms of the footprint, the Photo-Cat is significantly larger. It requires more than 40-60 ft2 of floor spacing for its operation, whereas the upflow photoreactor is smaller, requiring only 4-5 ft2 of floor spacing, and could easily and conveniently be mounted in the MobileNEWT (i.e., at testbed's wall). The Photo-Cat, on the other hand, is significantly larger and heavier in terms of its weight and footprint to the upflow photoreactor (Table 8.1). Moreover, the upflow photoreactor is a modular system and is lightweight. Due to heavier weight and size (footprint), the Photo-Cat cannot be accommodated inside the MobileNEWT testbed, not serving its purpose of having multiple treatment unit on a same treatment platform. Another essential but critical item to consider, the Photo-Cat requires a much higher amperage (larger power breaker). It also requires higher voltage (i.e., 220-230V), which could also be an issue, especially for field-study and testing (Table 8.1), especially if such a power supply cannot be arranged. Whereas the upflow photoreactor requires regular power (110-120V) supply, a standard wall outlet would be enough, which is easy to secure in a field setting. The equipment and

O&M cost (e.g., pump, lamp and membrane replacement, sensors, etc.) for the Photo-Cat will also be substantially higher. Thus, if the goal of the field-scale study is to screen optimal photocatalysts and treatment conditions, then the upflow (slurry) photoreactor at MobileNEWT could be utilized. However, if the goal is to implement a similarly designed photoreactor from the field to a larger scale design, then the Photo-Cat system would be the appropriate option. The Photo-Cat is a commercially available package product and currently is in operation at a larger scale. Overall, this study was able to show that all three photoreactors were effective in screening and assessing optimal treatment conditions for both pCBA and PFOA degradation and elucidated on E_{EO} values and their operational ease and challenges.

REFERENCES

Bolton, J. R., & Stefan, M. I. (2002). Fundamental photochemical approach to the concepts of fluence (UV dose) and electrical energy efficiency in photochemical degradation reactions. *Research on Chemical Intermediates*, *28*(7), 857-870.

Brame, J., Fattori, V., Clarke, R., Mackeyev, Y., Wilson, L. J., Li, Q., & Alvarez, P. (2014). Water disinfection using nanotechnology for safer irrigation: a demonstration project in Swaziland. *Environmental Engineer and Scientist: Applied Research and Practice*, *50*(2), 40-46.

Duan, L., Wang, B., Heck, K., Guo, S., Clark, C. A., Arredondo, J., ... & Wong, M. S. (2020). Efficient photocatalytic PFOA degradation over boron nitride. *Environmental Science & Technology Letters*, *7*(8), 613-619.

Etacheri, V., Di Valentin, C., Schneider, J., Bahnemann, D., & Pillai, S. C. (2015). Visible-light activation of TiO2 photocatalysts: Advances in theory and experiments. *Journal of Photochemistry and Photobiology C: Photochemistry Reviews*, *25*, 1-29.

Guo, Q., Zhou, C., Ma, Z., & Yang, X. (2019). Fundamentals of TiO2 photocatalysis: concepts, mechanisms, and challenges. *Advanced Materials*, *31*(50), 1901997.

Han, W., Zhang, P., Zhu, W., Yin, J., & Li, L. (2004). Photocatalysis of p-chlorobenzoic acid in aqueous solution under irradiation of 254 nm and 185 nm UV light. *Water research*, *38*(19), 4197-4203.

Herkert, N. J., Merrill, J., Peters, C., Bollinger, D., Zhang, S., Hoffman, K., ... & Stapleton, H. M. (2020). Assessing the effectiveness of point-of-use residential drinking water filters for perfluoroalkyl substances (PFASs). *Environmental Science & Technology Letters*, *7*(3), 178-184.

Lanzarini-Lopes, M., Garcia-Segura, S., Hristovski, K., & Westerhoff, P. (2017). Electrical energy per order and current efficiency for electrochemical oxidation of p-chlorobenzoic acid with boron-doped diamond anode. *Chemosphere*, *188*, 304-311.

Li, X., Li, Z., & Yang, J. (2014). Proposed photosynthesis method for producing hydrogen from dissociated water molecules using incident near-infrared light. *Physical review letters*, *112*(1), 018301.

Li, X., Zhang, P., Jin, L., Shao, T., Li, Z., & Cao, J. (2012). Efficient photocatalytic decomposition of perfluorooctanoic acid by indium oxide and its mechanism. *Environmental science & technology*, *46*(10), 5528-5534.

Li, N., Zou, X., Liu, M., Wei, L., Shen, Q., Bibi, R., ... & Zhou, J. (2017). Enhanced visible light photocatalytic hydrogenation of CO2 into methane over a Pd/Ce-TiO2 nanocomposition. *The Journal of Physical Chemistry C*, *121*(46), 25795-25804.

Nguyen, J. F. (2017). Degradation of gas-phase ethanol using TiO2 photocatalyst.

Sahu, S. P., Qanbarzadeh, M., Ateia, M., Torkzadeh, H., Maroli, A. S., & Cates, E. L. (2018). Rapid degradation and mineralization of perfluorooctanoic acid by a new petitjeanite Bi3O (OH)(PO4) 2 microparticle ultraviolet photocatalyst. *Environmental Science & Technology Letters*, *5*(8), 533-538.

Sörengård, M., Franke, V., Tröger, R., & Ahrens, L. (2020). Losses of poly-and perfluoroalkyl substances to syringe filter materials. *Journal of Chromatography A*, *1609*, 460430.

Stancl, H. O. N., Hristovski, K., & Westerhoff, P. (2015). Hexavalent chromium removal using UV-TiO2/ceramic membrane reactor. *Environmental Engineering Science*, *32*(8), 676-683.

Tugaoen, H. O. N., Garcia-Segura, S., Hristovski, K., & Westerhoff, P. (2018). Compact light-emitting diode optical fiber immobilized TiO2 reactor for photocatalytic water treatment. *Science of The Total Environment*, *613*, 1331-1338.

Venkatesh, K. (2020). *Adsorption of Perfluoroalkyl Substances from Groundwater Using Pilot and Lab Scale Columns*(Master's thesis, Arizona State University).

Westerhoff, P., Alvarez, P., Li, Q., Gardea-Torresdey, J., & Zimmerman, J. (2016). Overcoming implementation barriers for nanotechnology in drinking water treatment. *Environmental Science: Nano*, *3*(6), 1241-1253.

Xu, B., Ahmed, M. B., Zhou, J. L., Altaee, A., Wu, M., & Xu, G. (2017). Photocatalytic removal of perfluoroalkyl substances from water and wastewater: mechanism, kinetics and controlling factors. *Chemosphere*, *189*, 717-729.

Xu, B., Liu, S., Zhou, J. L., Zheng, C., Weifeng, J., Chen, B., ... & Qiu, W. (2021). PFAS and their substitutes in groundwater: Occurrence, transformation and remediation. *Journal of Hazardous Materials*, 125159.

Zhao, B., & Zhang, P. (2009). Photocatalytic decomposition of perfluorooctanoic acid with β-Ga2O3 wide bandgap photocatalyst. *Catalysis Communications*, *10*(8), 1184-1187.

Zhou, C., Lai, C., Zhang, C., Zeng, G., Huang, D., Cheng, M., ... & Jiang, L. (2018). Semiconductor/boron nitride composites: synthesis, properties, and photocatalysis applications. *Applied Catalysis B: Environmental*, *238*, 6-18.

APPENDIX A

SUPPORTING INFORMATION

1. Materials and Methods

Photocatalysts

There are three kinds of hBN with different affinities to water, as Figure S1. shows below.
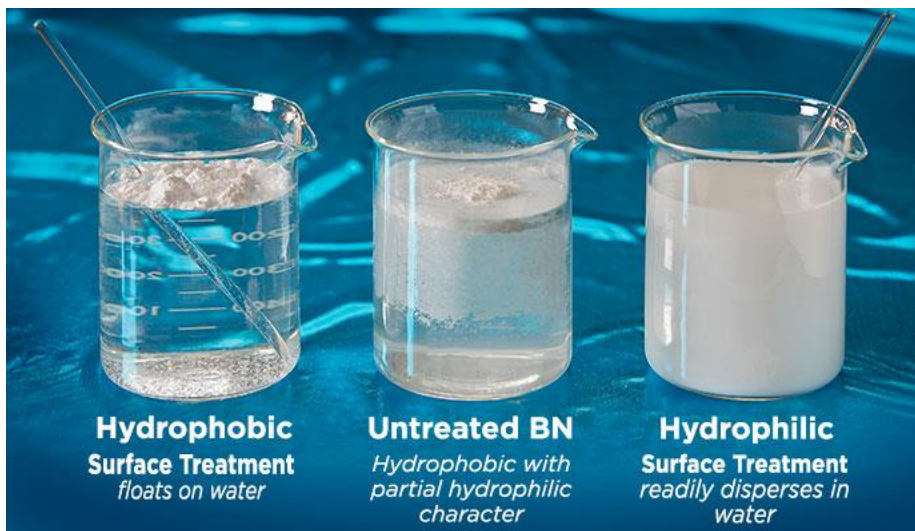
Figure S1. Three Kinds of hBN (https://www.bn.saint-gobain.com/technical-solutions/surface-properties)

hBN#1 used in this study, is a common, commercially available product, and belongs to one on the left one, which is hydrophobic and tends to float on water, which was observed in this study. While hBN#2 is more like the middle or the right one, which is less hydrophobic but more hydrophilic in character.

2. UV, UV/H$_2$O$_2$, and O$_3$/H$_2$O$_2$ PFAS Treatability Screening Using Real Groundwater

Objective

To screen potential of currently commercially available AOPs (UV, UV/H$_2$O$_2$, and O$_3$/H$_2$O$_2$) to remove PFASs from a groundwater.

Materials and Methods

Water samples (~55 gallons) were collected from a PFAS contaminated groundwater well in CA and filtered through 0.2 μm filters upon arrival to the laboratory. The water quality parameters were measured at ASU and the results are listed in Table S1. PFASs samples were measured according to method EPA 533 by Eurofins laboratories.

Table S1.

Water Quality Parameters for Groundwater

Parameters	Groundwater	PFASs	Groundwater (ng/L)
pH	7.61	PFDA (C10)	2
Conductivity (uS/cm)	843	PFNA (C9)	2
Alkalinity (mg/L as CaCO$_3$)	264	PFOA (C8)	580
Turbidity (NTU)	0.36	PFOS (C8)	52
DOC (mg/L)	0.69	PFHpA (C7)	67
UV 254 (cm^{-1})	0.003	PFHxA (C6)	70
Chloride (mg/L)	109.68	PFHxS (C6)	32
Nitrate (mg/L as N)	3.1	PFPeA (C5)	52
Sulfate (mg/L as SO$_4$)	54.3	PFPeS (C5)	6

UV, UV/ H$_2$O$_2$, and O$_3$/H$_2$O$_2$ experiments

UV and UV/H$_2$O$_2$ experiments were conducted using a pilot-scale Photo-Cat reactor (Purifics) (Figure 1). The system was occupied with four 75-Watt low-pressure mercury lamp with 45 μW/cm^2 UV output and operated in batch mode at a constant flow

rate of ~25 L/min. Before the experiments, 10-L of water sample was equilibrated to room temperature (22 ± 2°C), adjusted to pH 7.0, and transferred into the accumulator. The reactor was operated in batch mode up to 4 hr (UV dose ~2600 mJ/cm^2) and samples were collected from the ceramic UF filter effluent of the system and shipped to Eurofins laboratories with a cooler filled with ice packs (at ~4°C). For UV/H$_2$O$_2$ treatment, 20 mg/L of H$_2$O$_2$ was initially dosed into the reactor and run in batch mode for 10 min for the complete mixture of H$_2$O$_2$ in the reactor.

Table S2.

Concentrations of PFASs in Raw Groundwater and after by UV, UV/H$_2$O$_2$, O$_3$/H$_2$O$_2$, UV/Cat#1, UV/Cat#2, and UV/Cat#1+Cat#2 Treatment

PFASs	Concentrations (ng/L)						
	Raw Groundwater	UV	UV/H$_2$O$_2$	O$_3$/H$_2$O$_2$	UV/ Cat#1	UV/ Cat#2	UV/Cat#1+ Cat#2
PFDA (C10)	2	3	4	4	ND	ND	ND
PFNA (C9)	2	4	14	8	ND	ND	ND
PFOA (C8)	580	1700	950	89	1500	64	35
PFOS (C8)	52	33	29	39	30	ND	ND
PFHpA (C7)	67	490	280	150	380	670	390
PFHxA (C6)	70	470	300	250	350	840	570
PFHxS (C6)	32	28	31	37	38	ND	ND

PFPeA (C5)	52	270	210	130	270	490	320
PFPeS (C5)	6	6	6	8	ND	ND	ND
PFBA (C4)	51	140	130	150	200	290	210
PFBS (C4)	6	6	7	10	ND	ND	ND
Σ PFAS	920	3150	1961	875	2768	2354	1525

Cat#1: Commercially available catalyst

Cat#2: Novel catalyst

3. Degradation of para-Chlorobenzoic Acid at Upflow Photoreactor

Effect of pH (TiO$_2$)

Table S3.
pCBA Degradation with TiO$_2$ at pH=3 (Exp #4)

Time	UV	Loading Rate	pH	Conductivity	pCBA Concentration	Removal
(min)	(ON/OFF)	(mg/L)	(SU)	(uS/cm)	(ppb)	(%)
0	OFF		2.99	1250	2523	
10			3.07	1190	2509	1
20			3.12	1160	2310	8
30			3.07	1150	1840	27
60	ON	1000	3.18	1140	1593	37
90			3.19	1110	716	72
120			3.22	1050	487	81
150			3.22	1060	307	88
180			3.28	1040	180	93

Conductivity is due to the acid addition to DI water.

Table S4.
pCBA Degradation with TiO$_2$ at pH=7 (Exp #5)

Time	UV	Loading Rate	pH	Conductivity	pCBA Concentration	Removal
(min)	(ON/OFF)	(mg/L)	(SU)	(uS/cm)	(ppb)	(%)
0	OFF		6.66	100	4003	10
10			6.67	80	2475	44
20			6.70	80	2228	50
30			6.65	80	1918	57
60	ON	1000	6.58	90	1718	61
90			6.48	90	1255	72
120			6.35	100	798	82
150			6.20	100	481	89
180			6.15	110	302	93

Table S5.

pCBA Degradation with TiO$_2$ at pH=11 (Exp #6)

Time	UV	Loading Rate	pH	Conductivity	pCBA Concentration	Removal
(min)	(ON/OFF)	(mg/L)	(SU)	(uS/cm)	(ppb)	(%)
0	OFF		10.33	560	5333	1
10			10.44	540	5153	5
20			10.43	540	4904	9
30			10.37	550	4702	13
60	ON	1000	10.42	550	3996	26
90			10.30	530	3530	35
120			10.36	540	3374	38
150			10.30	530	2744	49
180			10.36	540	2426	55

Conductivity is due to the acid addition to DI water.

Effect of pH (hBN)

Table S6.

pCBA Degradation with hBN#1 at pH=3 (Exp #7)

Time	UV	Loading Rate	pH	Conductivity	pCBA Concentration	Removal
(min)	(ON/OFF)	(mg/L)	(SU)	(uS/cm)	(ppb)	(%)
0	OFF		3.10	820	2585	5
10			3.07	800	2468	9
20			3.16	770	2259	17
30			3.13	720	2110	23
60		1000	3.30	650	2144	21
90	ON		3.35	620	1286	53
120			3.36	590	981	64
150			3.36	580	448	84
180			3.35	570	312	89

Table S7.

pCBA Degradation with hBN#1 at pH=7 (Exp #8)

Time	UV	Loading Rate	pH	Conductivity	pCBA Concentration	Removal
(min)	(ON/OFF)	(mg/L)	(SU)	(uS/cm)	(ppb)	(%)
0	OFF		6.38	120	1952	9
10	ON	1000	6.29	120	1867	13
20			6.32	120	1677	22
30			6.43	120	1523	29
60			6.34	120	779	64
90			6.28	130	535	75
120			6.19	130	469	78
150			6.11	130	326	85
180			6.09	140	287	87

4. Degradation of Per-fluorootanoic Acid at Upflow Photoreactor

Effect of pH (hBN)

Table S8.

PFOA Degradation with hBN#1 at pH=3 (Exp #5)

Time	UV	Loading Rate	pH	Conductivity	pCBA Concentration	Removal
(min)	(ON/OFF)	(mg/L)	(SU)	(uS/cm)	(ppb)	(%)
0	OFF		3.02	1100	26734	3
10			3.09	1060	26689	3
20			3.05	1080	25973	6
30			3.23	1080	24846	10
60	ON	1000	3.25	1030	23424	15
90			3.23	1010	23519	15
120			3.29	970	23319	15
150			3.35	920	21384	22
180			3.37	910	22491	18

Table S9.

PFOA Degradation with hBN#2 at pH=3 (Exp #6)

Time	UV	Loading Rate	pH	Conductivity	pCBA Concentration	Removal
(min)	(ON/OFF)	(mg/L)	(SU)	(uS/cm)	(ppb)	(%)
0	OFF		2.89	1370	20054	5
10			2.91	1310	19762	6
20			2.86	1310	18888	10
30			2.98	1290	18786	11
60		1000	3.07	1250	16323	23
90	ON		3.09	1230	15660	26
120			3.02	1220	14867	29
150			3.11	1200	14881	29
180			3.04	1210	14595	31

Table S10.

PFOA Degradation with hBN#2 at pH=7 (Exp #7)

Time	UV	Loading Rate	pH	Conductivity	pCBA Concentration	Removal
(min)	(ON/OFF)	(mg/L)	(SU)	(uS/cm)	(ppb)	(%)
0	OFF		7.58	410	23586	2
10			7.45	420	21750	9
20			7.44	400	21670	10
30			7.46	400	21072	12
60		1000	7.49	410	21098	12
90	ON		7.57	430	21109	12
120			7.60	410	21661	10
150			7.53	400	20966	12
180			7.51	420	21151	12

Table S11.

PFOA Degradation with hBN#2 at pH=11 (Exp #8)

Time	UV	Loading Rate	pH	Conductivity	pCBA Concentration	Removal
(min)	(ON/OFF)	(mg/L)	(SU)	(uS/cm)	(ppb)	(%)
0	OFF		10.81	510	25867	
10			10.72	510	25392	2
20			10.78	510	25612	1
30			10.71	510	25049	3
60	ON	1000	10.85	490	25279	2
90			10.88	500	25539	1
120			10.83	500	24971	4
150			10.80	500	24533	5
180			10.83	490	24878	4